



LIBRARIES

UNIVERSITY OF WISCONSIN-MADISON

Transport of agricultural contaminants in sand aquifers affected by drainage ditches : July 1990 to September 1991 : final report. [1991?]

Bahr, Jean Marie et al.

Madison, Wisconsin: Wisconsin University, Madison, Department of Geology and Geophysics., [1991?]

<https://digital.library.wisc.edu/1711.dl/PKEXCIJFI7NDP8U>

<http://rightsstatements.org/vocab/InC/1.0/>

For information on re-use see:

<http://digital.library.wisc.edu/1711.dl/Copyright>

The libraries provide public access to a wide range of material, including online exhibits, digitized collections, archival finding aids, our catalog, online articles, and a growing range of materials in many media.

When possible, we provide rights information in catalog records, finding aids, and other metadata that accompanies collections or items. However, it is always the user's obligation to evaluate copyright and rights issues in light of their own use.

C2
7-31-92

FINAL REPORT

TRANSPORT OF AGRICULTURAL CONTAMINANTS IN SAND AQUIFERS
AFFECTED BY DRAINAGE DITCHES

July 1990 to September 1991

Principal Investigator: Jean M. Bahr

Research Assistants: Lucy W. Chambers, Lynn Raue

Undergraduate Assistants: Rod Rustad, Terrance Huettl

Department of Geology and Geophysics

University of Wisconsin - Madison

Water Resources Center
University of Wisconsin - **MSN**
1975 Willow Drive
Madison, WI 53706

ABSTRACT

The objectives of the project described in this report were to develop an improved understanding of the hydrologic and chemical factors affecting the fate of agricultural contaminants in sand aquifers and to evaluate the effectiveness of drainage ditches as passive barriers to contaminant migration. These objectives were addressed through detailed field studies conducted in the vicinity of an agricultural drainage ditch. The field studies included extensive sampling and hydraulic testing to characterize hydrogeologic and chemical properties, a conservative tracer experiment to delineate flow paths and groundwater velocities, and a reactive tracer experiment to evaluate the rate of in-situ denitrification. The field studies were accompanied by evaluations of existing models of ditch capture depth and aquifer dispersivity. At the field site, variations in hydraulic conductivity appear to generate stratification of flow and of groundwater chemistry. Comparison of hydraulic conductivity measured by slug tests with grain size distributions determined for vibracore and auger samples provides the basis for evaluating magnitudes of hydraulic conductivity variations within the aquifer. These variations can be used to estimate the anisotropy ratio. Chemical signatures, particularly the calcium/magnesium ratio, may be useful as "natural tracers" for mapping flow lines at the field site.

Conservative tracer experiments have confirmed that existing ditches in the central sand plain do create passive barriers to shallow migration of groundwater contaminants. However, a comparison of the experiment conducted in 1990 with a previous experiment from 1989 demonstrates that there can be large fluctuations in the depth of the capture zone due to seasonal or

longer term variations in gradients and ditch stage. Reasonable matches between the observed capture depth and predictions of a simple analytical model can be obtained by assuming an aquifer anisotropy ratio of 2, which is consistent with the magnitude of vertical variations in hydraulic conductivity. The reactive tracer test conducted in 1991 demonstrated that rapid denitrification occurs in shallow portions of the aquifer at the field site. The observed rate of denitrification is consistent with the hypothesis that rates of denitrification in anaerobic sandy aquifers are roughly proportional to concentrations of labile organic carbon. These results suggest that improved estimates of susceptibility to nitrate contamination in the central sand plain can be obtained through a regional survey of dissolved oxygen and dissolved organic carbon in groundwater.

TABLE OF CONTENTS

	Page
ABSTRACT	i
I. INTRODUCTION	1
II. MATERIALS AND METHODS	5
A. Field Site	5
B. Characterization of Physical and Chemical Heterogeneity	7
1. Hydraulic Conductivity Measurements	7
2. Grain Size Analyses	7
3. Groundwater Chemistry	10
C. Tracer Experiments	11
D. Model Evaluation	16
III. RESULTS AND DISCUSSION	17
A. Characterization of Physical and Chemical Heterogeneity	17
1. Physical heterogeneity	17
2. Chemical heterogeneity	25
B. Tracer Experiments	36
1. Conservative tracer experiment	36
2. Reactive tracer experiment	38
C. Model Evaluation	49
1. Comparison of observed and predicted capture depths	49
2. Estimates of apparent dispersivity	53
IV. CONCLUSIONS	57
REFERENCES	62
APPENDIX A - Slug Tests and Grain Size Analyses	
APPENDIX B - Chemical Analyses	
APPENDIX C - Bromide and Nitrate Concentrations, 1991 Experiment	
APPENDIX D - Paper published in Ottawa Conference Proceedings	

LIST OF TABLES

Page

Table 1 - Summary of tracer injections at Adams Co. site, 1990	12
Table 2 - Summary of tracer injections at Adams Co. site, 1991	15
Table 3 - Summary of slug test results	17
Table 4 - Summary of grain size analyses	19
Table 5 - Parameter estimates and predicted capture depths	52
Table 6 - Dispersivity estimates from breakthrough curve analysis	56

LIST OF FIGURES

Figure 1 - Locations at which slug tests were performed.	8
Figure 2 - Locations from which samples were collected for grain size analysis.	9
Figure 3 - Location of injection well and samplers employed during the 1991 tracer experiment.	14
Figure 4 - Average hydraulic conductivity determined from slug tests, plotted versus the midpoint of the well screen.	18
Figure 5 - Grain size distribution parameters versus sample elevation.	20
Figure 6 - Hydraulic conductivity predicted on the basis of grain size distribution using the models of Hazen (1893) and Masch and Denny (1966).	23
Figure 7 - Scaling between Masch and Denny predictions and measured hydraulic conductivities from slug tests.	24
Figure 8 - Locations at which samples were collected for chemical analyses.	26
Figure 9 - Profiles of specific conductance in micromhos/cm (μS).	27
Figure 10- Profiles of pH.	28
Figure 11- Profiles of calcium concentration (ppm).	29
Figure 12- Profiles of the ratio of calcium concentration (ppm) to magnesium concentration (ppm).	30
Figure 13- Profiles of iron concentration (ppm).	31
Figure 14- Profiles of manganese concentration (ppm).	32
Figure 15- Comparison of tracer paths for 1989 and 1990 tracer tests	37
Figure 16- Cross-section of total movement of the bromide cloud during the reactive tracer test of 1991.	39
Figure 17- Dimensionless breakthrough curves at mm57.	40
Figure 18- Dimensionless breakthrough curves at mm58.	41
Figure 19- Decrease in concentration of nitrate relative to bromide in mm57 and mm58.	44
Figure 20- Nitrate deficiencies at mm57 and mm58.	46
Figure 21- Dimensionless breakthrough curves at mm61 and mm64.	48
Figure 22- Profiles of dissolved organic carbon and dissolved inorganic carbon within the tracer zone, as measured in mm58.	50
Figure 23- Schematic diagram illustrating parameters of the two-dimensional solution of Zheng et al. (1988a).	51
Figure 24- Observed and calculated breakthrough curves for multilevels during the 1989 tracer experiment.	55

I. INTRODUCTION

Groundwater contamination by agricultural chemicals is a serious concern in irrigated areas such as the central sand plain of Wisconsin. Highly permeable soils and a shallow water table can permit relatively rapid transport through the unsaturated zone to groundwater. Detections of pesticides and high nitrate concentrations have resulted in the abandonment of both domestic and municipal wells in the region (Lulloff, 1987, Born et al., 1988). A number of research projects over the last decade (e.g. Rothschild et al., 1982; Chesters et al., 1982; Manser, 1983; Harkin et al., 1986; Brasino, 1986; Kung, 1990; Kraft, 1990) have been designed to assess the extent of groundwater contamination in the central sand plain and to identify the factors that control rates of transport in the vadose zone and below the water table. The results of these studies have highlighted the need for effective measures both to assess groundwater susceptibility to contamination and to limit contaminant migration in susceptible areas.

Groundwater susceptibility is generally assumed to be a function of soil, geologic and hydrologic characteristics of an area (Wisconsin Geol. and Nat. Hist. Survey, 1987). Geochemical characteristics of the groundwater system may be equally important in determining the ultimate fate of contaminants. For example, field studies by Trudell et al. (1986) and Starr and Gillham (1989) demonstrate the importance of dissolved organic carbon concentrations on the rate of transformation of nitrate to nitrogen gas (denitrification). Landreau et al. (1988) also suggest that groundwater redox conditions and sulfide concentrations in the aquifer matrix control rates of a second denitrification process. Transformation of pesticides

such as aldicarb can also vary significantly as a function of aquifer and groundwater geochemistry, as indicated by the microcosm studies of Kraft (1990). An improved understanding of the relationship between hydrologic and geochemical characteristics of aquifers in the sand plain should help to explain observed contaminant distributions and to distinguish between areas of low and high susceptibility to contamination.

Control of contaminant migration resulting from dispersed agricultural sources is virtually impossible using active pump-and-treat systems such as those designed to deal with more localized contaminant sources. However, Faustini (1985) suggested that the existing system of drainage ditches in the central sand plain may be creating passive barriers to shallow contaminant migration. Zheng et al. (1988a, 1988b) developed analytical and numerical models to simulate groundwater flow patterns in the vicinity of drainage ditches. These models predict the position of the streamline that divides the upper portion of the aquifer, which constitutes the "capture zone" of the drainage ditch, from the lower portion which contains water that will ultimately flow beyond the ditch. Initial field experiments conducted at a ditch in Adams County (Chambers, 1990; Chambers and Bahr, 1992) identified a capture zone depth of 12 to 16 ft and provided partial confirmation of model predictions of capture zone effectiveness. However, results of the field experiments also demonstrated the existence of significant local scale variations in groundwater velocity and a three-dimensional nature of the flow field that are not accounted for in the models. Additional uncertainties in model predictions of ditch capture zone depth are introduced by seasonal variations in flow directions, gradients and ditch stage, and by the paucity of data on anisotropy of the aquifer.

Further evaluation of existing drainage ditches and the design of improved ditch networks to limit contaminant migration requires quantitative studies of aquifer heterogeneity, particularly horizontal to vertical anisotropy, and of rates and magnitudes of variations in the groundwater flow field.

The overall objective of the project described in this report was to develop an improved understanding of the hydrologic and chemical factors affecting the fate of agricultural contaminants in sand aquifers. A related objective was to evaluate the effectiveness of drainage ditches as passive barriers to contaminant migration, in particular examining the effects of aquifer heterogeneity and flow field variability on ditch-groundwater interactions. These objectives were addressed through detailed field studies conducted in the vicinity of an agricultural drainage ditch at the Adams County site that was the subject of our previous investigations. The information on the flow field and capture depth at the site obtained in previous studies provided the necessary background information required in the design of additional field experiments conducted during this second study phase to examine physical and chemical heterogeneity of the sand aquifer at this location.

The field studies included extensive sampling and hydraulic testing to characterize hydrogeologic and chemical properties, a conservative tracer experiment to delineate flow paths and groundwater velocities, and a reactive tracer experiment to evaluate the rate of in-situ denitrification. The extensive network of wells and sampling devices that had been installed during the initial experiments provide the opportunity to collect water samples to examine the vertical and lateral variations in groundwater chemistry and to conduct slug tests and grain size analyses for a variety of

locations and depths. The flow paths and velocity ranges for conservative tracers determined during the previous experiments allowed for design of an additional conservative experiment with improved sampling strategies designed not only to delineate the capture zone but also to examine variations in advective velocity and apparent dispersivity within the aquifer. Results of this conservative tracer experiment were used in turn to design the reactive tracer experiment, confining the nitrate introduced to the aquifer to the ditch capture zone, thus insuring that any nitrate that was not converted to nitrogen by denitrification would not migrate in the aquifer beyond the ditch. The field studies were accompanied by evaluation of existing models. Development of improved models based on data obtained from the field studies is a major component of ongoing research motivated by the results of this project.

II. MATERIALS AND METHODS

The project involved three major categories of research activities: characterization of physical and chemical heterogeneity, tracer experiments and model evaluation. The methods employed in each of these activities are described following a review of the hydrogeologic setting and previous studies at the field site.

A. Field Site

The field site is located in the northeast corner of Adams County, nine miles west of Plainfield. According to maps of Clayton and Attig (1989), the site is located near the edge of the maximum extent of Glacial Lake Wisconsin. Drilling at the site revealed the presence of a silt and clay layer at a depth of approximately 30 ft. This layer probably is part of the New Rome Member which was deposited during the last filling of Glacial Lake Wisconsin. The sediment above the silt and clay layer is well sorted fine to medium sand, deposited near the margin of glacial lake Wisconsin and may be either stream or offshore deposits according to the map of Clayton and Attig (1989). A north-south trending ditch, approximately 10 feet wide, crosses the site. Mini-piezometers installed in the ditch indicate that head in the aquifer exceeds ditch stage by 0.1 to 0.2 feet. Based on a water table map of Adams County (Lippelt and Hennings, 1981), regional flow is to the west-southwest, roughly perpendicular to the ditch, and the horizontal gradient is between 0.001 and 0.002. Water level measurements at the site indicate that the water table gradient on the east side of the ditch ranges from greater than 0.007 down to 0.003. However, this observed water

table gradient is likely to represent a local, shallow perturbation caused by the ditch. It is the regional gradient, rather than local perturbations, that is assumed to determine the effective ditch capture depth in the analytical model of Zheng et al. (1988a).

Instrumentation of the site was initiated in the summer of 1988. By the fall of 1989, a dense array of monitoring points was available for field testing and sampling. The monitoring network included over 40 water table wells, 7 two-inch injection wells, 12 bundle-type multilevel sampling wells of the type described by Jackson et al. (1985), and over 50 miniature multilevels installed using the method described by Stites and Chambers (1991). Following a number of preliminary tests conducted at the site between August 1988 and June 1989, a multiple tracer experiment was initiated in July 1989. Results of this experiment are described in detail by Chambers (1990) and are summarized in Chambers and Bahr (1992). This multiple tracer test verified the existence of a capture zone in the vicinity of the drainage ditch with a depth of at least 12 feet below the water table. The observed capture depth was within the range of 5 feet to 34 feet predicted using the analytical model of Zheng et al. (1988a). The large range of predicted depths is primarily the result of solution sensitivity to the anisotropy ratio of the aquifer and the uncertainty in this parameter for the field site. It should also be noted that 1989 was a drought year and hydrologic conditions that summer cannot necessarily be considered typical.

B. Characterization of Physical and Chemical Heterogeneity

1. Hydraulic Conductivity Measurements

Estimates of field scale hydraulic conductivity were obtained from 25 slug tests conducted on 13 wells at the locations shown on Figure 1. Each slug test was initiated by rapidly adding or removing a solid polyvinyl-chloride rod, or slug, to the well. This caused a temporary perturbation in the static water level. Decay of the water level perturbation was monitored using a submerged pressure transducer connected via a cable to a Hermit 1000 data logger at the surface. The data logger was preprogrammed to collect pressure data at a logarithmic sampling interval. Data were transferred in the lab to a personal computer and analyzed using the code AQTESOLV (Geraghty and Miller, Inc., Reston, VA, 1989) which includes the solution developed by Bouwer and Rice (1976) for analysis of slug tests in unconfined aquifers. Results of these tests are discussed in Chapter III, section A.1 and AQTESOLV analyses are included in Appendix A.

2. Grain Size Analyses

Hydraulic conductivity measurements were compared to grain size distributions of samples collected during installation of the wells and from vibracore samples for the locations shown in Figure 2. Samples collected during well installation were obtained from the base of the solid stem auger used to drill the well. A vibracore sample is obtained by vibrating a length of aluminum irrigation pipe into the ground. A mechanical vibrator is attached to the pipe with a collar and additional weight is applied to the pipe to accelerate downward movement. When the pipe has reached the

Location of Slug Tests

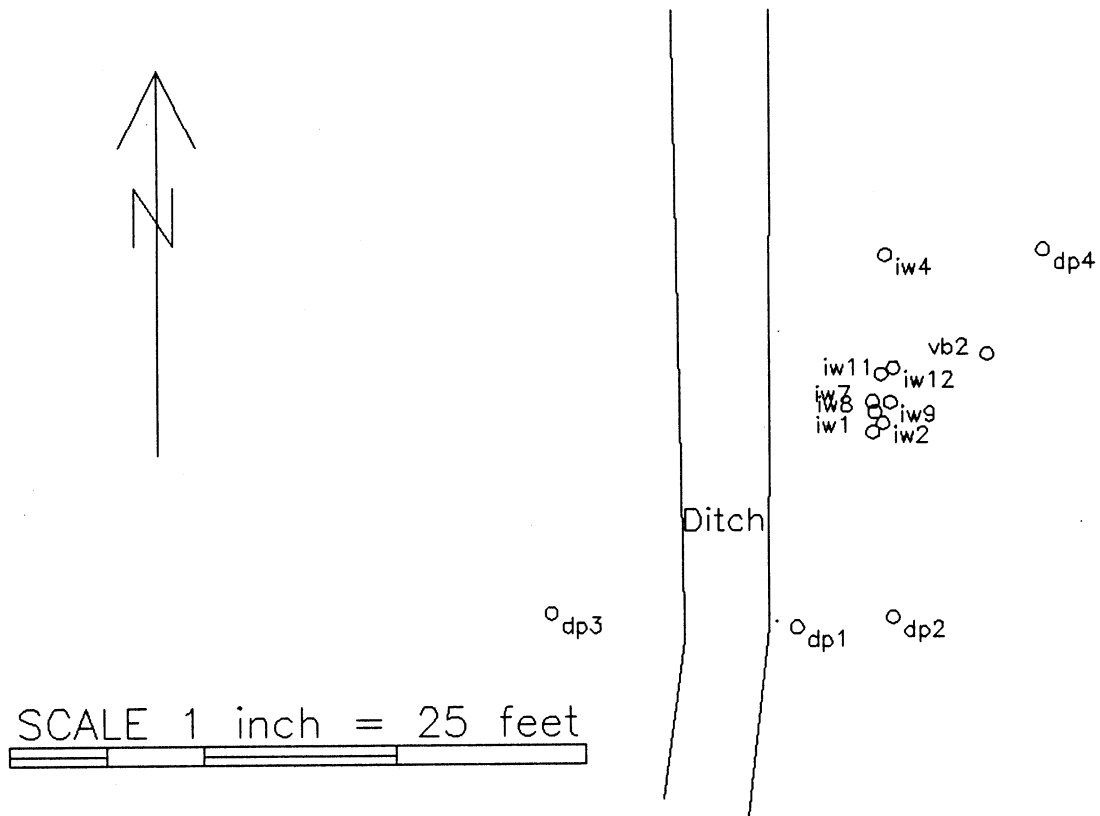


Figure 1 - Locations at which slug tests were performed.

Location of Grain Size Samples

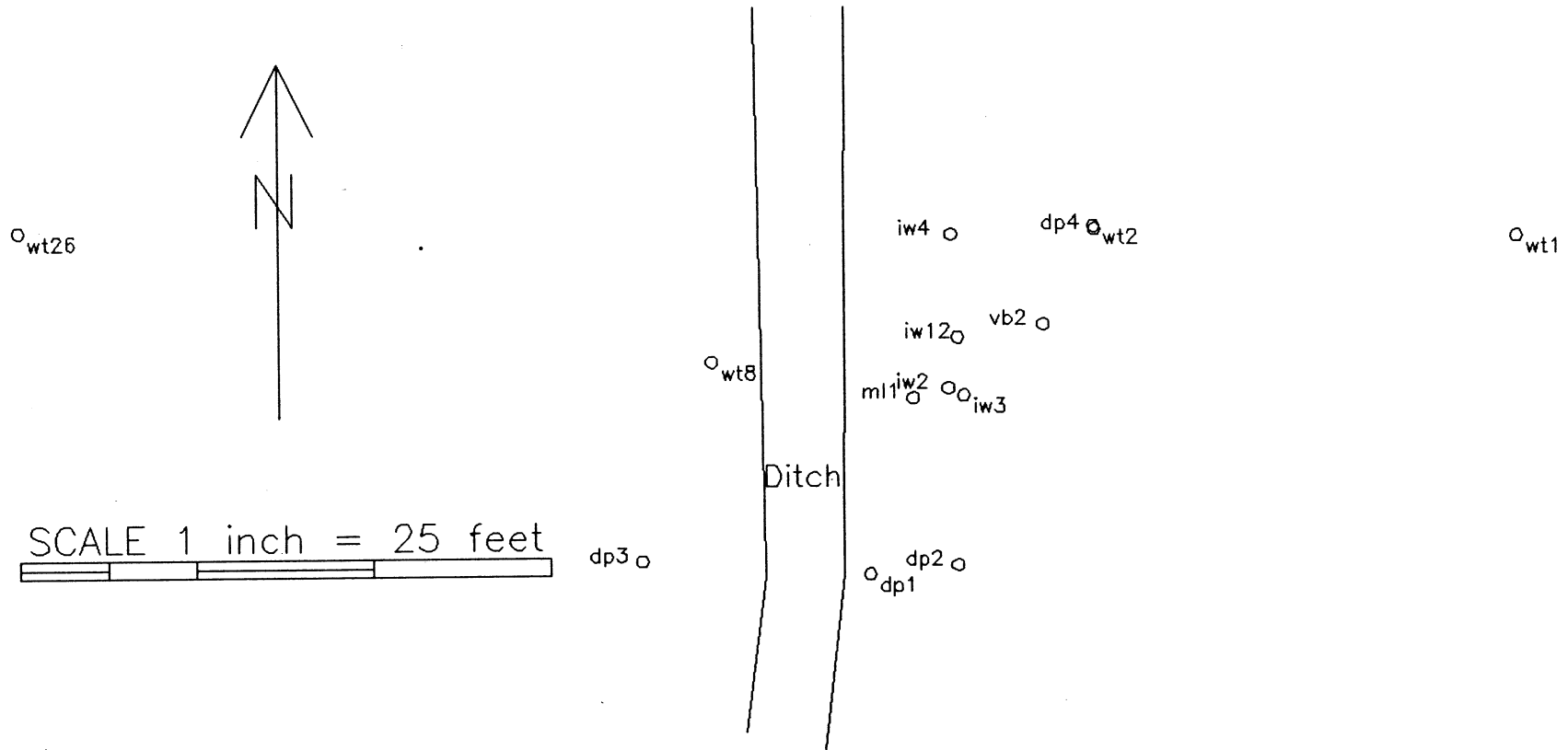


Figure 2 - Locations from which samples were collected for grain size analysis.

desired depth, it is retrieved using a tripod and block-and-tackle. Three vibracores were completed successfully at the site. Upon return to the laboratory these were cut in half lengthwise in order to observe stratification of the sediments. One vibracore was sampled for mechanical grain size analysis.

Mechanical sieve analyses were conducted employing sieves stacked in descending order with mesh sizes of 2 mm, 1 mm, 0.5 mm, 0.25 mm 0.125 mm and 0.0625 mm and a bottom pan to collect silt and clay size particles. Following oven drying, 35 to 40 grams of sediment was poured into the top sieve and the sieve stack was then placed on a shaker unit for 10 minutes. The cumulative grain size distribution was plotted on a logarithmic scale and a cubic spline was fit to the data in order to obtain a graphical estimate of D50, the mean grain diameter, D10, the diameter corresponding to the 10% finer or 90% coarser limit, and the standard deviation, σ , of grain size (measured in ϕ units). Plots of grain size distribution are included in Appendix A and results are compared to slug test analyses in Chapter III, Section A.2.

3. Groundwater Chemistry

A series of groundwater samples were collected in the summer and fall of 1990 and a second set of samples was collected in May and June of 1991. Samples were withdrawn from multilevel samplers using a peristaltic pump. Specific conductance, dissolved oxygen, temperature and pH were measured in the field. Nitrate concentrations were also determined for some samples in the field using a colorimetric technique (CHEMetrics, Inc., Calverton, VA). Samples for lab analysis were filtered using in-line 0.4 μ filters and

stored in a cooler. Samples for cation analysis were also acidified in the field using approximately 1 ml of 35% HNO_3 per 100 ml of groundwater. Cation and alkalinity analyses were performed on all samples at the Soil and Plant Analysis Laboratory, UW-Extension, Madison. Chloride, ammonia and nitrate analyses for the samples collected in 1990 were also performed at the Soil and Plant Analysis Laboratory. Concentrations of chloride, sulfate, and nitrate for samples collected in 1991 were determined using an ion chromatograph in the Department of Soil Science, UW - Madison. Results of chemical analyses are included in Appendix B and are discussed in Chapter III, Section A.2.

C. Tracer Experiments

An experiment employing bromide and iodide as conservative tracers was conducted during the summer and early fall of 1990. Injection wells for this experiment consisted of two of the wells that had been used in the July 1989 experiment. These were located approximately 20 feet east of the ditch and screened at two different depths below the water table. Iodide tracer solution was introduced to the shallow well on July 23. Bromide tracer solution was introduced to the deeper well two weeks later. The staggered injection times were chosen to avoid potential interference of the clouds as they approached the ditch. For each injection, tracer solution was prepared by pumping 500 to 700 L of groundwater from the aquifer into an insulated tank. A concentrated solution was prepared by combining a measured amount of potassium salt with approximately 20 L of groundwater in a carboy. Following thorough mixing of this solution, it was added to the tank. Water in the tank was then mixed using a rotary stirrer. Tracer solution was

pumped from the tank into the injection well using three peristaltic pumps connected to a single discharge line. The injection rate was monitored using an in-line flow meter and pumping rates were adjusted to maintain a steady injection rate. Injection dates, total volumes and concentrations for the experiments are summarized in Table 1 below.

TABLE 1 - SUMMARY OF TRACER INJECTIONS AT ADAMS CO. SITE, 1990

Injection Date	7/23/90	8/8/90
Depth (ft below water table)	7.1-11.5	18.1-22.5
Tracer	iodide	bromide
Concentration	0.5 g/L	0.5 g/L
Total Volume Injected	500 L	700 L

Samples were collected from multilevel and miniature multilevel points using a peristaltic pump. A volume of 150 to 500 mL, corresponding to two to three tube volumes, was removed from each multilevel point prior to sampling. Field measurements of electrical conductance provided a preliminary estimate of tracer concentration. Samples were collected in plastic cups and taken to Madison for laboratory analysis using specific ion electrodes. Sampling frequency ranged from at least daily during early stages of the test to weekly during later stages. An additional 20 miniature multilevels were installed prior to or during the experiment to provide improved definition of cloud geometry and flow paths. Over 1800 samples collected during the course of the experiments were analyzed for bromide and iodide.

Results of the 1989 and 1990 tracer experiments were used to design an experiment employing bromide as a conservative tracer and nitrate as a reactive tracer. This experiment was initiated in June 1991. A new injection well was installed for this experiment, located approximately 60 feet east of the ditch and screened approximately 7 to 12 feet below the land surface. The increased distance from the ditch and the shallow depth of the injection well were chosen to allow for approximately 2 months of horizontal transport with eventual discharge of the entire cloud to the drainage ditch. A total of 4 miniature multilevels, constructed using a smaller tubing size to allow for up to 8 points per sampler, were installed prior to the test. Additional miniature multilevels were installed during the experiment to provide samplers for breakthrough curve analysis at several distances from the injection well. Figure 3 shows the locations of the injection well and miniature multilevel devices employed in this experiment.

Tracer solution mixing and injection were accomplished by the procedures described above for the conservative experiment. Concentrations of nitrate-N and bromide in the injection solution were approximately 12 mg/L and 48 mg/L respectively. These concentrations were chosen to be within the DNR approved nitrate concentration for the experiment and to have approximately equal peak areas on the ion chromatograph used for laboratory analyses. Additional injection characteristics are included in Table 2 below. Samples were collected using a peristaltic pump. Because of the reduced tubing size, it was only necessary to collect a few tens of mL to remove several tube volumes prior to sampling.

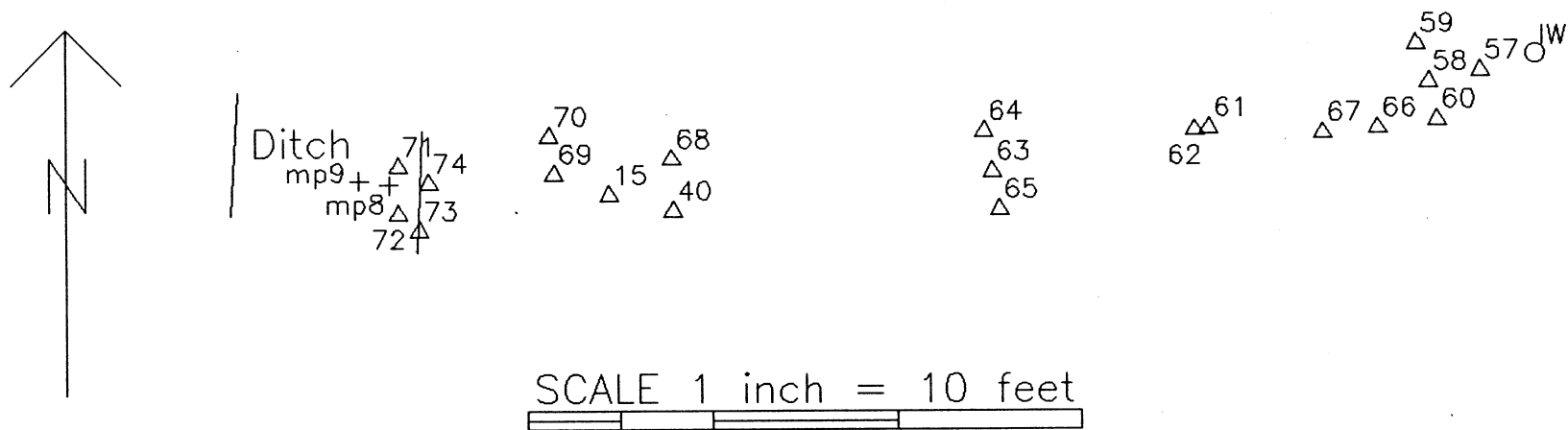


Figure 3 - Location of injection well (o) and samplers employed during the 1991 tracer experiment. Triangles are miniature multilevels and plusses are minipiezometers installed within the ditch.

TABLE 2 - SUMMARY OF TRACER INJECTION AT ADAMS CO. SITE, 1991

Injection Date	6/18/91
Depth (ft below water table)	6.0-10.4
Total Volume Injected	460 L
Injection Duration	4 hours
Injection Rate	115 L/hour
Tracer Concentration	NO ₃ -N: 12.3 mg/L bromide: 47.8 mg/L

Because of the relatively low concentrations in the tracer solution, it was not possible to monitor breakthrough using field measurements of specific conductance. A bromide specific ion electrode was therefore used to monitor breakthrough. Periodic analyses using a colorimetric method (CHEMetrics) were conducted to monitor nitrate concentrations. Results of field analyses of both tracers can only be considered approximate, however, because of difficulties associated with maintaining consistent calibrations under field conditions of fluctuating temperature. Samples for quantitative analysis using an ion chromatograph equipped with an auto-sampler in the Department of Soil Science, UW-Madison, were collected in plastic cups and transported to Madison. Following a repeated series of problems with this ion chromatograph, some of the remaining samples were analyzed by ion chromatography without the benefit of an auto-sampler in the Department of Geology and Geophysics, UW-Madison. Additional samples, for which previous ion-chromatography or field colorimetric analysis had indicated an absence of nitrate (i.e. samplers from locations at or beyond mm64) were analyzed

for bromide in the lab using a specific ion electrode. Bromide concentrations measured by specific ion electrode were used only to determine the path of the conservative tracer cloud. Results of laboratory analysis from this tracer test are included in Appendix C.

D. Model Evaluation

Two models were evaluated as part of this project: a simple equation resulting from the solution of an analytical model to predict ditch capture depth and a computer implementation of an analytical model to evaluate apparent dispersivity. In the case of the first model, estimates of the appropriate parameters obtained at the field site were used to solve the equation for the predicted capture depth. The ranges of predicted depth computed from the analytical model were compared to the capture depths observed during the tracer experiments of 1989 and 1990. Using the results of the two experiments allowed calibration to provide improved estimates of the anisotropy ratio for the aquifer at the field site. In the case of the second model, the model was calibrated using values of advective velocity, initial cloud dimensions and longitudinal dispersivity in order to fit breakthrough curves from the 1989 experiment.

III. RESULTS AND DISCUSSION

A. Characterization of Physical and Chemical Heterogeneity

1. Physical heterogeneity

Locations of wells in which slug tests were performed and from which samples were collected for grain size analyses are shown on Figures 1 and 2 in the preceding chapter. Slug test and grain size analysis results are included in Appendix A, summarized in Tables 3 and 4, and illustrated graphically in Figures 4 and 5.

TABLE 3 - SUMMARY OF SLUG TEST RESULTS

Well Number	Screen Elevation (fasl)	# of Tests	K (ft/min)	K_{ave} (ft/min)
iw2	1012.2-1018.8	2	0.015-0.027	0.021
iw4	1012.9-1019.8	1	0.018	0.018
dp1	1013.3-1016.0	2	0.023-0.024	0.024
iw12	1014.4-1019.1	4	0.022-0.026	0.024
dp2	1014.8-1017.7	2	0.021	0.021
dp4	1015.3-1018.1	2	0.011-0.015	0.013
dp3	1015.7-1018.4	1	0.030	0.030
iw1	1022.5-1028.8	1	0.035	0.035
iw11	1024.4-1029.1	2	0.032-0.036	0.034
iw9	1024.4-1029.1	2	0.033-0.038	0.036
vb2	1029.4-1032.4	2	0.015-0.018	0.017
iw7	1033.4-1034.8	2	0.012-0.018	0.015
iw8	1033.5-1034.9	2	0.020-0.027	0.024

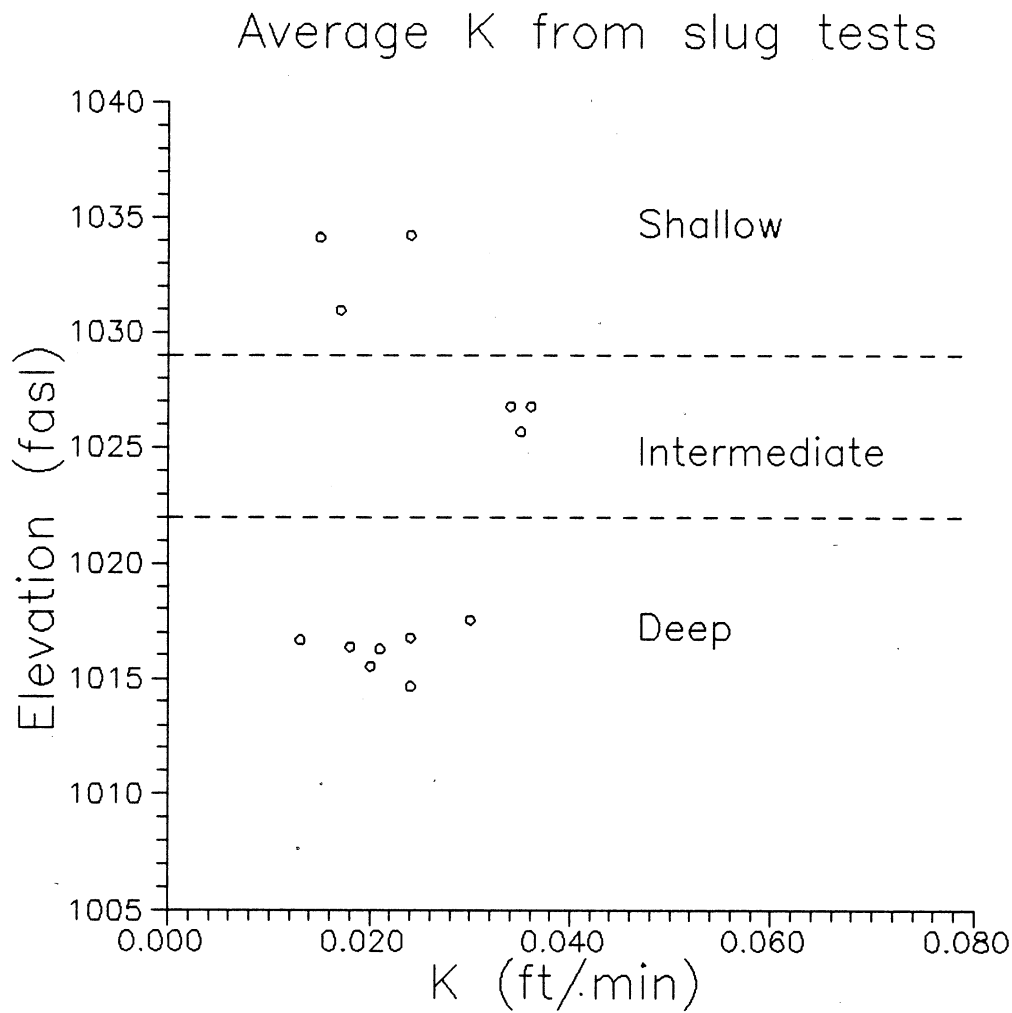


Figure 4 - Average hydraulic conductivity determined from slug tests, plotted versus the midpoint of the well screen. Screen lengths ranged from 1.4 to 6.9 ft. Also shown are approximate boundaries between 3 hydraulic conductivity zones.

TABLE 4 - SUMMARY OF GRAIN SIZE ANALYSES

Well Number	Elevation (ft)	D10 (mm)	D50 (mm)	σ (ϕ units)
iw3	1009.0	0.06	0.13	0.65
iw2	1013.9	0.13	0.22	0.48
iw4	1013.2	0.07	0.18	0.82
iw12	1014.0	0.09	0.17	0.52
dp2	1014.0	0.13	0.22	0.43
dp1	1014.0	0.11	0.22	0.58
dp3	1015.0	0.15	0.22	0.38
dp4	1015.0	0.09	0.22	0.63
dp2	1023.2	0.18	0.25	0.40
dp1	1023.2	0.18	0.25	0.40
m11	1024.0	0.17	0.26	0.48
dp3	1024.0	0.15	0.24	0.43
wt26	1026.0	0.18	0.25	0.29
wt2	1027.9	0.17	0.27	0.43
dp1	1029.7	0.18	0.25	0.35
wt24	1029.5	0.14	0.24	0.45
vb2	1031.6	0.14	0.22	0.35
wt1	1031.7	0.17	0.25	0.43
m11	1032.0	0.15	0.27	0.69
vb2	1032.5	0.18	0.25	0.43
dp1	1033.2	0.17	0.29	0.74
vb2	1034.2	0.24	0.47	0.59
wt2	1035.8	0.19	0.28	0.35
wt8	1036.0	0.18	0.29	0.63

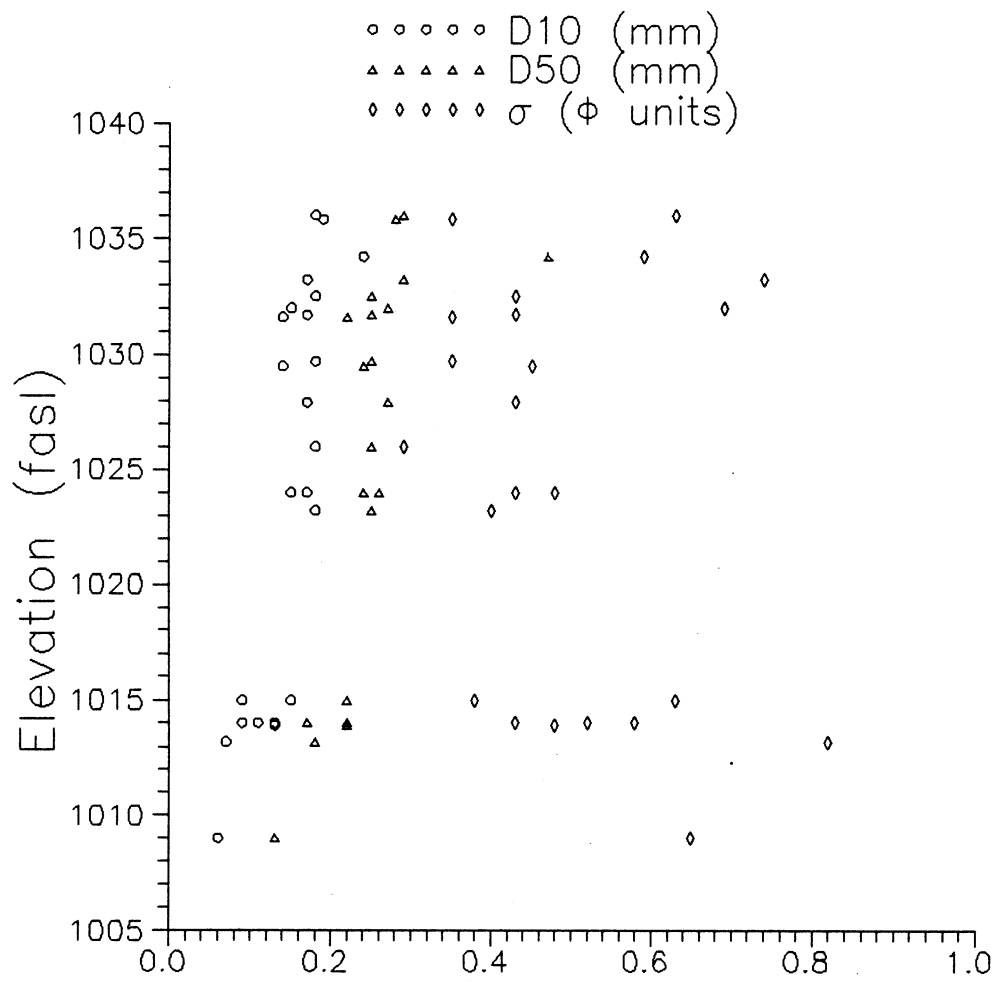


Figure 5 - Grain size distribution parameters plotted versus sample elevation.

On the basis of slug test results, the aquifer can be divided into the three zones that appear to be relatively continuous over the area tested. Approximate depth ranges of the zones are indicated on Figure 4. The deep zone, spanning elevations of approximately 1012 - 1022 feet above sea level (fasl) has hydraulic conductivities in the range of 0.011 - 0.030 ft/min. A middle zone, from approximately 1022 - 1029 fasl, has higher conductivities in the range of 0.033 to 0.038 ft/min. The shallow zone, above 1029 fasl, has conductivities in the range of 0.012 to 0.026 ft/min, similar to those of the deep zone. These three zones also correspond to three distinct velocity zones inferred from results of the 1989 tracer experiment. Observed velocities in the shallow zone were approximately 1 ft/day while velocities in the middle and deep zones fell in the ranges of 0.6-0.8 ft/day and 0.4-0.5 ft/day respectively. The increase in velocity from the deep zone to the middle zone is consistent with the measured increase in hydraulic conductivity. The further increase in velocity from the middle zone to the shallow zone, however, is not consistent with the measured hydraulic conductivity trends and must be explained by an increase in horizontal gradients near the water table.

The grain size parameters illustrated on Figure 5 do not show clear evidence of the three zones identified on the basis of slug test analyses. A variety of correlations were attempted between grain size distribution parameters and the values of hydraulic conductivity obtained from slug tests. The mean grain size D50 and the 10% finer size D10, which is frequently considered an "effective grain size" for estimates of hydraulic conductivity (Fetter, 1988), both show trends of slight decreases with increasing depth in Figure 5. The standard deviation, σ , has high values in

both the shallow and deep zones but is somewhat lower values in the intermediate zone. Because hydraulic conductivity is expected to increase with better sorting of unconsolidated sediments, this trend is qualitatively consistent with the observed variation in hydraulic conductivity from slug tests. Figure 6 shows average hydraulic conductivities from slug tests along with hydraulic conductivities predicted by two grain size correlation models. The model of Hazen (1893) assumes that hydraulic conductivity is proportional to the square of the effective grain size D_{10} . Masch and Denny (1966) generated a series of curves relating hydraulic conductivity to mean grain size, D_{50} , and the standard deviation, σ . It can be seen that the slug test values generally fall between the predictions of these two models. As shown in Figure 7, however, the Masch and Denny model provides a reasonable match to the relative trends in the slug test data when it is scaled by a factor of 4. This suggests that a scaled version of the Masch and Denny model could allow for detailed mapping of hydraulic conductivity variations at the field site using grain size analyses.

The systematic scaling between the slug test measurements and the Masch and Denny model may result from the fact that Masch and Denny used repacked, and hence relatively compacted, samples for their permeability measurements. It may also be a reflection of the "scale effect" of hydraulic conductivity that has been noted by other workers (e.g. Bradbury and Muldoon, 1988). The results obtained in this study, nevertheless, indicate that grain size distribution parameters can be related to hydraulic conductivity and can therefore be used as a means to quantify the distribution of physical transport properties which control contaminant migration.

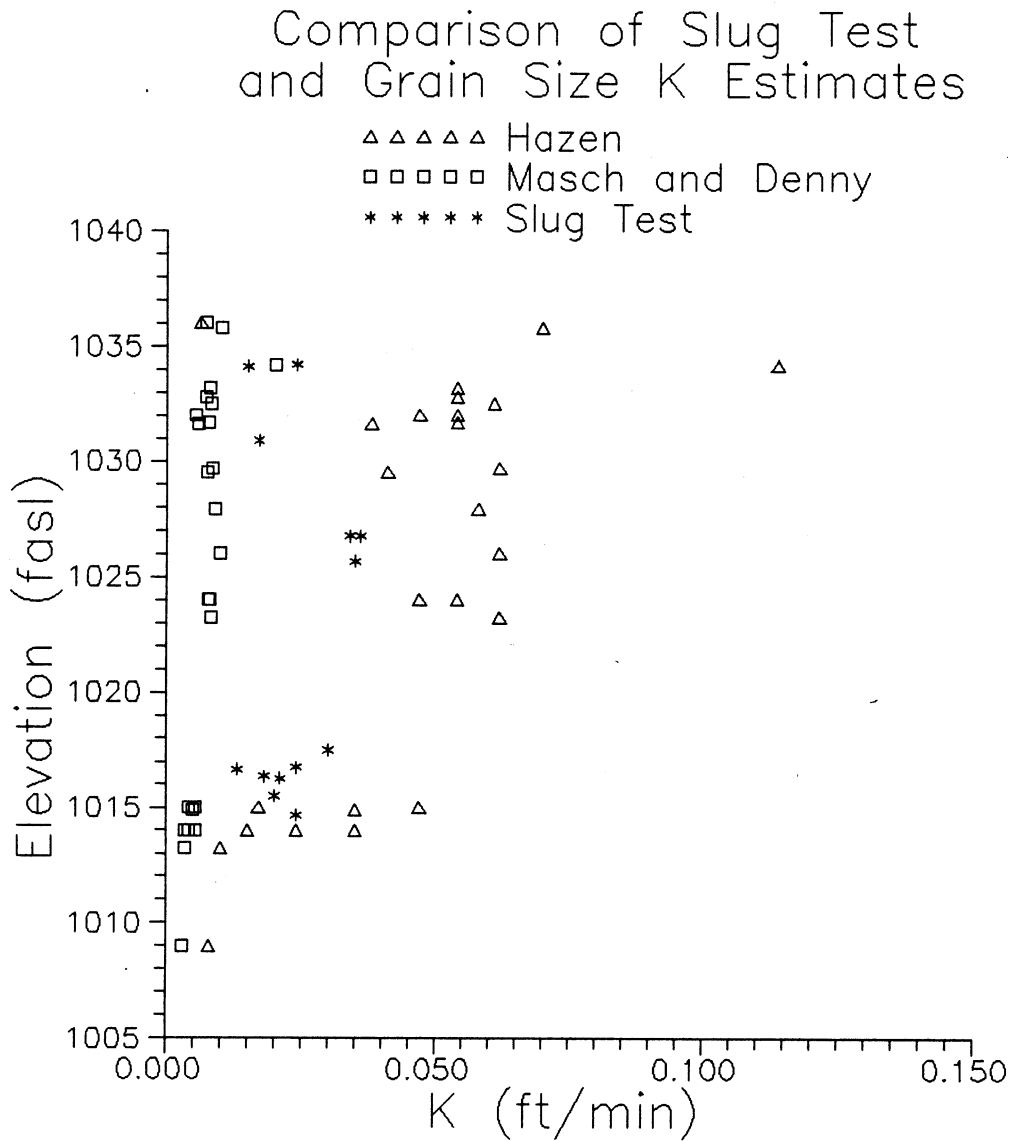


Figure 6 - Hydraulic conductivity predicted on the basis of grain size distribution using the models of Hazen (1893) and Masch and Denny (1966). Also shown are hydraulic conductivity values measured by slug tests.

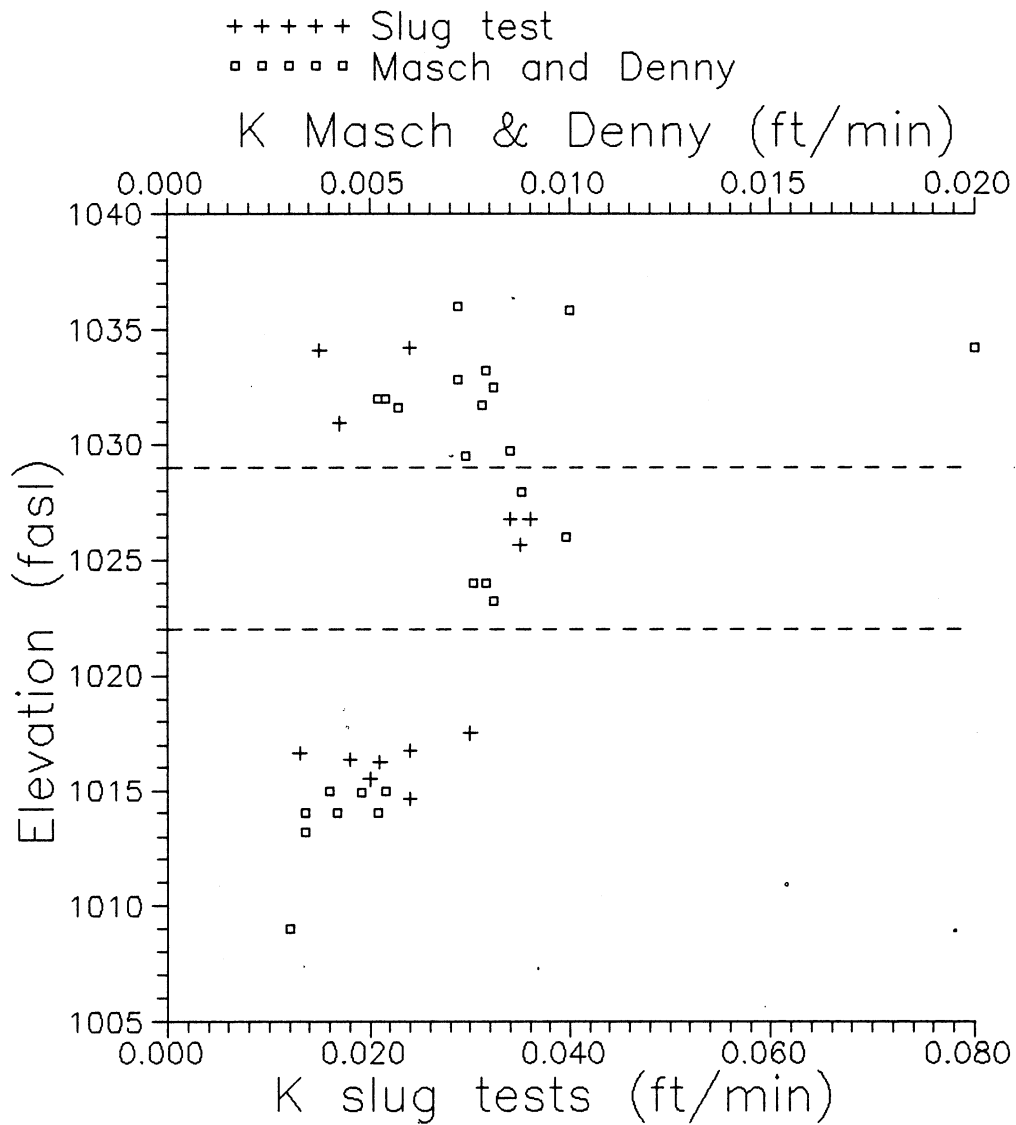


Figure 7 - Scaling between Masch and Denny predictions and measured hydraulic conductivities from slug tests. A good match is obtained when the hydraulic conductivity obtained from the Masch and Denny correlation multiplied by a factor of 4 is compared to the slug test values. Also shown are approximate boundaries between 3 hydraulic conductivity zones.

The extremes of hydraulic conductivity predicted on the basis of a scaled Masch and Denny model can be used to estimate the anisotropy ratio of the aquifer. Assuming an aquifer composed of two equal layers, one with a hydraulic conductivity of 0.080 ft/min and the other with a hydraulic conductivity of 0.012 ft/min, the anisotropy ratio computed according to methods outlined in Domenico and Schwartz (1990, pg. 69) is 2.2. If these are the true extremes of hydraulic conductivity in the aquifer, this would be a maximum estimate. Any combinations of layers with hydraulic conductivities intermediate to the two extremes, or any combination of layers with unequal thickness, would yield a lower anisotropy ratio. The actual anisotropy ratio could be higher, however, if the range of hydraulic conductivities is greater than that estimated from the available grain size analyses.

2. Chemical heterogeneity

The three zones identified on the basis of hydraulic conductivity variations and tracer cloud velocities also appear to have distinct chemical signatures. Results of chemical analyses for 1990 and 1991 samples, collected from the locations shown in Figure 8, are included in Appendix B. Figures 9 through 14 illustrate vertical profiles of specific conductance, pH, calcium, calcium/magnesium ratio, iron and manganese from 1 multilevel (ml7) located west of the ditch and 5 multilevels and miniature multilevels (mm7, mm20, ml8, ml9, and mm38) located east of the ditch.

The shallowest groundwater sampled at each distance from the ditch has the highest specific conductance. It also has the highest dissolved oxygen concentration, up to approximately 2 ppm, and generally the lowest pH. Specific conductance decreases from values of approximately 300 micromhos/cm

Chemical Sampling Locations

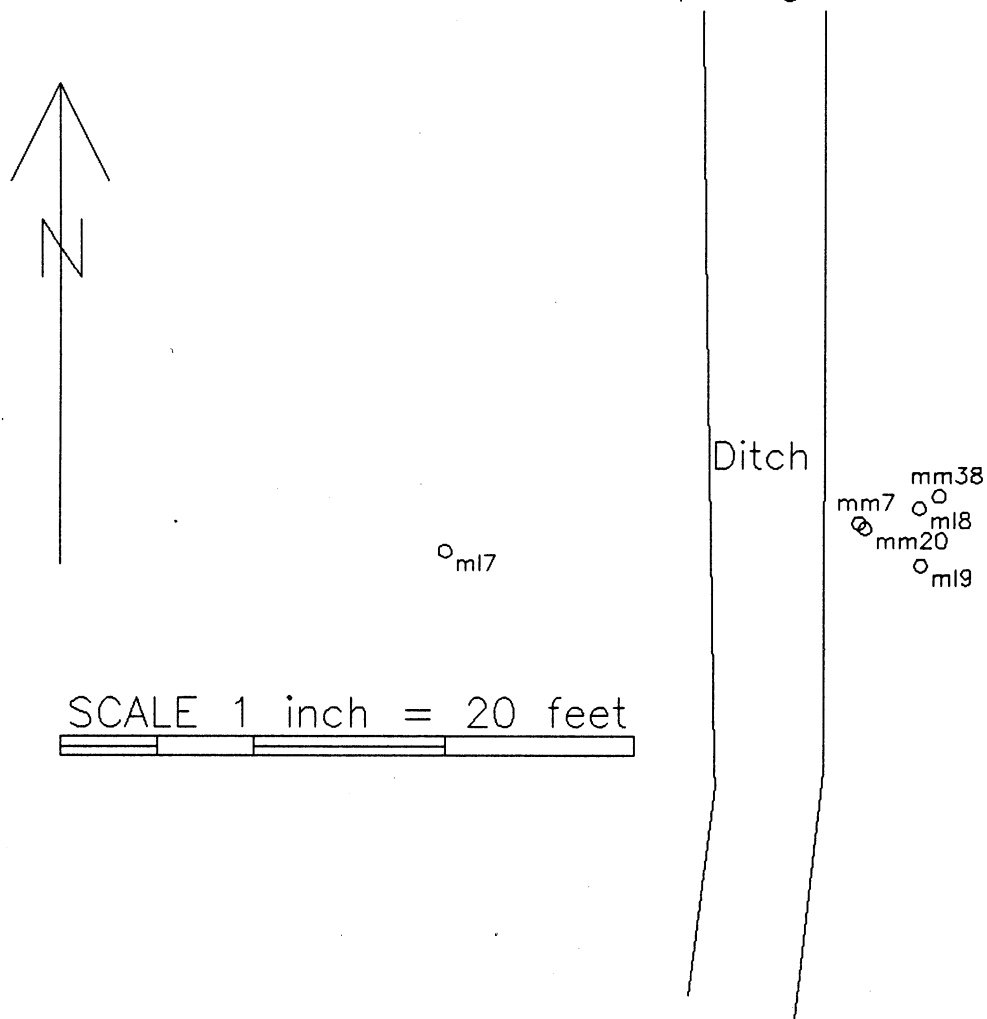


Figure 8 - Locations at which samples were collected for chemical analyses.

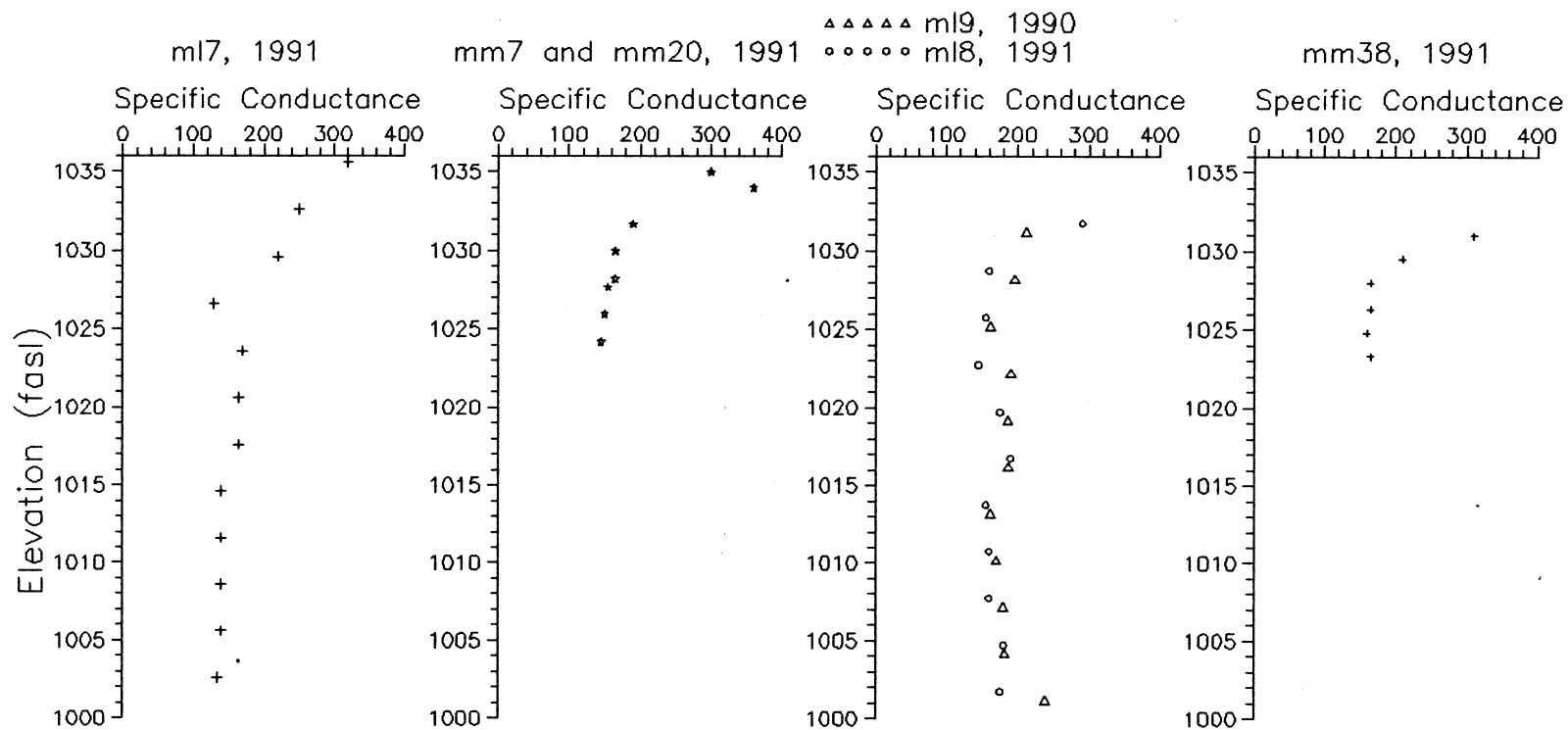


Figure 9 - Profiles of specific conductance in micromhos/cm (μS).

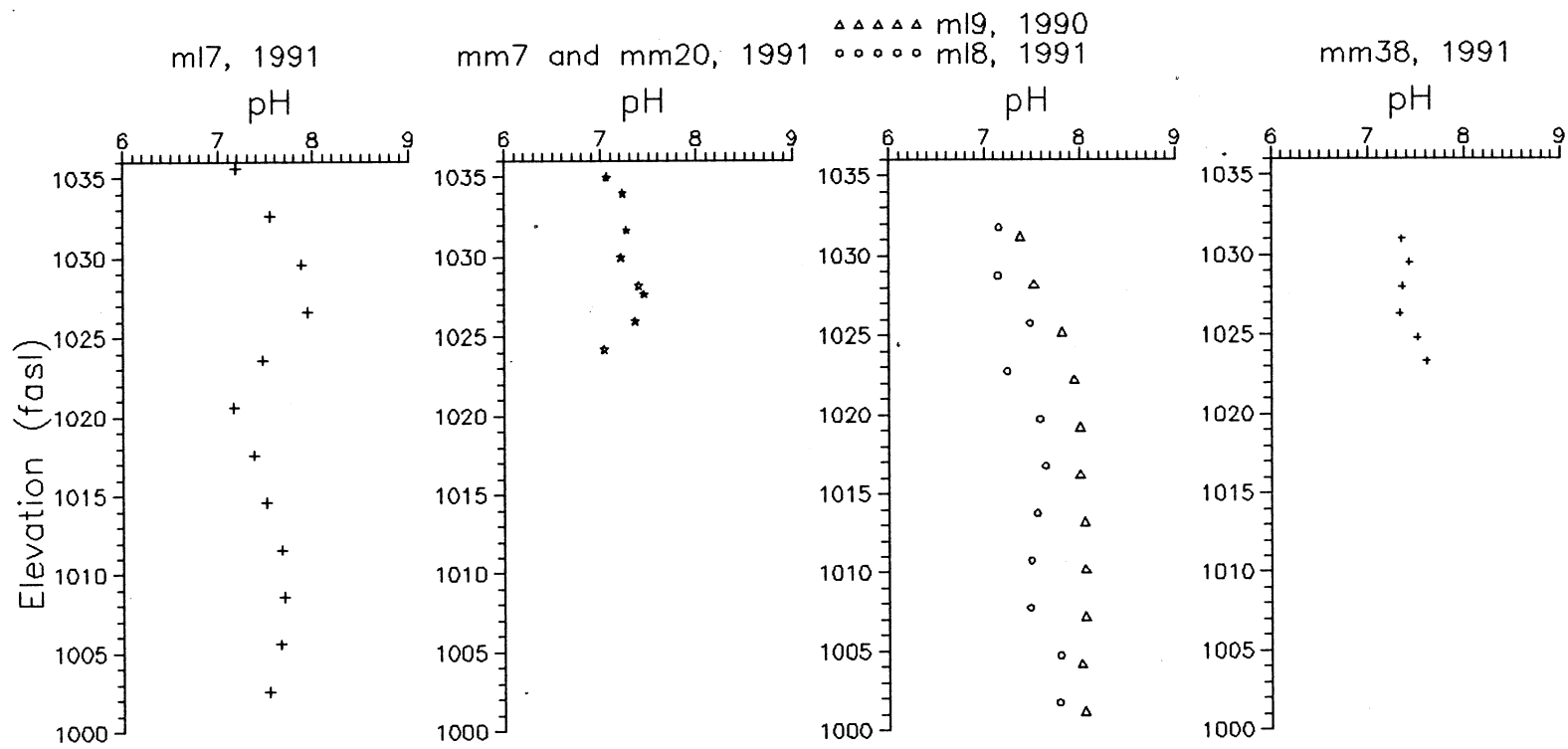


Figure 10 - Profiles of pH.

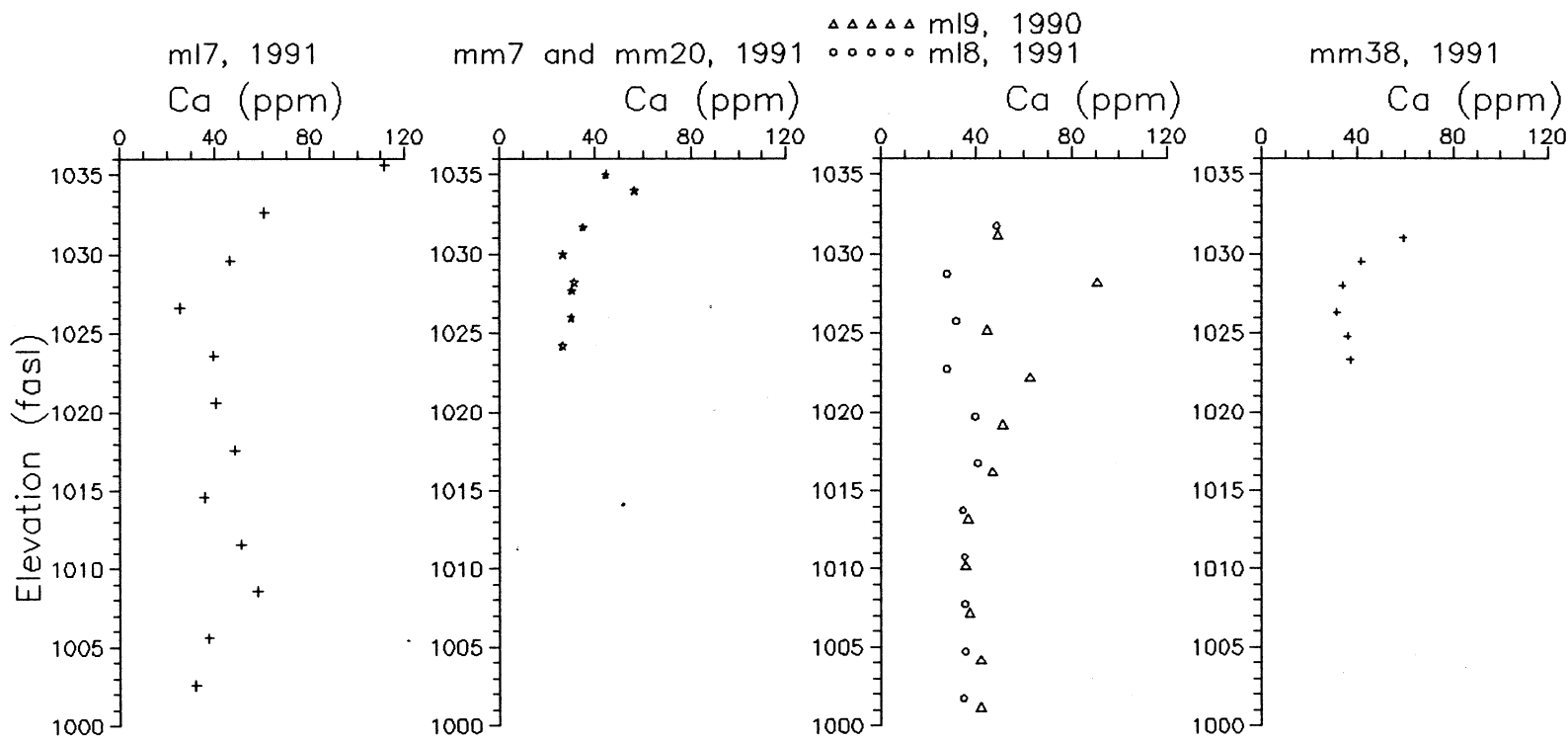


Figure 11 - Profiles of calcium concentration (ppm).

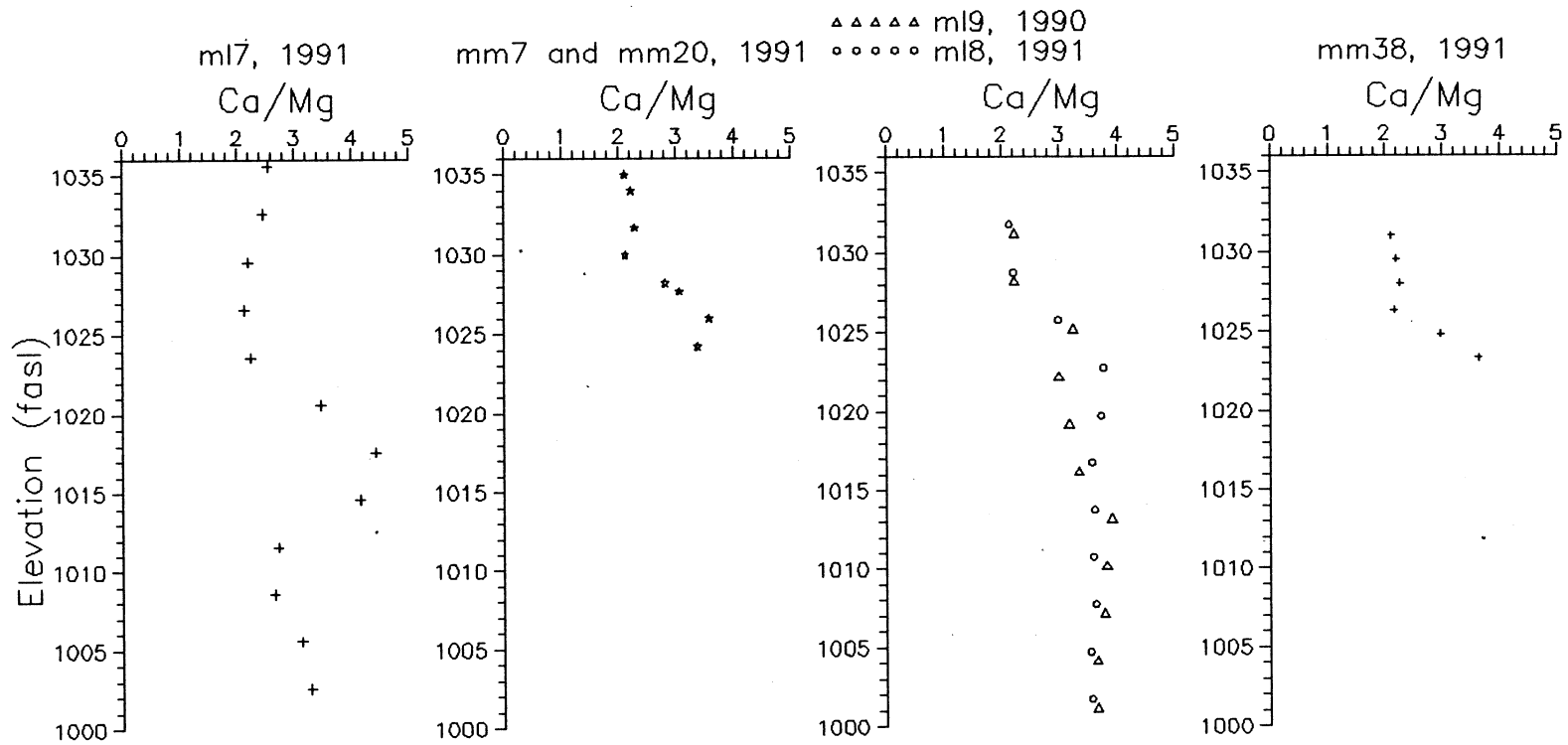


Figure 12 - Profiles of the ratio of calcium concentration (ppm) to magnesium concentration (ppm).

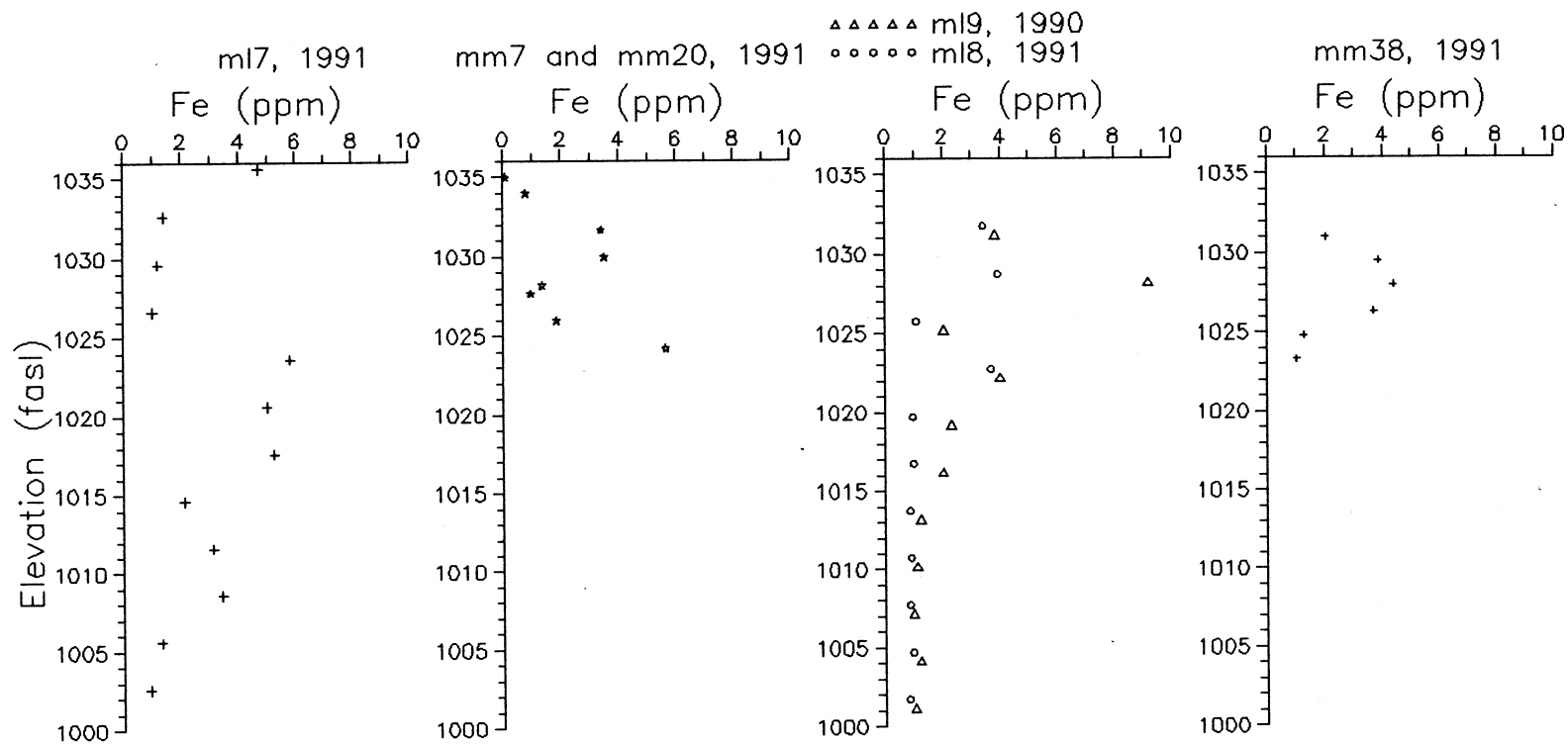


Figure 13 - Profiles of iron concentration (ppm).

Location	Depth (m)	Description	As ppm	Cu ppm	Pb ppm	Zn ppm	Mo ppm	Ni ppm	Co ppm	Sr ppm	Mn ppm	Cr ppm	S %	Fe %	Al %	Mg %	Ca %	Na %	K %
SB-1	21.64	dolomite, mineralized veins	73	145	21	13	6	81	46	39	715	26	3.95	4.45	0.08	8.39	13.93	0.04	0.06
MW-1	22.25	dolomite, mineralized veins	23	11	3	7	3	24	9	67	1009	20	1.05	1.71	0.08	10.05	16.59	0.03	0.07
MW-1	23.16	mineralized zone, purple	161	109	53	32	37	154	113	5	387	434	0.02	12.67	0.04	0.04	0.04	0.01	0.01
MW-1	23.47	sandstone, white to gray-brown	1.8	7	7	6	38	14	6	5	153	628	<0.01	2.27	0.02	0.02	0.16	<0.01	0.01
MW-1	23.93	mineralized nodule, purple	510	83	585	56	53	234	196	9	168	632	0.5	21.4	<0.01	0.06	0.04	<0.01	<0.01
MW-2	23.99	sandstone, white	16	7	12	7	32	23	10	18	206	513	0.03	1.54	0.03	2.07	3.43	0.01	0.01
MW-2	24.02	sandstone, orange	13	10	12	55	47	35	10	5	138	764	<0.01	2.55	0.02	0.11	0.18	<0.01	0.01
MW-2	24.14	sandstone, white	2.8	8	7	5	31	12	3	3	56	502	<0.01	0.72	0.02	<0.01	0.02	<0.01	0.01
MW-2	24.51	sand, light gray	8	149	10	61	10	16	6	32	412	107	0.24	1.11	0.15	7.85	11.62	0.03	0.05
MW-2	23.96	SCH	585	129	442	85	29	378	241	20	681	241	17.9	20	0.11	0.25	0.77	0.01	0.02
MW-2	25.3 - 26.5*	sandstone, white	1.8	16	4	10	15	6	2	9	135	232	0.1	0.57	0.04	1.8	3.27	0.01	0.02
MW-2	28.3 - 29.6*	sandstone	<1	3	<2	<1	15	4	2	3	48	218	0.04	0.45	0.02	0.38	0.75	0.01	<0.01
MW-2	29.9 - 31.1*	sandstone	1.9	28	2	15	14	7	3	6	48	208	0.03	0.53	0.02	0.25	0.5	<0.01	0.01
MW-2	31.4 - 32.6*	sandstone	4	13	<2	<1	15	5	3	4	34	214	0.16	0.68	0.03	0.1	0.19	0.01	0.04
MW-2	32.9 - 34.1*	sandstone	<1	11	<2	<1	16	7	3	2	33	243	0.11	0.47	0.02	0.04	0.07	0.01	0.02
MW-2	34.1 - 34.7*	sandstone, muddy matrix	12	67	8	3	17	66	38	47	134	237	0.58	1.37	1.32	1.37	2.53	0.02	0.85

* indicates sample was from drill cuttings and is likely to have more mixing of materials than samples selected from core

date	well id	water type	As µg/L diss.	Mo µg/L diss.	Ni µg/L diss.	Zn µg/L diss.	Co µg/L diss.	Mn µg/L diss.	Ca mg/L diss.	Mg mg/L diss.	Na mg/L diss.	K mg/L diss.	Fe mg/L diss.	Cl mg/L total	SO4 mg/L total	Alk as CaCO3 mg/L total	NO3 +NO2 mg/L total	organic carbon mg/L diss.	P mg/L total	Sulfide µg/L total
5/3/01	MW-1	aquifer	<3.7	<1.3	2.0Q	12	0.94Q	45	45	41	9.8	1.7	0.120	3.3	14	270	<0.015			
8/2/01	MW-1	borehole	15.5																	
8/24/01	MW-1	aquifer	5.8						46	41	11	1.4	<0.25	2.9	14	280			<0.1	
8/31/01	MW-1	borehole	22						38	40	14	1.6	0.970	3.2	15	280			<0.1	
9/11/01	MW-1	aquifer	<4.4										0.011		13					
9/27/01	MW-1	borehole	10										1.500		16			0.816	0.054	
9/27/01	MW-1	aquifer	<4.4										0.190		15			0.659	0.036	
1/21/02	MW-1	borehole	15	2.9	9.9	11	0.55	60					2.900		24					
1/21/02	MW-1	aquifer	2.4	<0.52	1.3	5.8	0.60	47					0.140		33					
4/1/02	MW-1	aquifer	6.4		2.2	12	0.27	46	42	36	8.8	1.7	0.470	4.0	18	280				
5/3/01	MW-2	aquifer	<3.7	5.0	3.6Q	11	6.3	56	60	41	14	3	0.059	5.8	52	270	<0.015			
4/1/02	MW-2-1	aquifer	21		0.75	5.6	0.22	22	36	40	9.8	1.6	0.850	5.2	19	270				
4/1/02	MW-2-2	aquifer	23		0.39	5.2	0.24	22	38	40	9.5	1.5	0.710	5.4	18	280				
4/1/02	MW-2-3	aquifer	7.2		1.2	4.1	0.54	85	55	36	7.6	2.2	0.890	2.5	16	310				
4/1/02	MW-2-4	aquifer	12						64	37	6.7	2.4	1.400	2.4	17	350				

"Q" indicates result was greater than the detection limit but less than the limit of quantification
results reported as dissolved were filtered to 0.45 microns; total indicates sample was not filtered

(μS) to less than 200 micromhos/cm over a vertical distance of about 2 ft. Calcium concentrations are somewhat variable within this zone of decreasing specific conductance. This is particularly noticeable comparing samples collected in 1990 from ml9 to samples collected in 1991 from ml8. Despite this variability, the ratios of calcium to magnesium (ppm/ppm) for samples from the shallowest part of the aquifer are all quite close to 2. For the samples from ml7, on the west side of the ditch, iron concentrations are relatively high at the water table 1036 fasl) but then drop to below 2 ppm in the shallow zone of low calcium/magnesium (Ca/Mg) ratio. For samples from the east side of the ditch, iron concentrations are low near the water table but rise to approximately 4 ppm within the shallow zone of uniform Ca/Mg ratio. On both sides of the ditch, manganese concentrations reach a maximum between elevations of 1025 and 1030 fasl, generally near the base of the uniform Ca/Mg zone.

At some depth below the water table, the calcium/magnesium ratio begins to increase steadily up to a value of approximately 4. This transition in Ca/Mg ratio occurs over a vertical interval of approximately 5 ft. At ml8 and ml9, the elevation range spanned by this transition is 1023 to 1028 fasl, which corresponds fairly closely to the middle hydraulic conductivity zone, from 1022 to 1029 fasl, identified from hydraulic conductivity testing. At other locations to the east of the ditch, the transition zone is shallower in mm7 and mm20, the miniature multilevels located closer to the ditch, and it is slightly deeper in mm38 which is several feet farther from the ditch than ml8 and ml9. This geometry suggests rising flow lines as groundwater approaches the ditch, consistent with the flow affected by a

ditch capture zone. In ml7 on the west side of the ditch, the Ca/Mg transition occurs considerably deeper, between 1017 and 1022 fasl. On this down-gradient side of the ditch, flow lines would be expected to move downward as recharge is added to the aquifer. The observed increase in transition zone depth at this location is consistent with downward moving flow lines.

Within the Ca/Mg transition zone, pH shows some variability with depth, generally increasing with depth near the top of the transition zone but then decreasing slightly near the base of the zone. Specific conductance is fairly constant within this zone. The dissolved oxygen is lower than in the shallow zone, decreasing to 1 ppm or less. On the west side of the ditch, iron concentrations are relatively high throughout this zone. To the east, iron concentrations are low at the top of the zone, but appear to increase steadily with depth and in some cases reach higher concentrations than those observed in the shallow zone. The low dissolved oxygen concentrations and high concentrations of dissolved iron are indicative of moderately reducing conditions. In contrast to iron, manganese concentrations are considerably lower than in the shallow zone and remain low throughout this zone. Given alkalinities on the order of 100 mg/L in the aquifer, diagrams of Mn-CO₂ systems in the text by Garrels and Christ (1965) indicate that manganese concentrations in solution may be limited by the solubility of manganese carbonate minerals.

To the east of the ditch, the base of the transition zone described above varies from an elevation of approximately 1026 fasl at mm7 and mm20 to approximately 1023 fasl at ml8 and ml9. The deepest point in mm38, at 1023.3 fasl, also appears to be near the base of the transition zone based

on the measured Ca/Mg ratio. Below the transition zone, calcium concentrations are approximately 40 ppm and Ca/Mg ratios are relatively constant in multilevels ml8 and ml9, which extend below the base of the unconfined aquifer at approximately 1005 fasl. Specific conductance in the deep portion of the aquifer is approximately 200 μ S. The pH tends to increase very gradually with depth, and dissolved oxygen decreases to near or below the detection limit of field electrode (0.1 ppm). Iron and manganese concentrations are uniformly low, consistent with low solubility of iron and manganese minerals under more strongly reducing and or higher pH conditions (Garrels and Christ, 1965).

To the west of the ditch at ml7, the base of the transition zone defined by increasing Ca/Mg ratio is at approximately 1017 fasl. The Ca/Mg ratio exceeds 4 in samples from 1014.6 and 1017.6 fasl, but then drops back to values of less than 3 in the two deepest points above the base of the unconfined aquifer at 1005 fasl. Calcium shows more variability near the base of the aquifer at this site compared to ml8 and ml9 east of the ditch. Iron decreases significantly between 1017.6 and 1014.6 fasl but it remains above 2 ppm, considerably higher than the concentrations in ml8 and ml9 at corresponding elevations. Manganese concentrations show an increase near the base of the aquifer, between 1006 and 1012 fasl.

This chemical zonation is likely to reflect, in part, the chemical evolution of groundwater during predominantly horizontal flow from recharge areas, which are located at increasing distances from the field site for samples obtained from increasing depths in the aquifer. The shallowest groundwater is probably from local recharge while the deepest water may come from a considerable distance from the site. However, the relatively abrupt

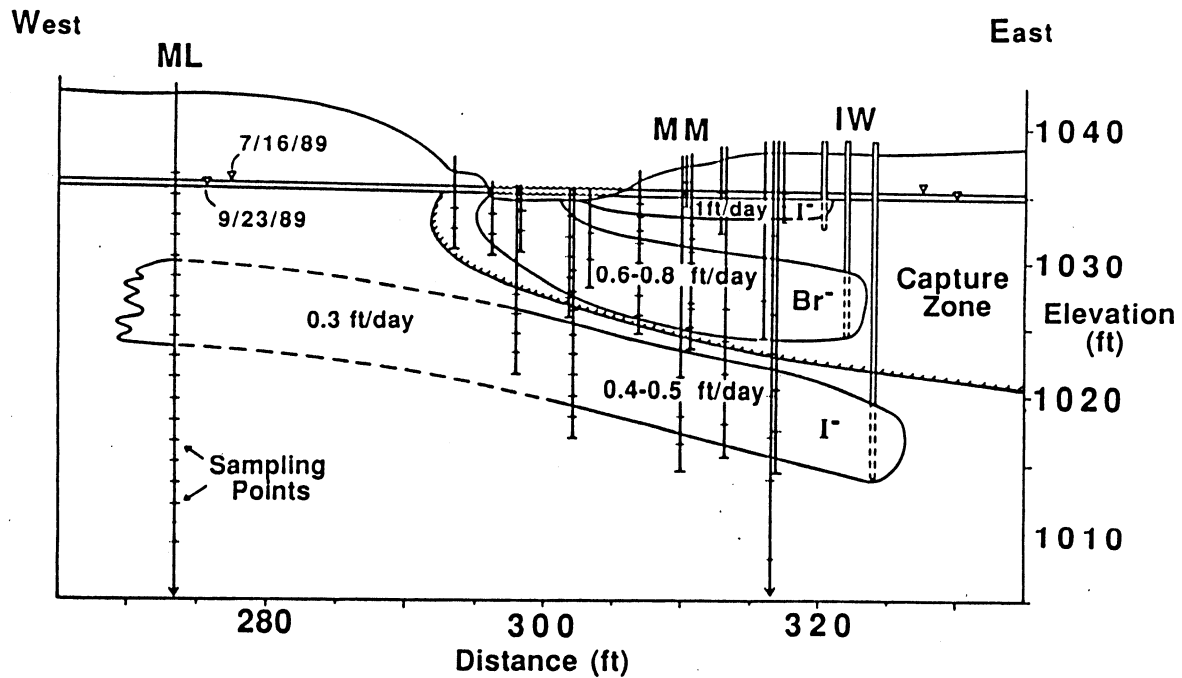
changes in chemical characteristics between zones and possibly within zones, as indicated by cation ratios, specific conductance, iron and manganese, are also consistent with flow segregation that could result from hydraulic conductivity contrasts. Thus, the chemical signatures provide independent evidence of the importance of stratification of hydraulic conductivity in controlling contaminant migration in sand aquifers of the central sand plain. Of the parameters examined, the Ca/Mg ratio appears to provide a relatively simple means of identifying major stratification and may also be useful as a "natural tracer" for mapping flow lines at the field site or elsewhere within the sand plains.

B. Tracer Experiments

1. Conservative tracer experiment

The conservative tracer experiment conducted during the summer and fall of 1990 defined a capture zone that extends to considerably greater depth than that observed in the summer of 1989. Tracer injected at both depths discharged to the ditch. Figure 15 compares the tracer paths from the 1989 and 1990 experiments. In 1990, both clouds showed a much larger component of vertical flow compared to 1989. The capture depth for the 1990 experiment was at least 24 feet below the water table. The dramatic variation in tracer flow paths between the two years appears to result in part from transient flow conditions. Precipitation data and water level measurements indicate larger than normal recharge events in July and August 1990. In addition to generating a deeper capture zone, conditions during the summer of 1990 also generated higher groundwater velocities for both the shallow

Flow Path of Tracer, 1989



Flow Path of Tracer, 1990

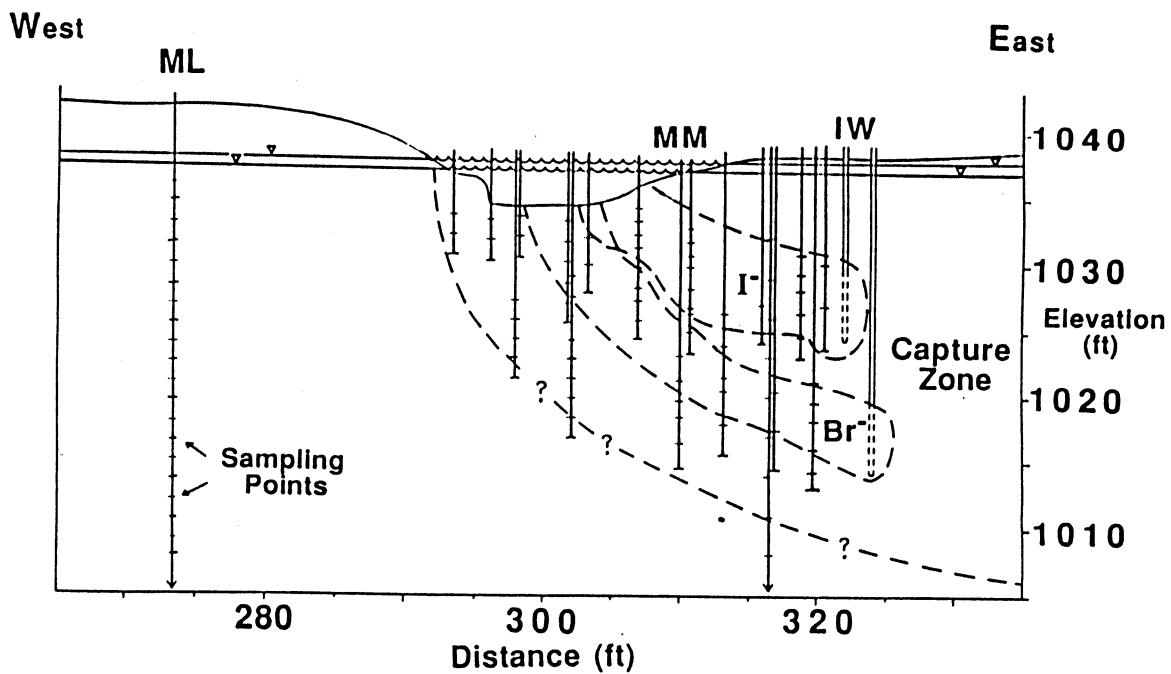


Figure 15 - Comparison of tracer paths for 1989 and 1990 tracer tests.

and deep tracers. A comparison of the observed capture depth for this experiment and model predictions is included in the section on model evaluation.

2. Reactive tracer experiment

The nitrate experiment initiated in June of 1991 was designed to measure in-situ rates of denitrification in the shallow portion of the aquifer. The total path of the conservative bromide tracer in this experiment is shown in Figure 16. Breakthrough curves for monitoring points at mm57 and mm58, at distances of 3 and 6 feet respectively from the injection well, are shown in Figures 17 and 18. Concentrations have been normalized by dividing by the input concentrations of 47.8 mg/L for bromide and 12.3 mg/L nitrate-nitrogen. In each miniature multilevel, the sampling points are separated by a vertical distance of 1 foot. The deepest point at mm57 (mm57-1) is at an elevation of 1024.75 ft above sea level (fasl) while the deepest point at mm58 (mm58-1) is at an elevation of 1025.63 fasl.

The shapes in corresponding points in the two miniature multilevels (e.g. mm57-1 and mm58-1) are quite similar in all cases when one accounts for the fact that the breakthrough curves would be expected to show more spreading due to dispersion at greater distances from the injection well. Comparing shapes and areas under the bromide curves for points at mm57 to curves for points at mm58, it appears that the vertical velocity and concentration distributions within the tracer cloud remain relatively constant over the 3 foot travel distance between these miniature multilevels. The narrow breakthrough curves at mm57-1 and mm58-1 and the low peak concentrations at mm57-7 and mm57-8 indicate that considerably less mass passed by

Tracer Test 1991

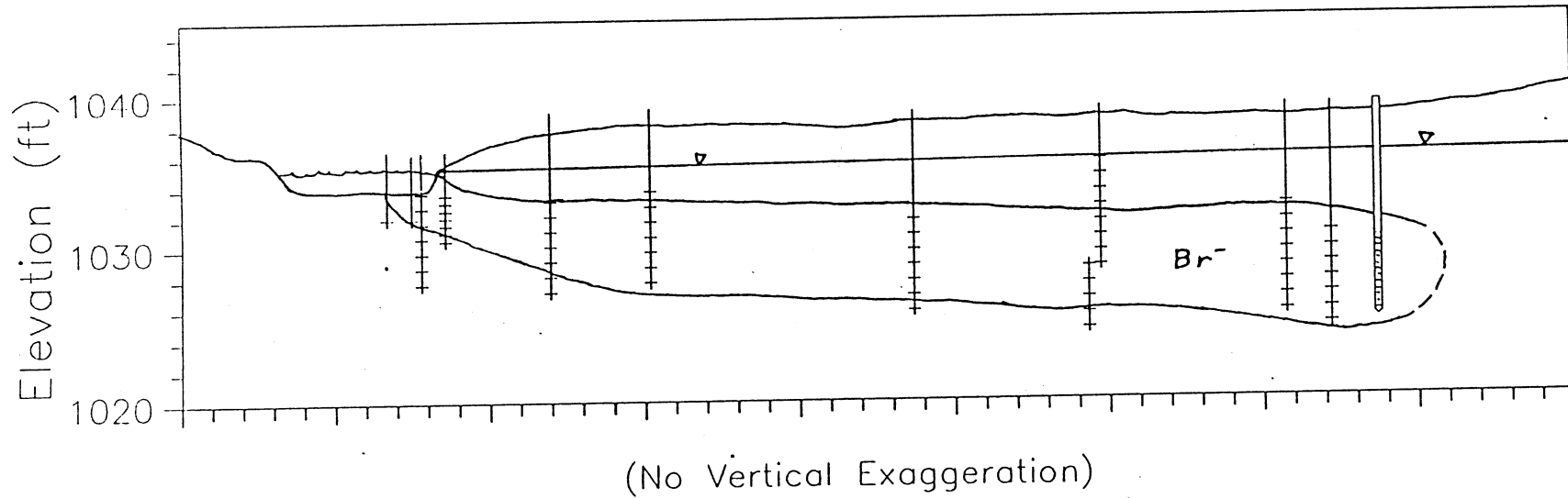


Figure 16 - Cross-section of total movement of the bromide cloud during the reactive tracer test of 1991.

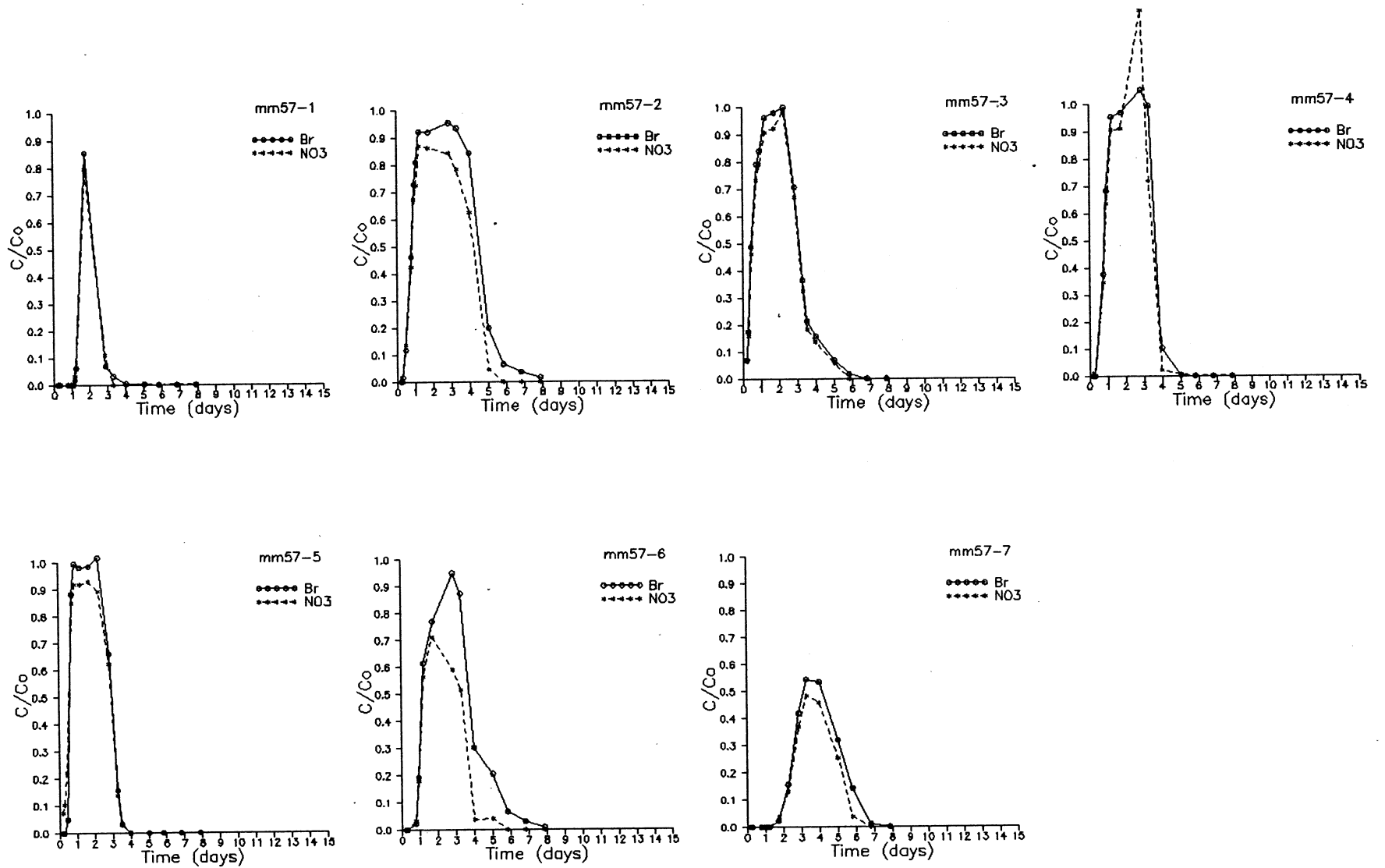


Figure 17 - Dimensionless breakthrough curves at mm57. Concentrations of bromide and nitrate are normalized to concentrations measured in the injected tracer solution.

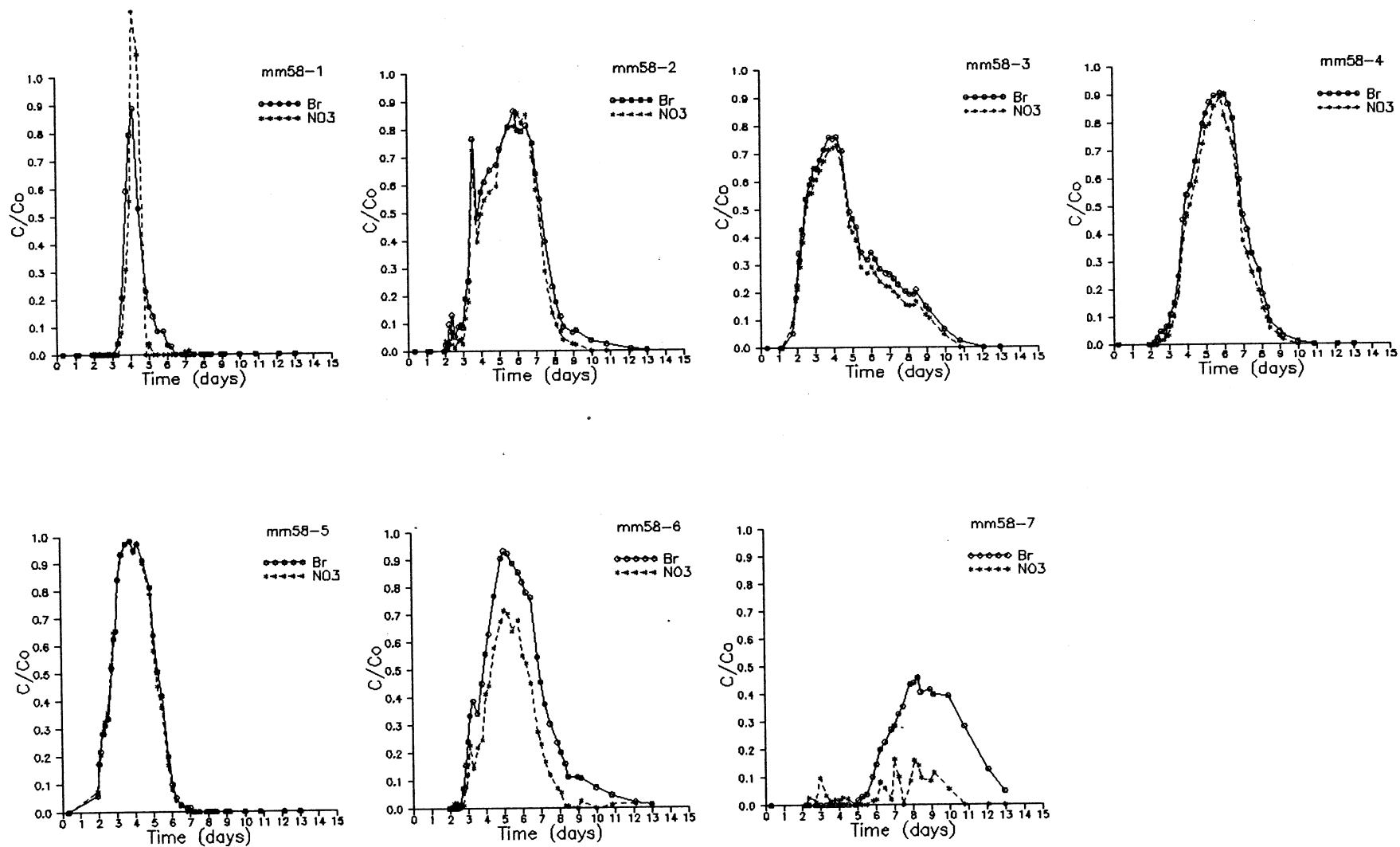


Figure 18 - Dimensionless breakthrough curves at mm58. Concentrations of bromide and nitrate are normalized to concentrations measured in the injected tracer solution.

the shallowest the deepest point at each location than by the intermediate points, suggesting that the shallowest and deepest points at each location are near the vertical limits of the tracer cloud. Given the elevation difference of 0.88 ft between mm57-1 and mm58-1, which is also the elevation difference between mm57-7 and mm58-7, it appears that the tracer cloud rose almost 0.9 ft as it travelled 3 feet in the horizontal direction between these two points.

One measurement of nitrate concentration at mm57-4 and two measurements at mm58-1 exceed the input concentration (normalized concentration greater than 1.0). These values are probably in error as a result of calibration errors for the ion-chromatograph at high concentrations. It is also possible that these samples might have been contaminated by measurement with the bromide electrode in the field, which can release potassium nitrate filling solution to the sample. Separate samples were collected for field and laboratory measurement, but a few samples intended for laboratory analysis by ion-chromatography were analyzed with the electrode by mistake during the first days of the experiment. Where this is known to have occurred, the nitrate analyses for these samples were deleted from the data base.

Based on the peak arrival times for bromide and nitrate at these two miniature multilevels, there is little evidence of retardation of the nitrate tracer relative to bromide. In the absence of retardation, it is possible to compare nitrate concentrations directly to the bromide concentrations to determine the extent of nitrate loss by processes such as denitrification. With the exception of the anomalous high nitrate measurements mentioned above, there is a general decrease in normalized nitrate concentration relative to the normalized bromide concentration, particularly

on the falling limbs of the breakthrough curves. Figure 19 illustrates this relative decrease in nitrate concentration for sampling points in mm57 and mm58, plotted as the ratio of normalized nitrate concentration to normalized bromide concentration on a logarithmic scale versus time on the arithmetic scale. A straight line with negative slope on this type of plot corresponds to a first-order (or pseudo-first-order) decay process, that is, a reaction that proceeds according to a rate law of the form

$$\frac{dC}{dt} = -k C \quad (1)$$

where C is the concentration and k is a rate constant with units of inverse time ($1/T$). The first-order rate constant k can be calculated from the slope of the line on this semilog plot. At both mm57 and mm58 there appears to be an initial lag time during which little loss of nitrate occurs. This lag time is approximately 2 days at mm57 and 4 days at mm58. Following the initial lag, nitrate loss is relatively steady and can be approximated as a first order process. A first-order rate constant of 0.0027/hr, which corresponds to a half-life of about 11 days, provides a reasonable fit to early time data, particularly in the intermediate sampling points, at both mm57 and mm58. For later time and particularly for sampling points in the shallowest portions of the tracer cloud, a much more rapid decrease in nitrate concentrations appears to occur, corresponding to a first-order rate constant of 0.019/day, or a half-life of 1.5 days.

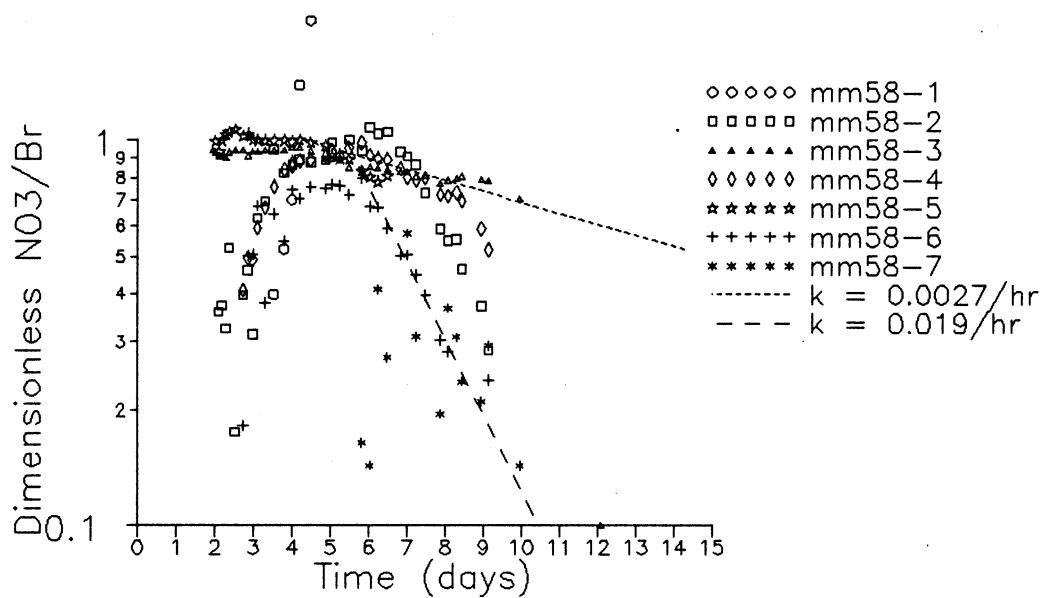
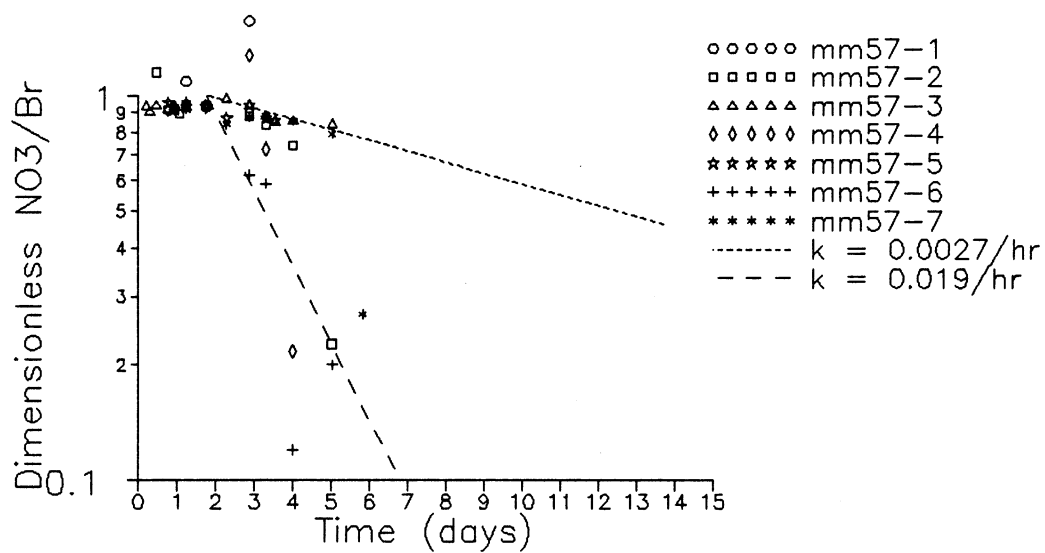


Figure 19 - Decrease in concentration of nitrate relative to bromide in mm57 and mm58, measured as $(C_{\text{NO}_3\text{-N}}/C_{0\text{NO}_3\text{-N}}) \div (C_{\text{Br}}/C_{0\text{Br}})$

Microbially mediated processes such as denitrification are frequently assumed to follow zero-order rather than first-order kinetics. A zero-order rate law has the form

$$\frac{dC}{dt} = -k \quad (2)$$

In this case the rate is independent of concentration and the rate constant has units of concentration/time (M/L³-T). Both first-order kinetics and zero-order kinetics are limiting cases of Monod kinetics which characterize enzyme or catalytic processes and has the rate law

$$\frac{dC}{dt} = -\frac{kXC}{K_s + C} \quad (3)$$

where k is a rate constant, X is a concentration of microorganisms and K_s is the "half-saturation constant". First-order kinetics corresponds to cases in which the substrate (nitrate in this case) is limiting, in other words K_s is much greater than C . Zero-order kinetics would apply if the substrate were abundant, i.e. $C \gg K_s$, in which case the size or activity of the microbial population, X , would be the limiting factor.

In order to test the hypothesis of zero-order kinetics, the nitrate concentrations were converted to nitrate "deficiencies" by subtracting the observed concentration from the theoretical concentration for a given time and sampling point that had been computed on the basis of the observed bromide concentration. For sampling points at mm57, this analysis produced the highly scattered plot shown in Figure 20a. The data from mm58-6 suggest a decay rate of 0.8 mg/L-day following zero-order kinetics during the rising

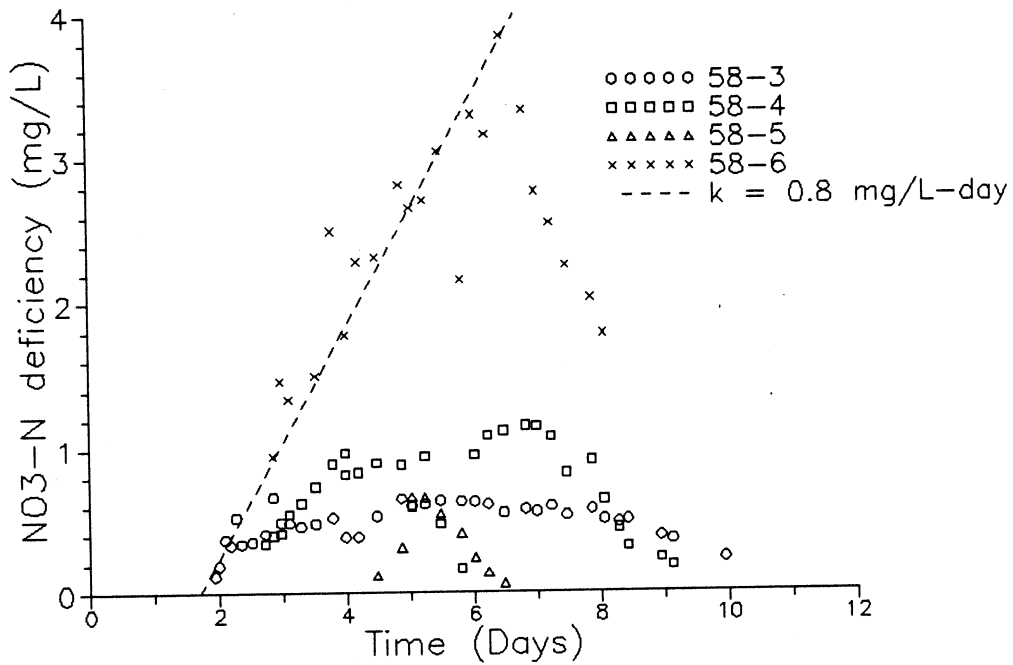
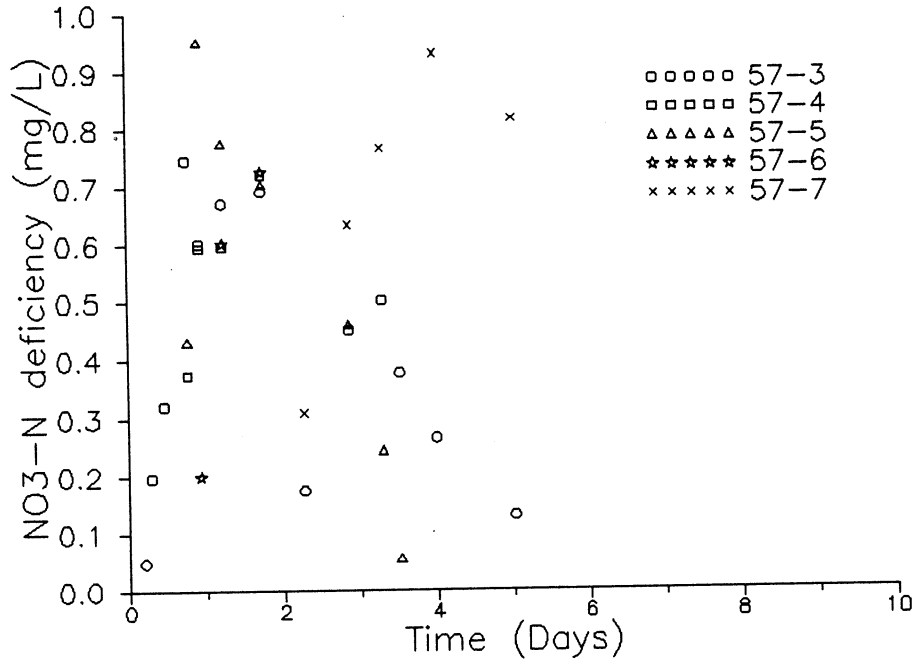


Figure 20 - Nitrate deficiencies at a) mm57 and b) mm58, measured as

$$[(C_{Br}/C_{0Br}) * C_{0NO3-N}] - C_{NO3-N}$$

limb of the breakthrough curve (see Figure 20b). This rate also appears to bound the data from other sampling points in mm58.

A conceptual model to explain the lag time and apparent switch from zero-order to first-order kinetics is as follows. When nitrate is first introduced to an aquifer with low background nitrate concentration, a finite acclimation period is required before the microbial population initiates denitrification. It may also have been necessary for excess dissolved oxygen introduced with the nitrate containing water (in this case the tracer solution) to be consumed before nitrate is utilized as an electron acceptor for microbially mediated redox reactions. Following this acclimation period, the microbial population is limited in size and denitrification follows zero-order kinetics. As the denitrifiers multiply in the aquifer, nitrate becomes limiting and the rate changes from the zero-order limit to the first-order limit of Monod kinetics.

By the time the bromide cloud reached mm61, at a distance of 18 feet from the injection well (corresponding to a travel time of approximately 12 days) no nitrate was detected during bromide breakthrough (see Figure 21). Assuming zero-order kinetics, this observation indicates a minimum denitrification rate of approximately 1 mg/L-day, which is slightly higher than the rate inferred from breakthrough data at mm58-6. This suggests accelerated rates of denitrification as the tracer cloud migrated through the aquifer and the denitrifiers became more active or abundant. The complete loss of nitrate within the tracer cloud was confirmed by breakthrough in mm64 at 30 feet from the injection well (also shown in Figure 21).

The zero-order denitrification rate of 1 mg/L-day is approximately twice the rate determined by Starr and Gillham (1989) for an anaerobic sandy

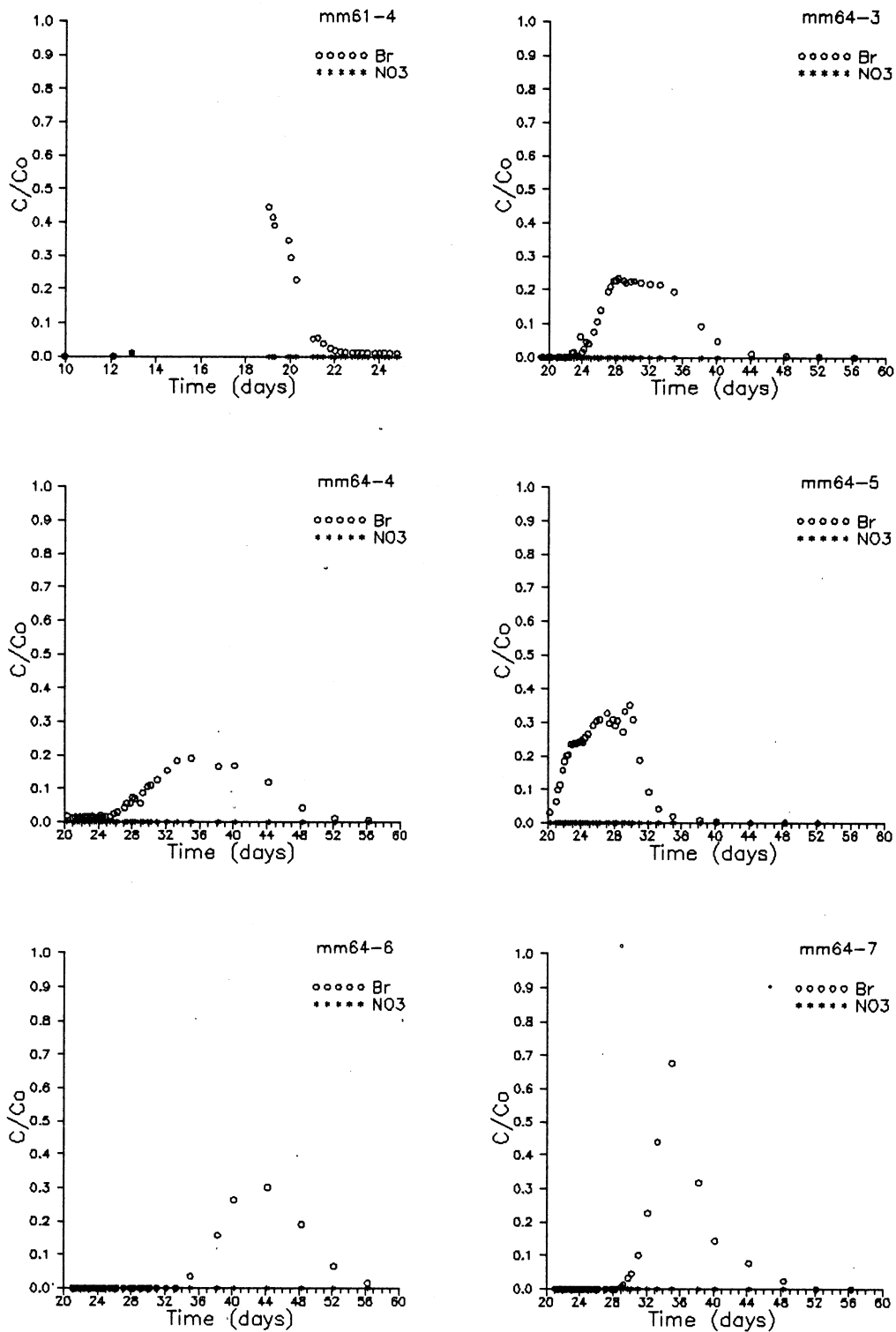


Figure 21 - Dimensionless breakthrough curves at mm61 and mm64. Concentrations of bromide and nitrate are normalized to concentrations measured in the injected tracer solution.

aquifer in southern Ontario. At the Ontario site, dissolved organic carbon concentrations were on the order of 7 to 10 mg/L. At the Adams County site dissolved organic carbon concentrations ranged from 17 to 29 mg/L in the injection zone (see Figure 22). Thus, the results of the reactive tracer experiment support the hypothesis that rates of denitrification in anaerobic sandy aquifers are roughly proportional to concentrations of labile organic carbon.

C. Model Evaluation

1. Comparison of observed and predicted capture depths

The analytical results of Zheng et al. (1998a) lead to an equation for the capture depth, D , of a ditch as a function of the ditch width, w , the difference between ditch stage and aquifer head, H , the regional gradient, I , and the ratio of horizontal to vertical conductivity, R (see Figure 23). This equation has the form

$$D = [(2wH)/(\pi IR)]^{1/2} \quad (4)$$

The measured and estimated values of parameters appearing in equation (4) for the tracer experiments of 1989 and 1990 are listed in Table 5. The width of the water-filled portion of the ditch can be measured directly and was found to vary spatially along the ditch and temporally with changes in ditch stage at the Adams County site. The difference between ditch stage and aquifer head can be measured using mini-piezometers installed in the ditch and screened below any fine-grained ditch sediment. The observed difference between ditch stage and aquifer head at the Adams County site was

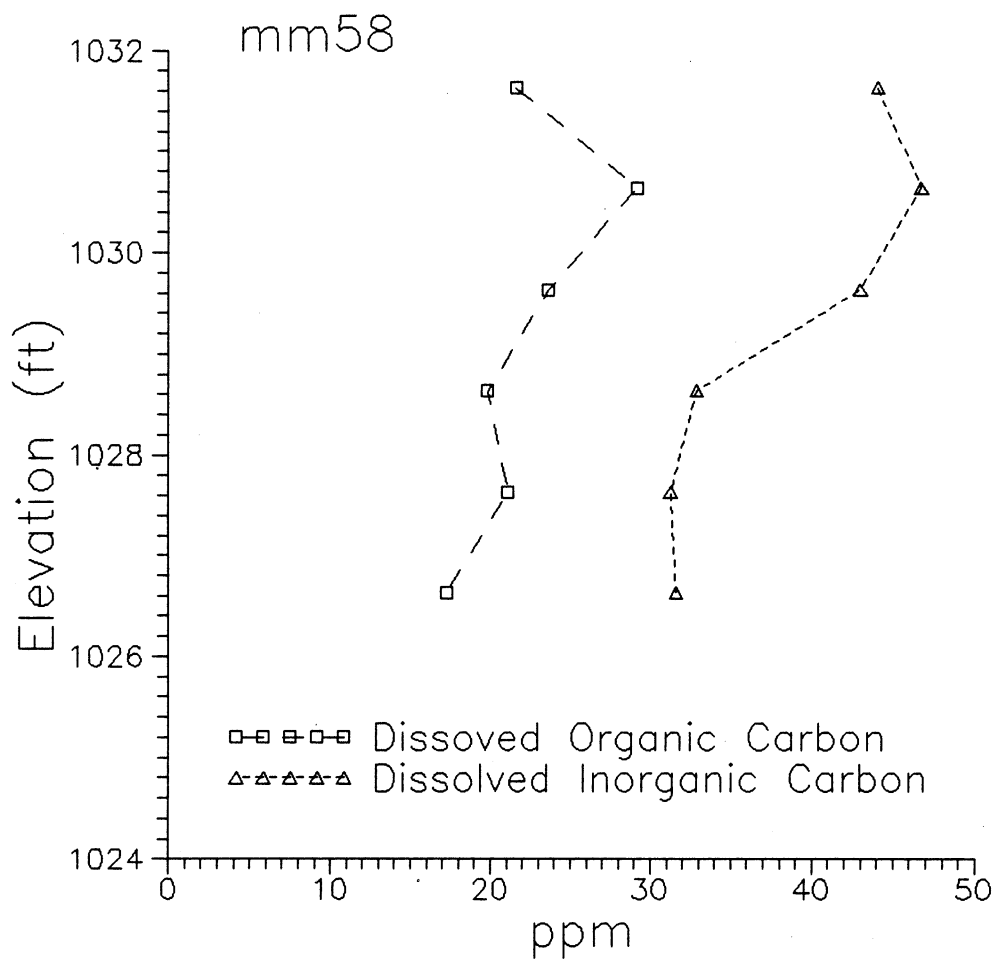


Figure 22 - Profiles of dissolved organic carbon and dissolved inorganic carbon within the tracer zone, as measured in mm58.

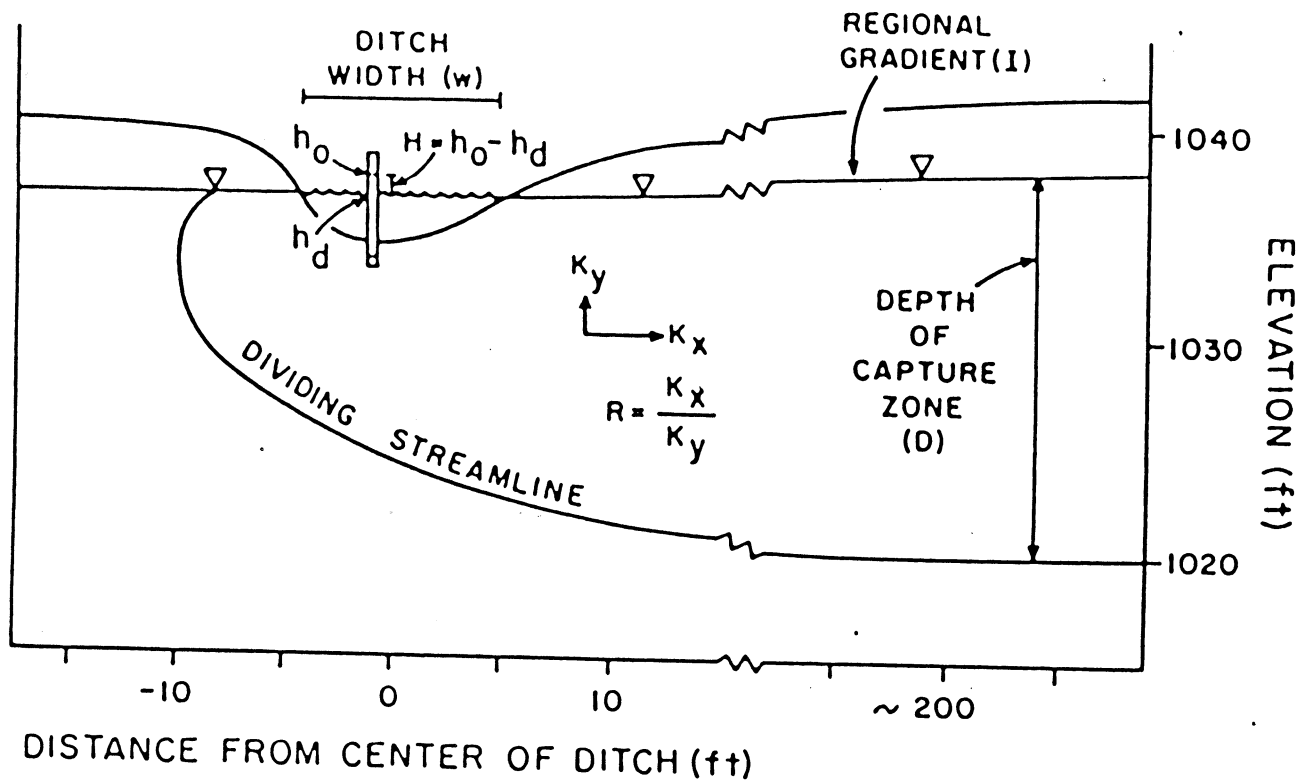


Figure 23 - Schematic diagram illustrating parameters of the two-dimensional solution of Zheng et al. (1988a). R is the ratio between the horizontal (K_x) and vertical (K_z) hydraulic conductivity. H is the difference between the water level in the ditch (h_d) and the potentiometric surface in the aquifer below the ditch (h_o).

also found to vary temporally in response to changes in ditch stage and recharge events. The regional gradient at the field site was estimated from the water table map of Lippelt and Hennings (1981). The anisotropy ratio, R, was the most difficult parameter to constrain for the field site. Weeks (1969) presented a method for determining the anisotropy ratio using results of pumping tests specifically designed for the purpose of evaluating this parameter. In the absence of such pumping tests at a site, the anisotropy ratio for the sand plain can only be estimated to fall within the range of 1 to 7 cited by Weeks and Stangland (1971).

TABLE 5 - PARAMETER ESTIMATES AND PREDICTED CAPTURE DEPTHS

	1989 Range	1989 Median	1990 Range	1990 Median
w (ft)	7.5-10	8.5	10-20	16
H (ft)	0.08-0.18	0.12	0.10-0.24	0.17
I	0.001-0.002	0.0015	0.001-0.002	0.0015
R	1-7	2.2*	1-7	2.2*
D (calculated)	5-34	14.0*	7-55	24.0*
D (observed)	11.3-15.7		>22.5	

* A value of 2.2 is assumed for R in computing D for median values of other parameters.

Using the extremes of the ranges of the estimated parameters for the field site during the two experiments, equation (1) predicts a capture depth

in the range of 5 to 34 feet for the summer of 1989 and 7 to 55 feet for the summer of 1990. These can be compared to observed capture depths of between 11.3 and 15.7 feet for 1989 and greater than 22.5 feet for 1990. Using median observed values of ditch width and difference between aquifer head and ditch stage along with a regional gradient of .0015, good matches to the observed capture depths for both years are obtained assuming an anisotropy ratio of 2.2, as estimated based on hydraulic conductivity results in section III.A.1. Good matches for both years would also be achieved with anisotropy ratios as low as 1.8, which would also be consistent with the measured hydraulic conductivity values. The good agreement between the anisotropy ratio calculated on the basis of grain size data and that determined from calibration of the capture zone model indicates that grain size analyses can be used to constrain estimates of capture zone effectiveness in the central sand plain.

2. Estimates of apparent dispersivity

A one-dimensional analytical solution based on that described by Moltzaner and Killey (1988) was used to evaluate apparent dispersivities within the middle zone of the aquifer from bromide breakthrough curves measured during the 1989 tracer experiment. Results of this analysis are described in Chambers and Bahr (1990, also included as Appendix D) and are summarized below. The model has the form

$$c(x,t) = 0.5 c_o \{ \text{erf}[(x + x_o/2 - vt)/(2Dt)] - \text{erf}[(x - x_o/2 - vt)/(2Dt)] \} \quad (5)$$

and assumes that the tracer is added instantaneously to the aquifer at time $t=0$. At the moment the tracer is added to the system, the cloud has width of x_0 and an initial concentration c_0 . D is the coefficient of longitudinal dispersion, v is the cloud velocity and x is the distance from the source.

Figure 24 shows the observed and calculated breakthrough curves for 3 miniature multilevels along the axis of the cloud. Transport between the injection well and mm19 was predominantly horizontal. During transport between mm19 and mmd12 the vertical component of flow increased. Velocity variations due to stratification, apparent in the breakthrough curves for points in mm19, decrease noticeably in the breakthrough curves for mm22 and mmd12 which are affected by cross-stratification flow.

Table 6 summarizes dispersivity values, α , equal to the ratio D/v , for each breakthrough curve. Also included in Table 5 are other parameter values used to fit the model to observed breakthrough curves. In some cases it was necessary to adjust the value of the initial cloud width or initial concentration in order to obtain a good fit. The need to adjust the parameters may be attributed to the initial heterogeneity of the cloud. With the exception of the slow moving region of tracer at point 5 in mm19, the apparent dispersivity values show a general trend of increasing as the upward component of flow increases. This increase in apparent dispersivity probably reflects flow of the cloud across rather than parallel to aquifer stratification.

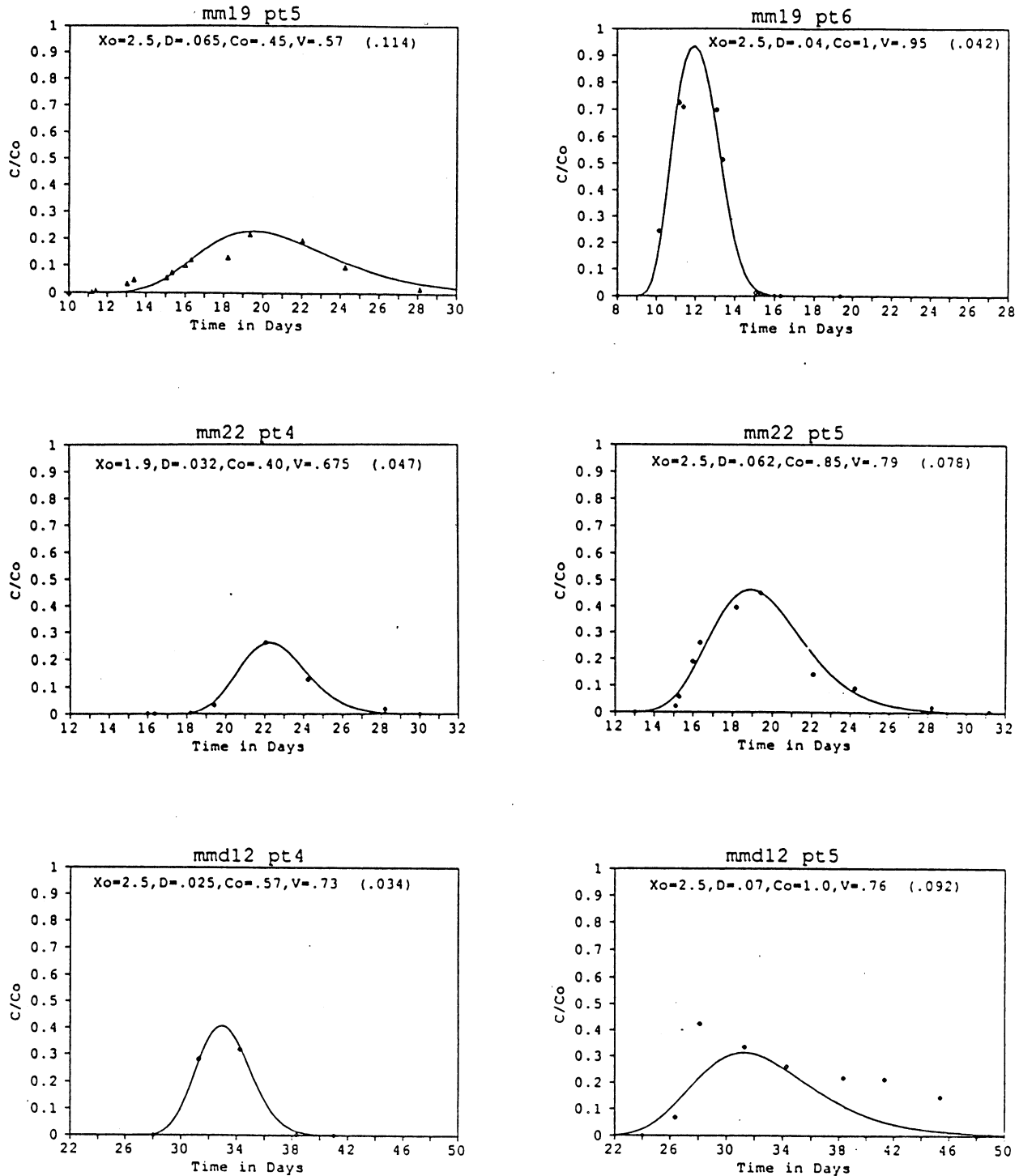


Figure 24 - Observed and calculated breakthrough curves for multilevels during the 1989 tracer experiment. Dots represent measured concentrations and solid lines are model fits.

TABLE 6 - DISPERSIVITY ESTIMATES FROM BREAKTHROUGH CURVE ANALYSIS

Sampling Point	Elevation (ft)	v (ft/d)	x_0 (ft)	c_0^*	α (ft)
mm19 pt7	1030.65	0.73	1.6	0.70	0.027
mm19 pt6	1029.89	0.95	2.5	1.00	0.042
mm19 pt5	1028.14	0.57	2.5	0.45	0.11
mm19 pt4	1026.39	0.72	1.6	0.63	0.027
mm22 pt6	1031.50	0.76	1.8	0.38	0.039
mm22 pt5	1030.00	0.79	2.5	0.85	0.078
mm22 pt4	1028.50	0.68	1.9	0.40	0.047
mm22 pt3	1027.73	0.71	2.5	0.80	0.066
mm22 pt2	1026.23	0.81	2.5	0.36	0.037
mm12 pt6	1032.97	0.77	2.5	0.40	0.042
mm12 pt5	1031.47	0.76	2.5	1.00	0.092
mm12 pt4	1029.97	0.73	2.5	0.57	0.034
mm12 pt3	1028.54	0.82	2.5	1.00	0.046

* Initial concentration used in model divided by measured concentration in the injection solution.

IV. CONCLUSIONS

The field and modeling studies conducted in this project have served to identify relationships between physical and chemical heterogeneity in a sand aquifer in central Wisconsin. Variations in hydraulic conductivity can lead to stratification of flow which in turn can lead to stratified chemical characteristics of groundwater. At the field site in Adams County, the ratio of calcium to magnesium concentration appears to be a good indicator by which to discriminate between zones of shallow groundwater that is likely to be the product of local recharge and deeper groundwater that may have its source at a greater distance from the sampling site. Stratification of the aquifer leads to a relatively thin, intermediate mixing zone between groundwater of local and more distant origin, characterized by transitional Ca/Mg ratios. Additional studies of cation ratio profiles in recharge and discharge areas of the sand plains could be used to determine if this type of indicator has more general applicability. If cation ratios can be correlated in a general way to groundwater age or recharge area location, they could prove quite useful in identifying whether local or more distant sources are responsible for observed contaminants at particular locations or depths within the sand plains aquifer system. As an example, such an analysis could be used to determine if nitrate contamination in a residential subdivision originated from failure of nearby septic systems or from more diffuse agricultural inputs upgradient of the subdivision.

Heterogeneities of the type observed at the Adams County site can exert important controls on shallow contaminant migration and spreading of con-

taminant plumes. Stratification of hydraulic properties may serve to confine contaminants to zones of relatively thin vertical extent within an aquifer. This can have important consequences for design of monitoring wells in the sand plains. If long screens are used, the maximum concentrations present in the aquifer will not be determined during sampling because of dilution with uncontaminated water in the strata surrounding the contaminated zone. Although monitoring wells constructed with long screens may be adequate for detection monitoring, they may provide a misleading picture of the distribution of contaminants in the aquifer. On the other hand, if only a few monitoring wells with very short screens are installed at a particular site, a contaminant plume could be missed completely. Monitoring designed to determine the distribution of contaminants for the purpose of source identification or the design of efficient remedial pumping schemes in stratified sand aquifers of the sand plain is therefore likely to require a fairly dense network of vertically spaced samplers.

Assessment of groundwater susceptibility to contamination in the central sand plain depends on groundwater chemistry as well as on physical hydrogeologic factors. In particular, the nitrate tracer experiment conducted as part of this project demonstrates that rapid denitrification can be expected under conditions of low dissolved oxygen and high dissolved organic carbon concentrations. These results indicate that improved estimates of susceptibility to contamination by nitrate in the central sand plain can be obtained through a regional survey of dissolved oxygen, dissolved organic carbon, and nitrate in groundwater. Such a survey should examine both the vertical distribution of these parameters at individual

sites and the variations between sites. Because dissolved oxygen is generally expected to decrease from recharge areas to discharge areas, attempts should be made to correlate measured concentrations with information on position within the regional flow field. Land use factors that may contribute to available dissolved organic carbon within the aquifer should also be identified and related to the measured values. This information would contribute to the development of management strategies to enhance microbial denitrification. For example, information on the regional distribution of dissolved oxygen and organic carbon could be used to identify areas in which denitrification is currently limited low concentrations of dissolved organic carbon. In these areas it might be possible to modify tillage practices to enhance leaching of dissolved organic carbon to the water table. In areas where denitrification appears to be limited by both high dissolved oxygen and low organic carbon, measures to enhance organic carbon leaching might also be effective, but the required organic carbon load would probably be considerably higher. In such areas, an increased organic carbon load would first increase the rate of oxygen consumption below the water and, following depletion of oxygen, serve as a carbon source for denitrifiers.

Tracer experiments designed to identify a ditch capture zone have confirmed that existing ditches in the central sand plain do create passive barriers to shallow contaminant migration. A simple model to predict capture zone depth is limited by the uncertainty in the anisotropy ratio for central sand plain aquifers. Results of this study suggest that uncertainty in the anisotropy ratio can be reduced by obtaining data on grain size distributions of aquifer sediments. Additional information on the regional distribution of anisotropy would significantly reduce the uncertainty in

estimates of average capture depth for existing ditches that can be made using equation (4) along with relatively simple measures of ditch width, water table gradient and head difference between the ditch and the aquifer. Improved estimates of capture depth will aid in identifying existing ditches that are currently intercepting significant volumes of shallow ground water.

For ditches that currently create only very shallow capture zones, a number of modifications could be undertaken to improve their effectiveness for contaminant removal. If the water depth in the ditch is a foot or deeper, it may be possible to lower the ditch stage by modifying downstream controls such as culverts or check dams. This would have the effect of increasing H , the difference between ditch stage and potentiometric surface in the aquifer, thereby increasing the capture depth. The required change in ditch stage, assuming that lowering the water level in the ditch would have little immediate effect on the aquifer potentiometric surface, could be determined from equation (4). If the water level in the ditch is too shallow to be reduced significantly by downstream controls, a second alternative would be to increase the depth of the ditch by dredging in the desired capture area as well as downstream. Following excavation and establishment of a new flow regime in the ditch, it might also be possible to decrease ditch stage further through additional downstream control modifications. Increasing ditch width is a third alternative that would increase the capture depth. However, because widening the ditch is likely to be more costly and disruptive to existing land uses than dredging, it is expected that this alternative would be chosen only if other alternatives were not effective or feasible.

The experiments conducted as part of this research have also demonstrated that there can be large seasonal fluctuations in the depth of the capture zone. Additional field work and modeling are currently being conducted to obtain a better understanding of the magnitudes and time scales of these fluctuations. It is hoped that the results of these ongoing studies will lead to effective monitoring techniques and control strategies that might be employed to minimize short term and seasonal variations in capture depth while at the same time maximizing contaminant removal by ditches.

REFERENCES

- Born, S. M., D. A. Yanggen, A. R. Czecholinski, R. J. Tierney, and R. G. Hennings, 1988. Well head protection districts in Wisconsin: an analysis and test application. Wisc. Geol. and Nat. Hist. Survey Special Report, no. 10. 75 pp.
- Bouwer, H. and R. C. Rice, 1976. A slug test for determining hydraulic conductivity of unconfined aquifers with completely or partially penetrating wells. Water Resour. Res., v. 12, pp. 423-428.
- Bradbury, K. R. and M. A. Muldoon, 1990. Hydraulic conductivity determinations in unlithified glacial and fluvial materials. in D. M. Nielson and A. I. Johnson, eds. Ground Water and Vadose Zone Monitoring. ASTM STP 1053, Philadelphia PA.
- Brasino, J. S., 1986. A simple stochastic model predicting conservative mass transport through the unsaturated zone into groundwater. PhD thesis, Dept. of Soil Science, UW-Madison
- Chambers, L. W., 1990. A field evaluation of drainage ditches as barriers to contaminant migration. MS thesis, Dept. of Geology and Geophysics, UW-Madison
- Chambers, L. W. and J. M. Bahr, 1989. Tracer study for evaluation drainage ditches as controls on ground water contamination. Ground Water, vol. 27(5). p. 724. (abstract)
- Chambers, L. W. and J. M. Bahr, 1990. Tracer study in a complex three-dimensional flow system. in Proceedings of International Conference and Workshop on Transport and Mass Exchange Processes in Sand and Gravel Aquifers: Field and Modeling Studies, Ottawa, Canada, October 1-4 1990. pp. 355-372.

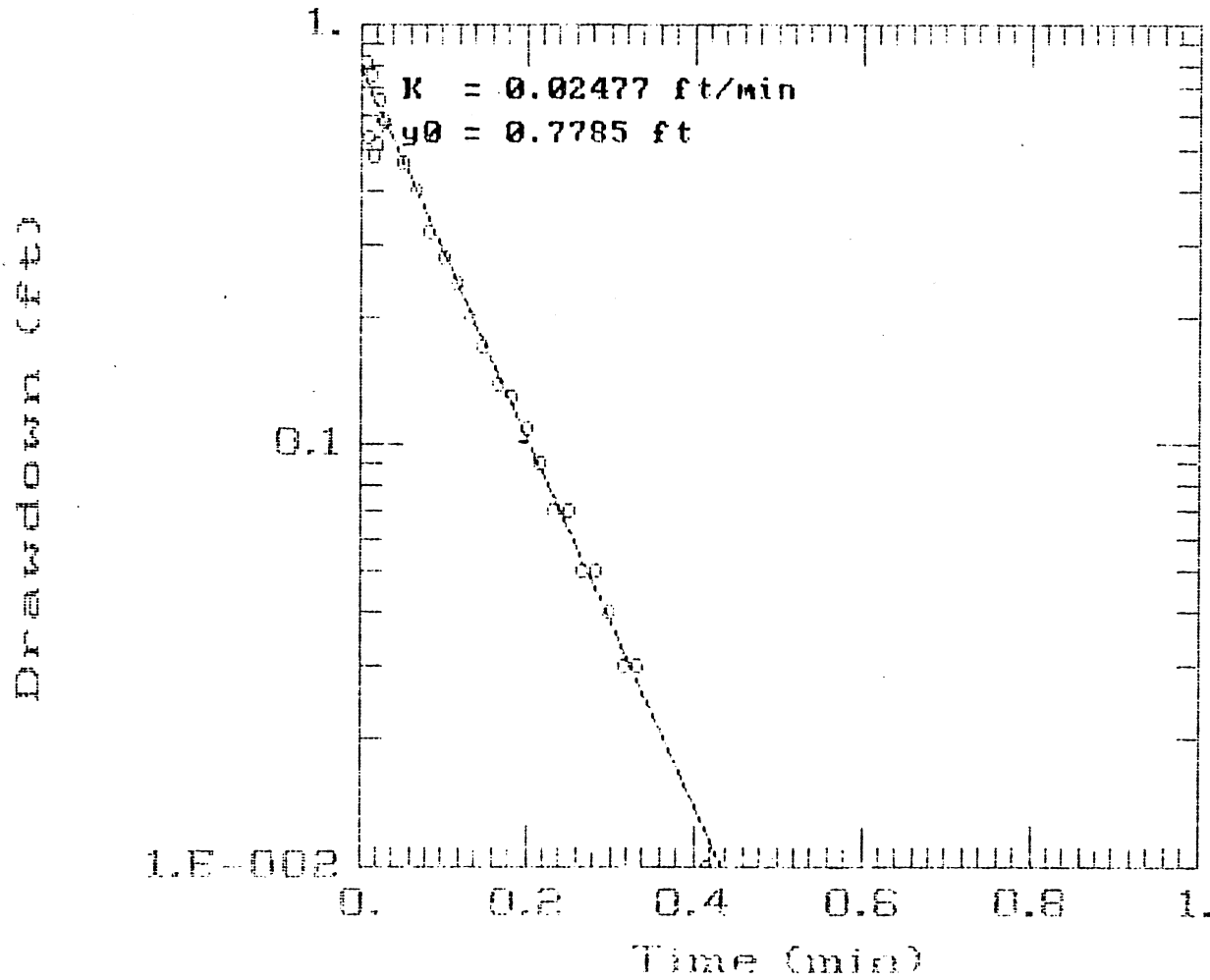
- Chambers Lucy. W. and J. M. Bahr, 1992. Tracer test evaluation of a drainage ditch capture zone. Ground Water (in press).
- Chesters, G., M. P. Anderson, B. H. Shaw, J. M. Harkin, M. Meyer, E. Rothschild, and R. Manser, 1982. Aldicarb in groundwater. Water Resources Center Report. Madison, WI, 38 pp.
- Clayton, L. and J. W. Attig, 1989. Glacial Lake Wisconsin. Geol. Soc. Am. Memoir 173, Boulder CO 80 p.
- Faustini, J. M. 1985. Delineation of groundwater flow patterns in a portion of the central sand plains of Wisconsin. MS thesis, Dept. of Geology and Geophysics, UW-Madison
- Fetter, C. W., 1988. Applied Hydrogeology. Columbus, Ohio: Merrill Publishing Co., 592.
- Garrels, R. M. and C. L. Christ, 1965. Solutions, Minerals, and Equilibria. San Francisco: Freeman, Cooper & Co., 450 pp.
- Gillham, R. W., 1990. Nitrate contamination of groundwater in southern Ontario and the evidence for denitrification, Proceedings NATO Advanced Workshop on Nitrate Contamination, Exposure, Consequences & Control, Lincoln NE, September 9-14, 1990.
- Harkin, J. M., G. Chesters, F. A. Jones, R. N. Fathulla, E. K. Dantzor and D. G. Kroll, 1986. Fate of aldicarb in Wisconsin groundwater. Water Resources Center Tech. Rept., WIS-WRC, 86-01.
- Hazen, A. 1893. Some physical properties of sands and gravels with special reference to their use in filtration. Mass. State Board of Health 24th Annual Report, pp. 553.
- Jackson, R.E., R.J. Patterson, B.W. Graham, J. Bahr, D. Belanger, J. Lockwood and M. Priddle, 1985. Contaminant Hydrogeology of Toxic

- Organic Chemicals at a Disposal Site, Gloucester, Ontario. 1. Chemical concepts and site assessment. Inland Waters Directorate Scientific Series no. 141, Environment Canada, Ottawa, Ontario, 114 p.
- Kraft, G., 1990. Fate of aldicarb residues in a groundwater basin near Plover, Wisconsin. PhD dissertation, Dept. of Soil Science, UW-Madison.
- Kung, K-J.S., 1990. Preferential flow in a sandy vadose zone: 1. Field observation, *Geoderma*, 46, pp. 51-58.
- Landreau, A., A. Mariotti and B. Simon, 1988. La dénitrification naturelle dans les eaux souterraines. *Hydrogéologie*, no.1, pp 35-43.
- Lippelt, I. D. and R. G. Hennings, 1981. Irrigable lands inventory- Phase I, Groundwater and related information. *Wisc. Geol. and Nat. History Survey Misc. Paper 81-1*.
- Lulloff, A. R., 1987. Groundwater quality in Wisconsin. Wisconsin DNR PUBL WR-156-87.
- Manser, R. J., 1983. An investigation into the movement of aldicarb residue in groundwater in the central sand plains of Wisconsin. MS thesis, Dept. of Geology and Geophysics, UW-Madison
- Masch, F. D. and J. J. Denny, 1966. Grain size distribution and its effect on the permeability of unconsolidated sands. *Water Resour. Res.*, v. 2(4). pp. 663-667.
- Moltyaner, G. L. and R. W. D. Killey, 1988. Twin Lake tracer test: longitudinal dispersion, *Water Resour. Res.*, v. 24(10), pp. 1613-1627.
- Rothschild, E. R., R. J. Manser, and M. P. Anderson, 1982. Investigation of aldicarb in ground water in selected areas of the central sand plain of Wisconsin, *Ground Water*, 20(4), pp. 437-445.

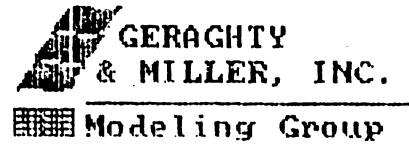
- Trudell, M. R. W. Gillham, and J. A. Cherry, 1986. An in-situ study of the occurrence and rate of denitrification in a shallow unconfined sand aquifer. *J. Hyd.*, 83, pp 251-268.
- Starr, R. C. and R. W. Gillham, 1989. Controls on denitrification in shallow unconfined aquifers., in *Contaminant Transport in Groundwater*, Kobus and Kinzelbach, eds., Balkema, Rotterdam, ISBN 90 6191 7890.
- Stites, W. and L. W. Chambers, 1991. A method for installing miniature multilevel sampling wells. *Ground Water*, vol. 29, pp. 430-432.
- Weeks, E. P. 1969. Determining the ratio of horizontal to vertical permeability by aquifer test analysis; *Water Resour. Res.* v. 5(1), pp. 196-214.
- Weeks, E. P. and H. G. Stangland, 1971. Effects of irrigation on streamflow in the central sand plain of Wisconsin. *U. S. G. S. Open File Rept.*, 113 pp.
- Wisconsin Geological and Natural History Survey, 1987. *Groundwater Contamination Susceptibility in Wisconsin (map)*, Madison WI.
- Zheng, C., K. R. Bradbury, and M. P. Anderson, 1988a. Role of interceptor ditches in limiting the spread of contaminants in ground water; *Ground Water*, vol. 26, no. 4. pp 734-742.
- Zheng, C., H. F. Wang, M. P. Anderson and K. R. Bradbury, 1988b. Analysis of interceptor ditches for control of groundwater pollution, *J. Hydr.*, vol. 98, pp. 67-81.

APPENDIX A - Slug Tests and Grain Size Analyses

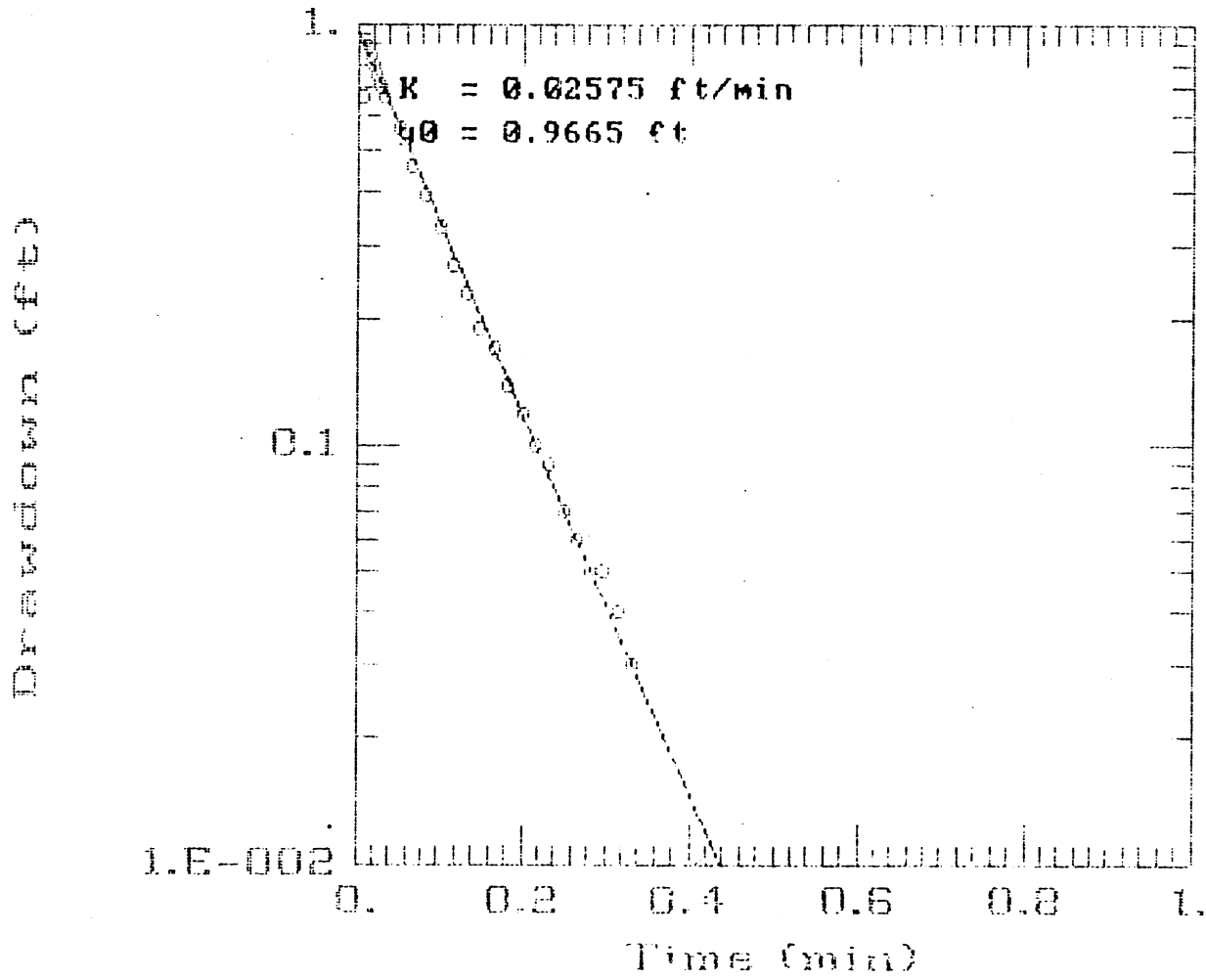
Aqt0 IW12 Elev 1014.4-1019.1



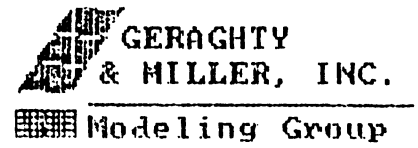
AQTESOLV



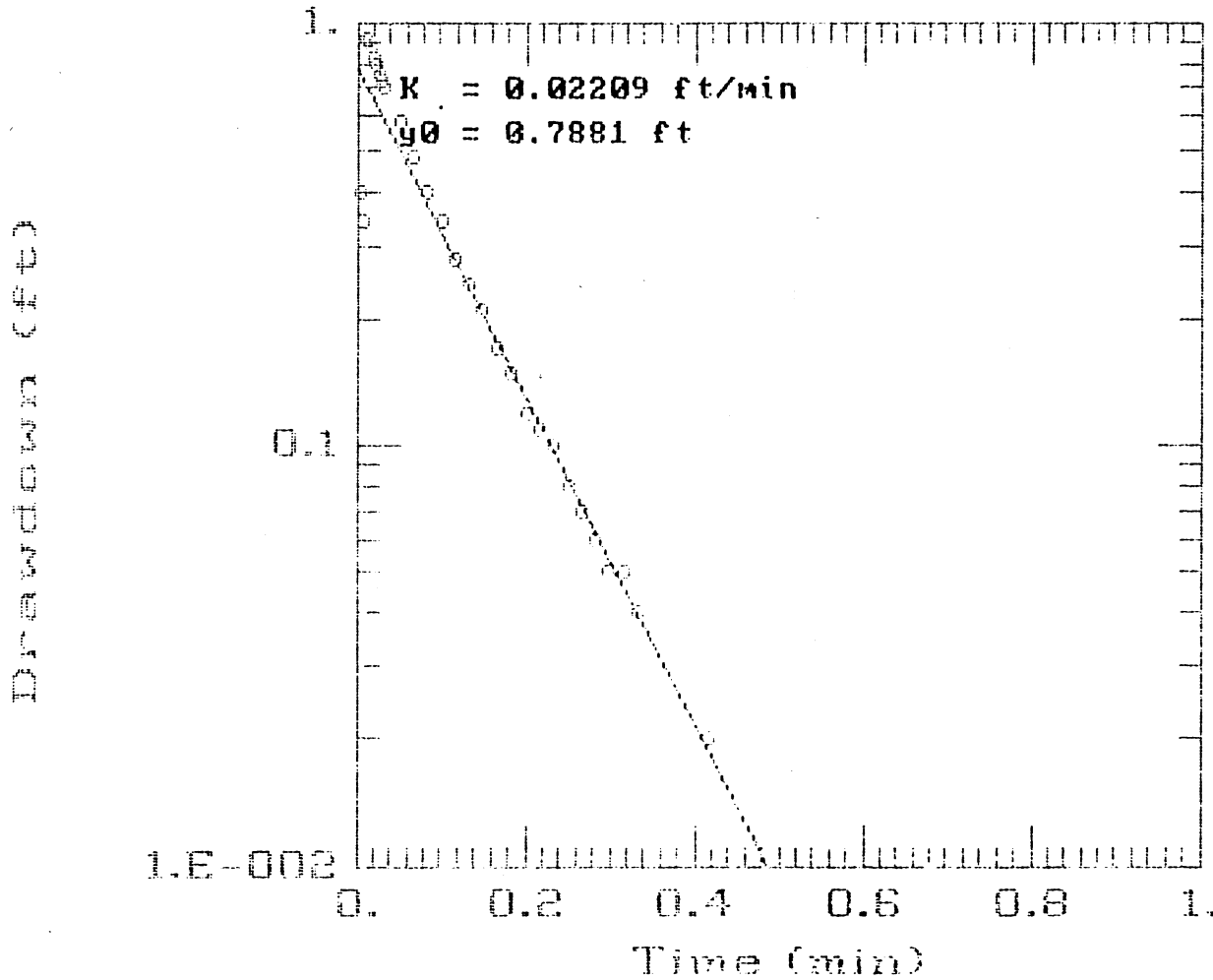
Aqt1 IW12 Elev 1014.4-1019.1




AQTESOLV



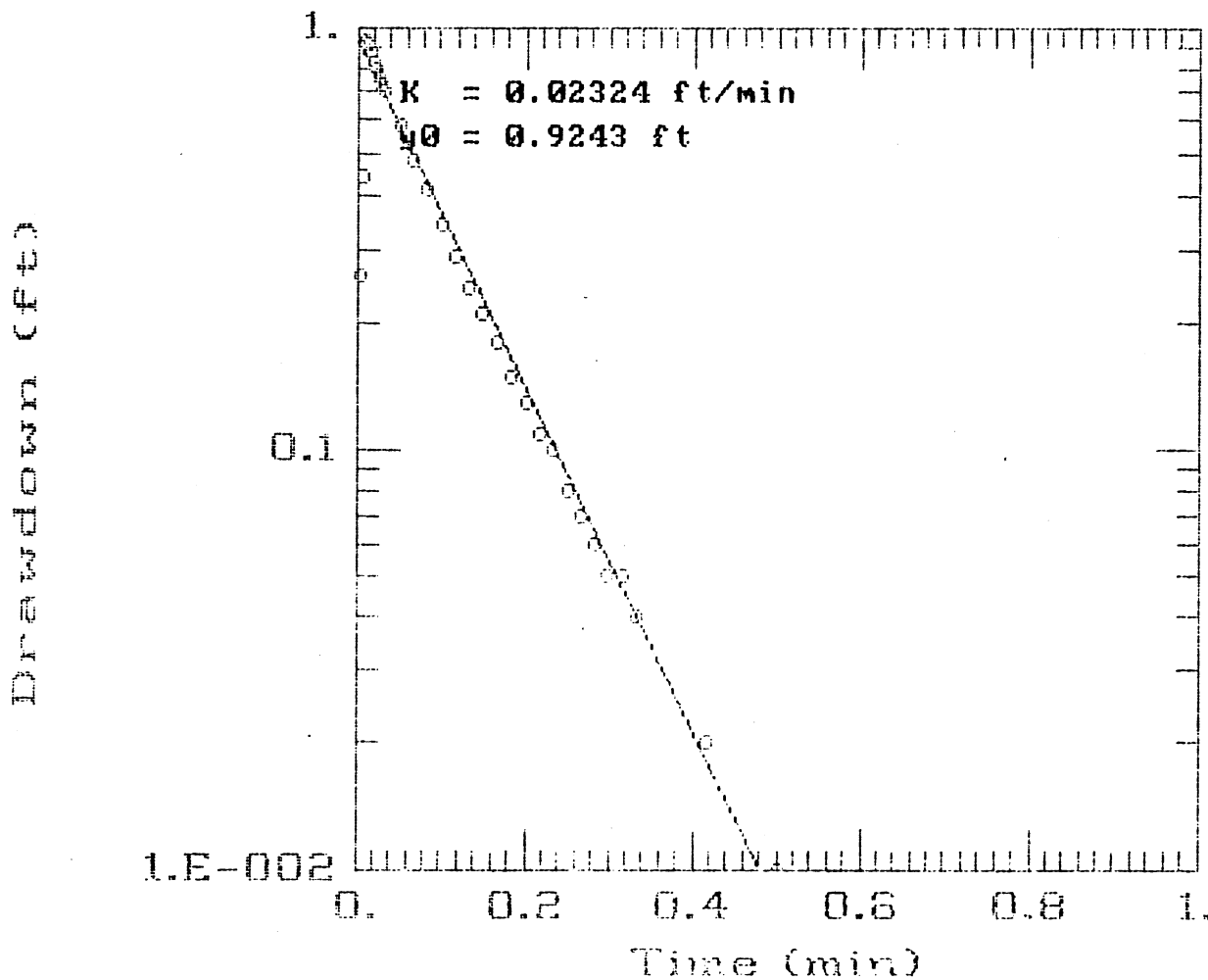
Aqt2 IW12 Elev 1014.4-1019.1



AQTESOLV

 GERAGHTY
& MILLER, INC.
Modeling Group

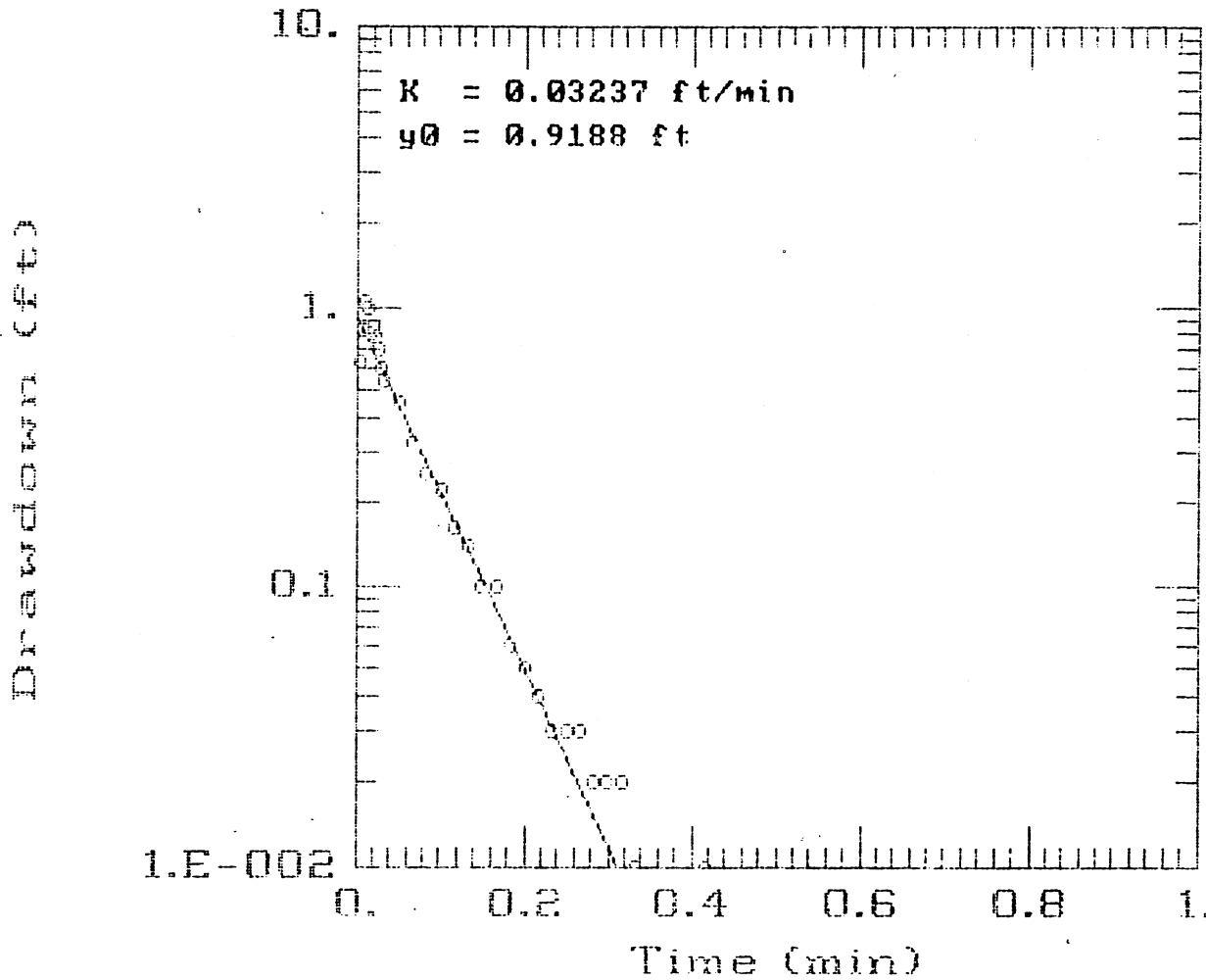
Aqt6 IW12 Elev 1014.4-1019.1





AQTESOLV

 GERAGHTY
& MILLER, INC.
Modeling Group

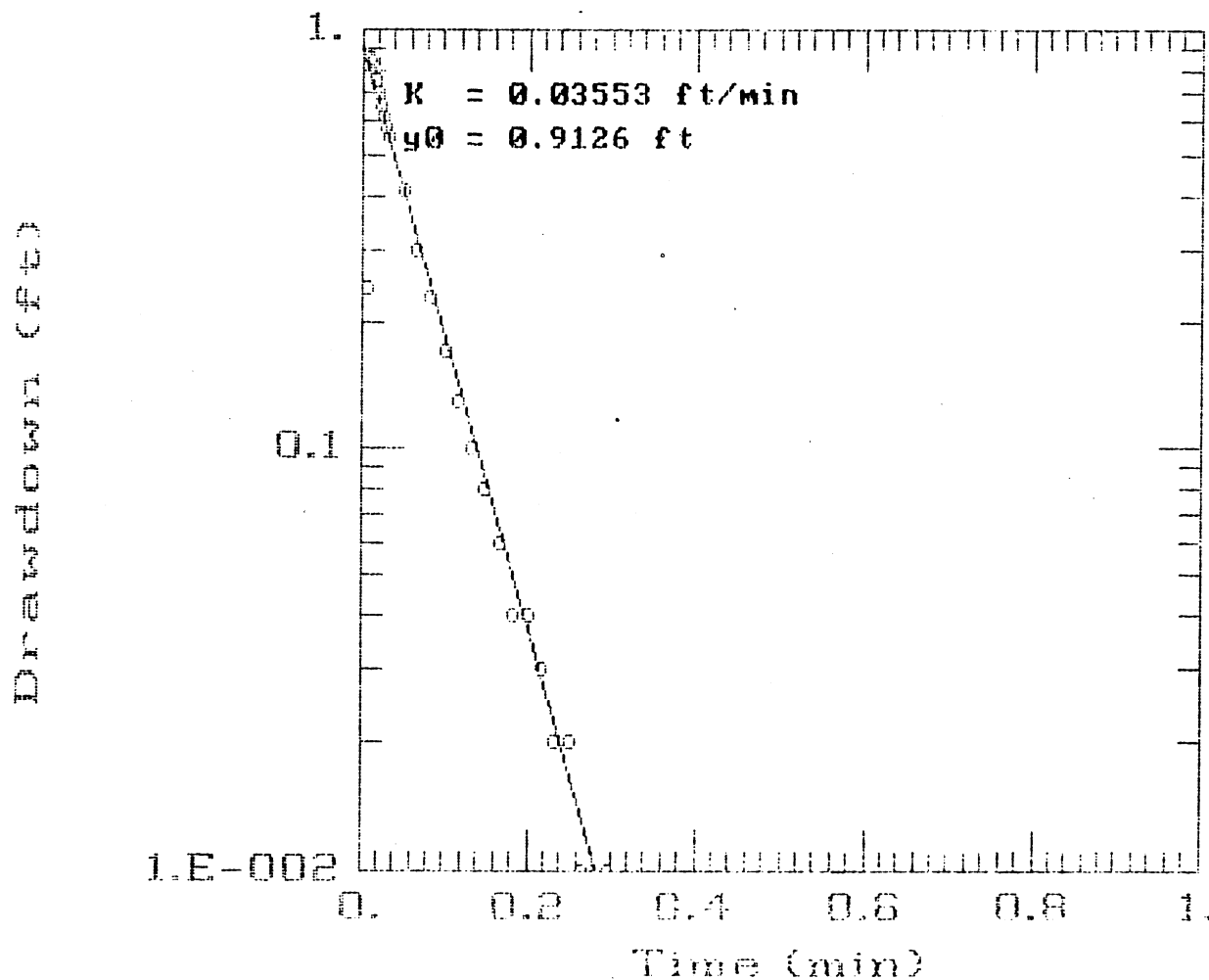
Aqt3 IW11 Elev 1024.4-1029.1



AQTESOLV

 GERAGHTY
& MILLER, INC.
 Modeling Group

Aqt4 IW11 Elev 1024.4-1029.1



AQTESOLV

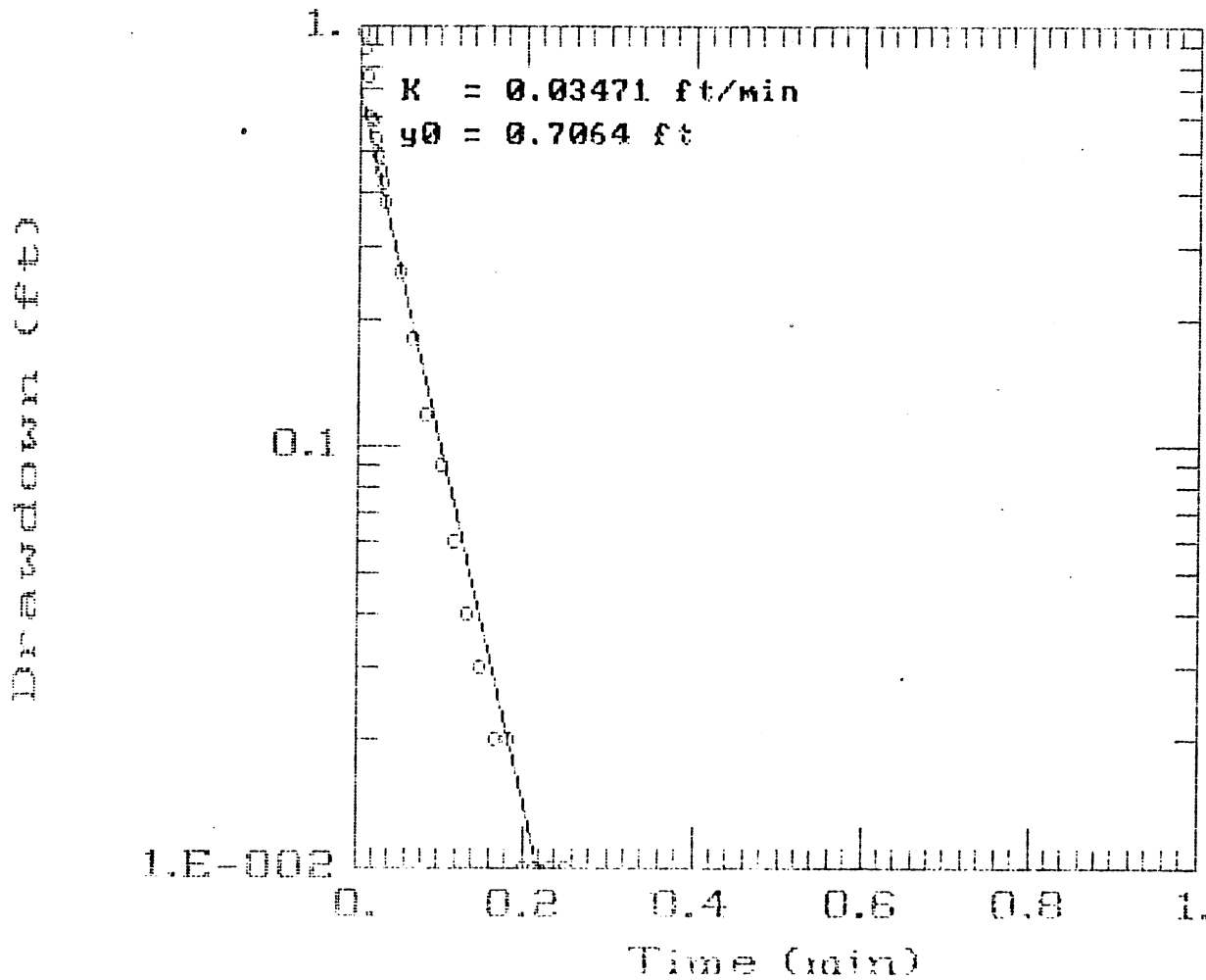


GERAGHTY
& MILLER, INC.





Modeling Group

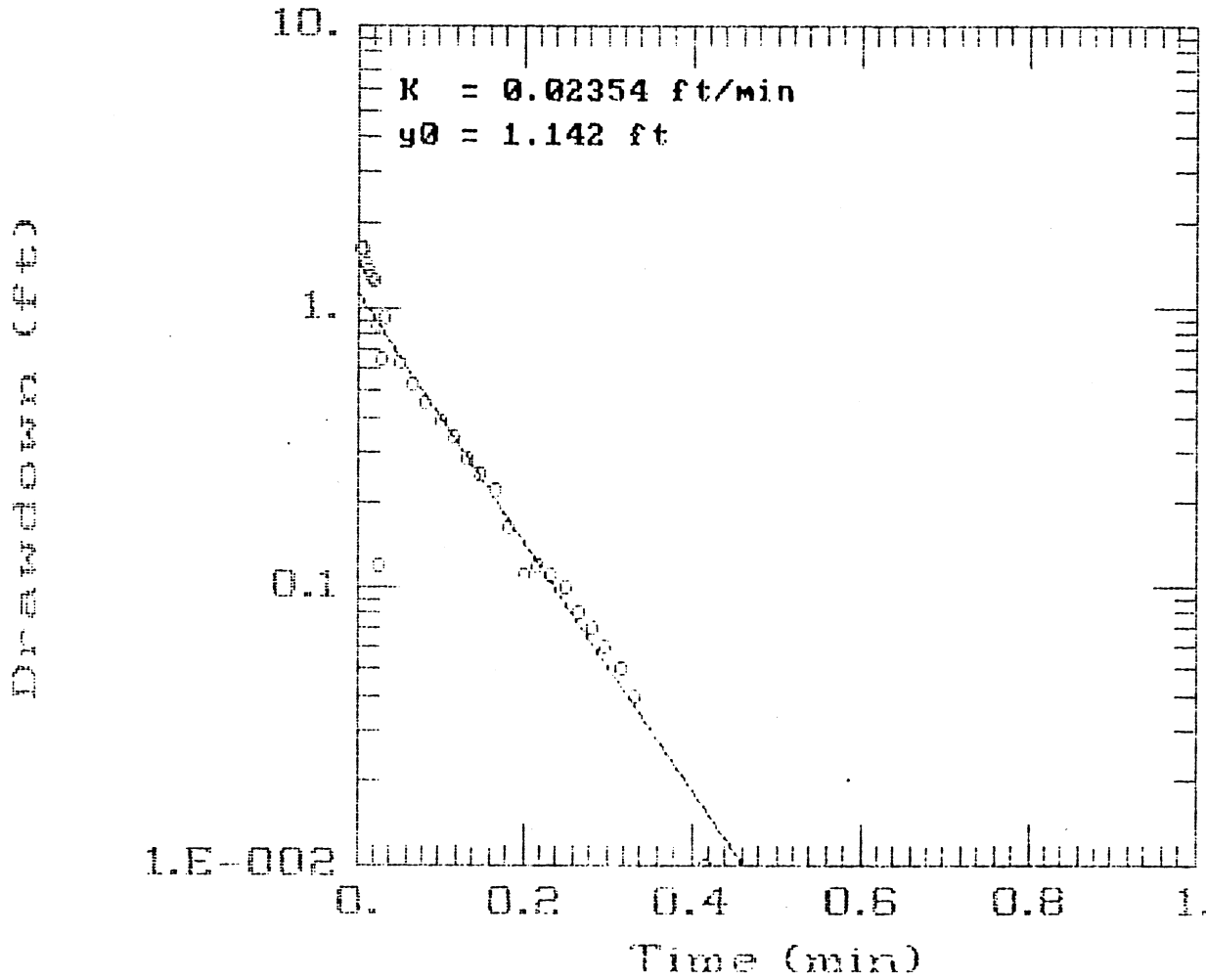
Aqt5 IW1 Elev 1022.5-1028.8




AQTESOLV

 GERAGHTY
& MILLER, INC.
 Modeling Group

Aqt0a DP1 Elev 1013.3-1016.0

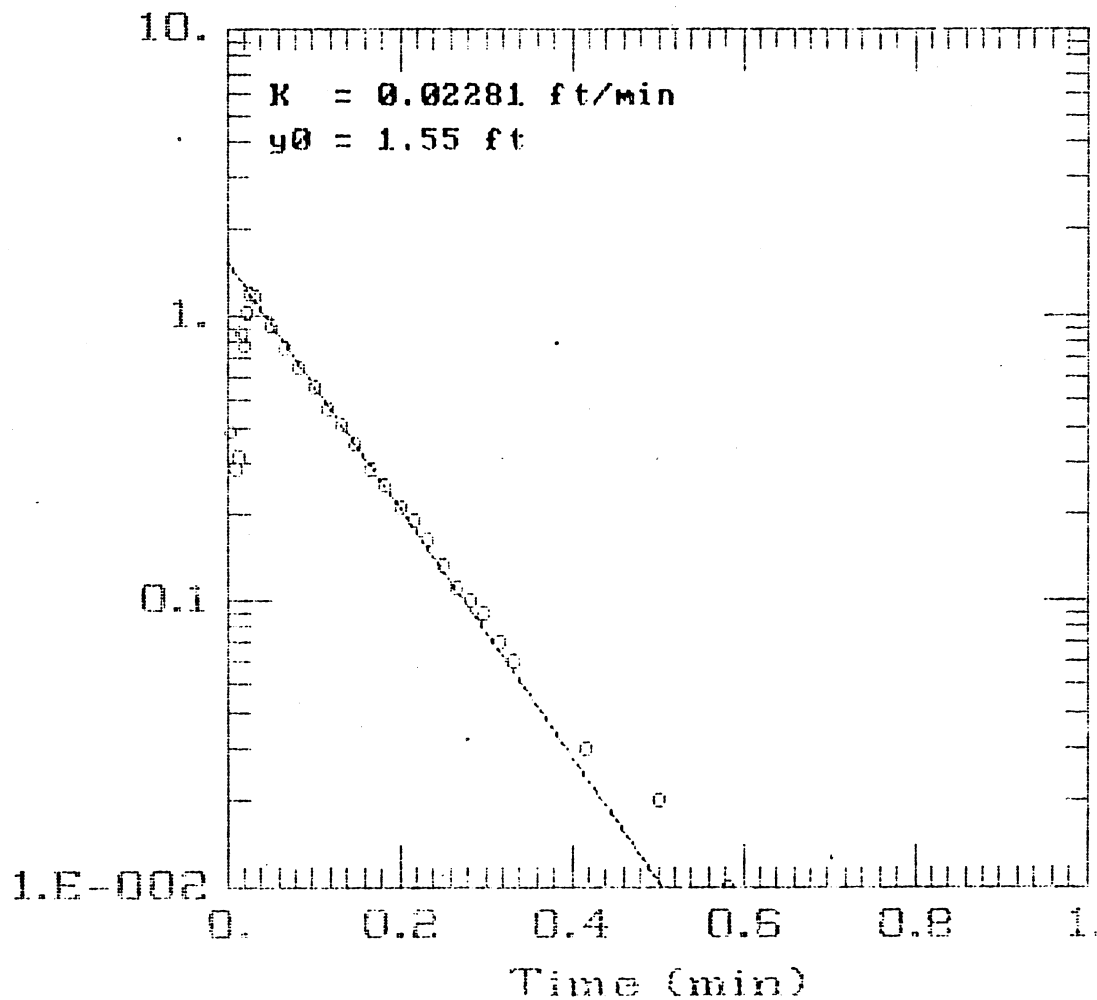


AQTESOLV

 GERAGHTY
& MILLER, INC.
Modeling Group

Aqt1a DP1 Elev 1013.3-1016.0

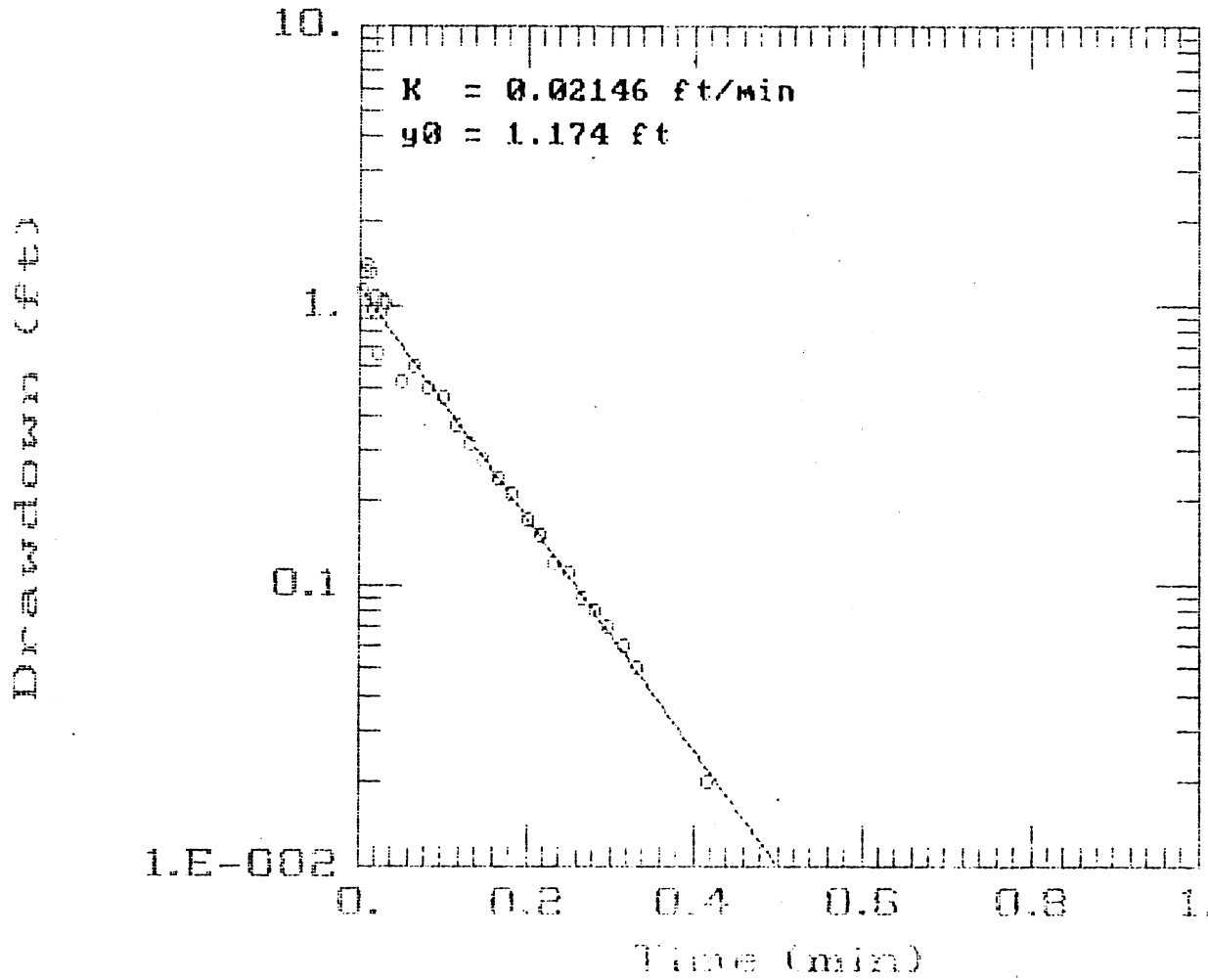
Drawdown (ft)




AQTESOLV

 GERAGHTY
& MILLER, INC.
Modeling Group

Aqt2a DP2 Elev 1014.8-1017.7

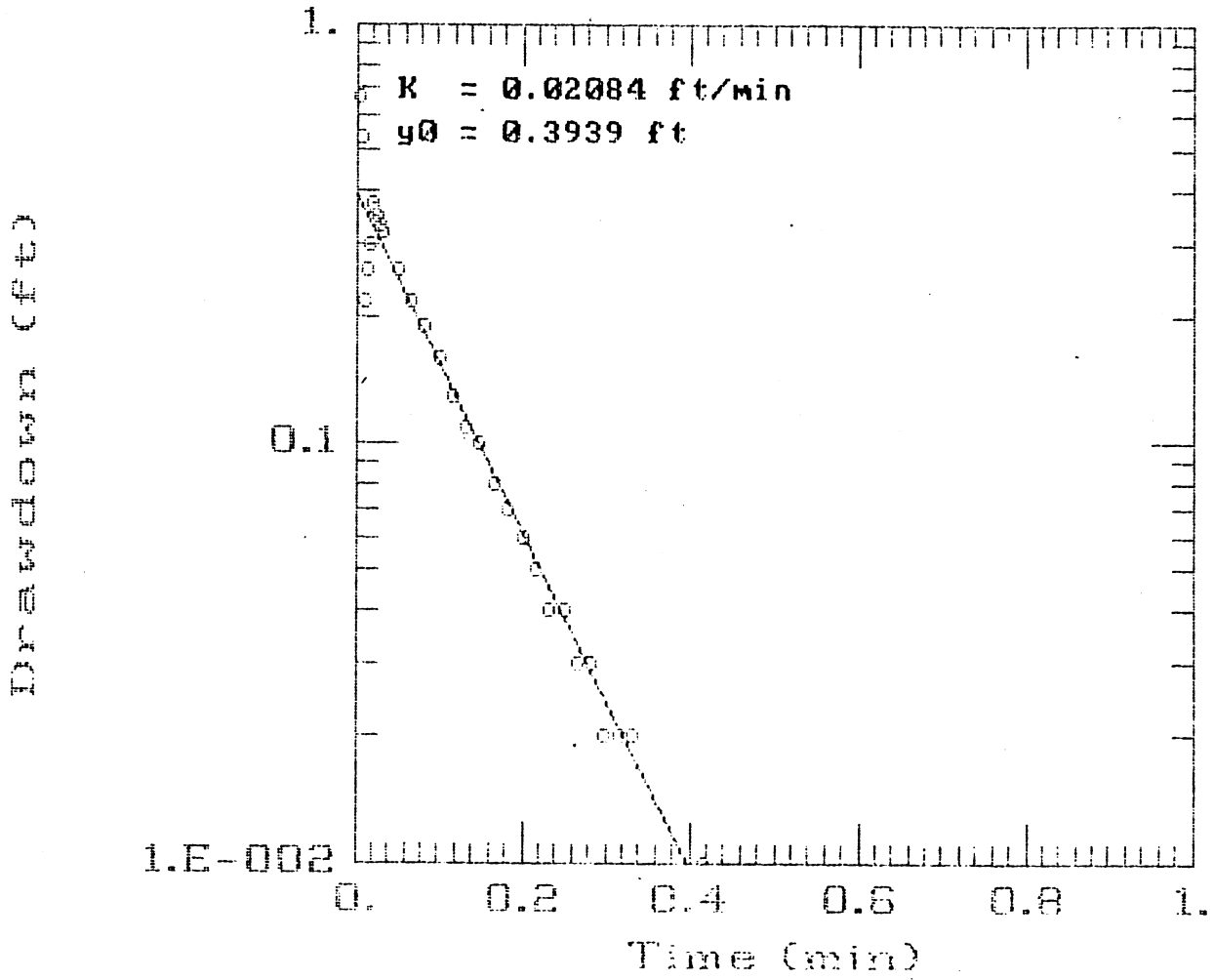


AQTESOLV

 GERAGHTY
& MILLER, INC.

Modeling Group

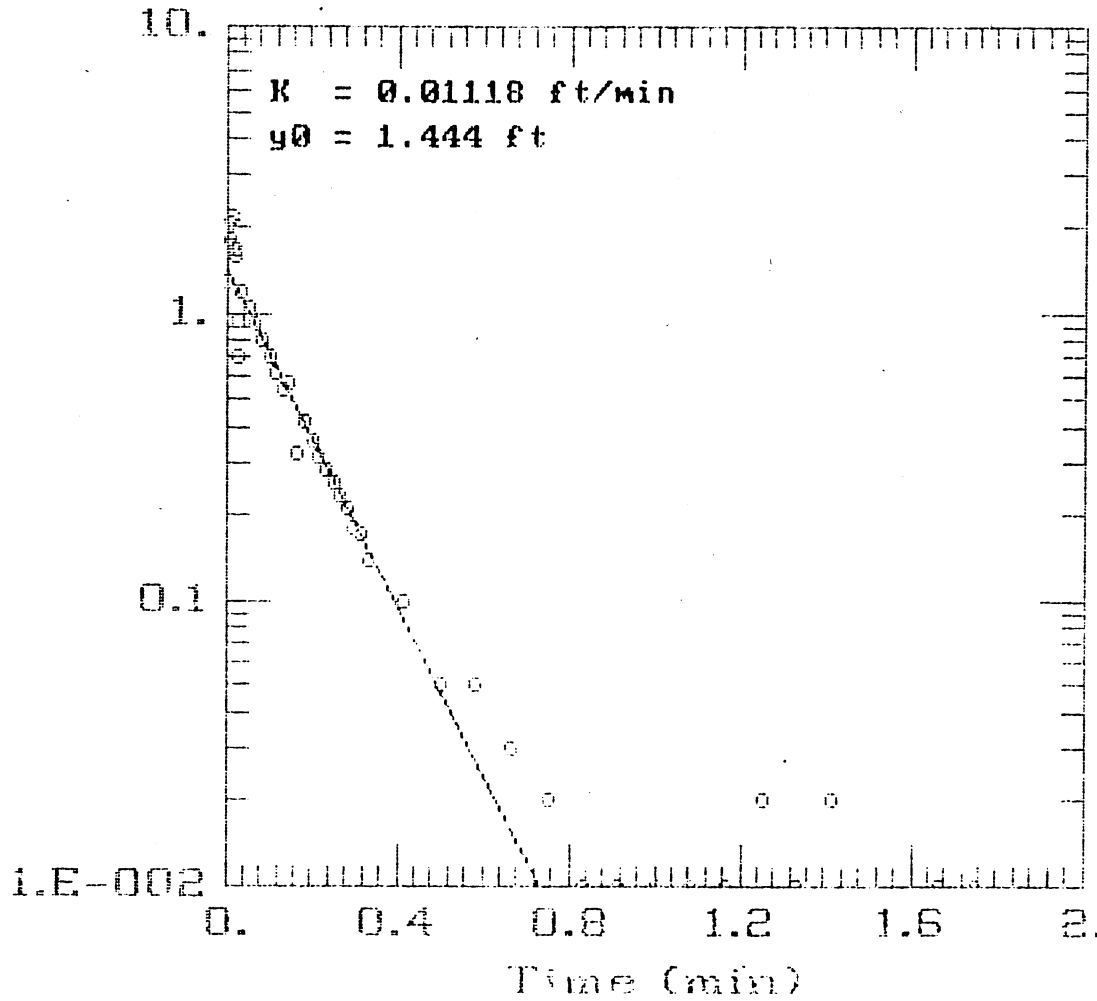
Aqt3a DP2 Elev 1014.8-1017.7





AQTESOLV
GERAGHTY
& MILLER, INC.
Modeling Group

Aqt4a DP4 Elev 1015.3-1018.12

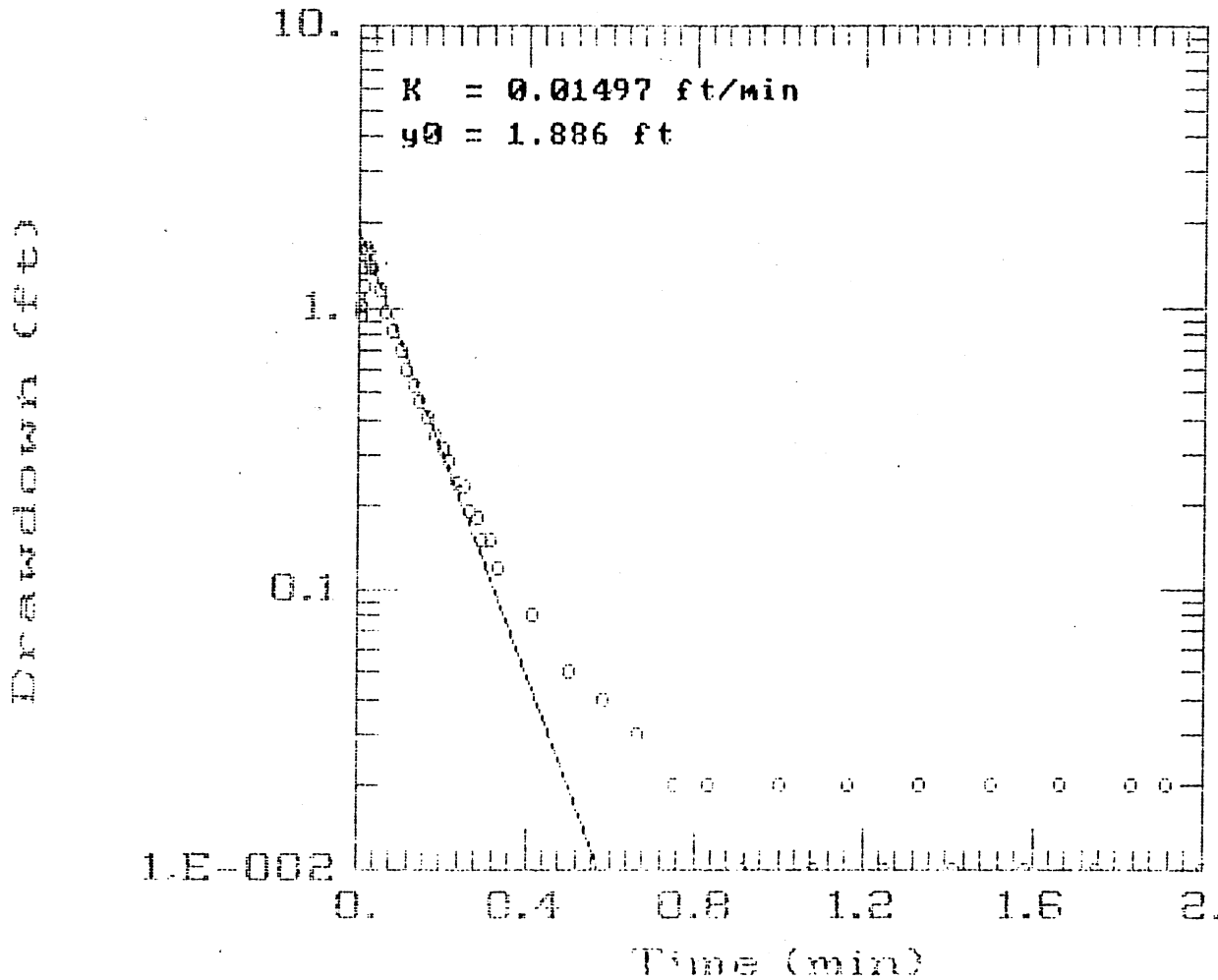
Drawdown (ft)




AQTESOLV

 GERAGHTY
& MILLER, INC.
 Modeling Group

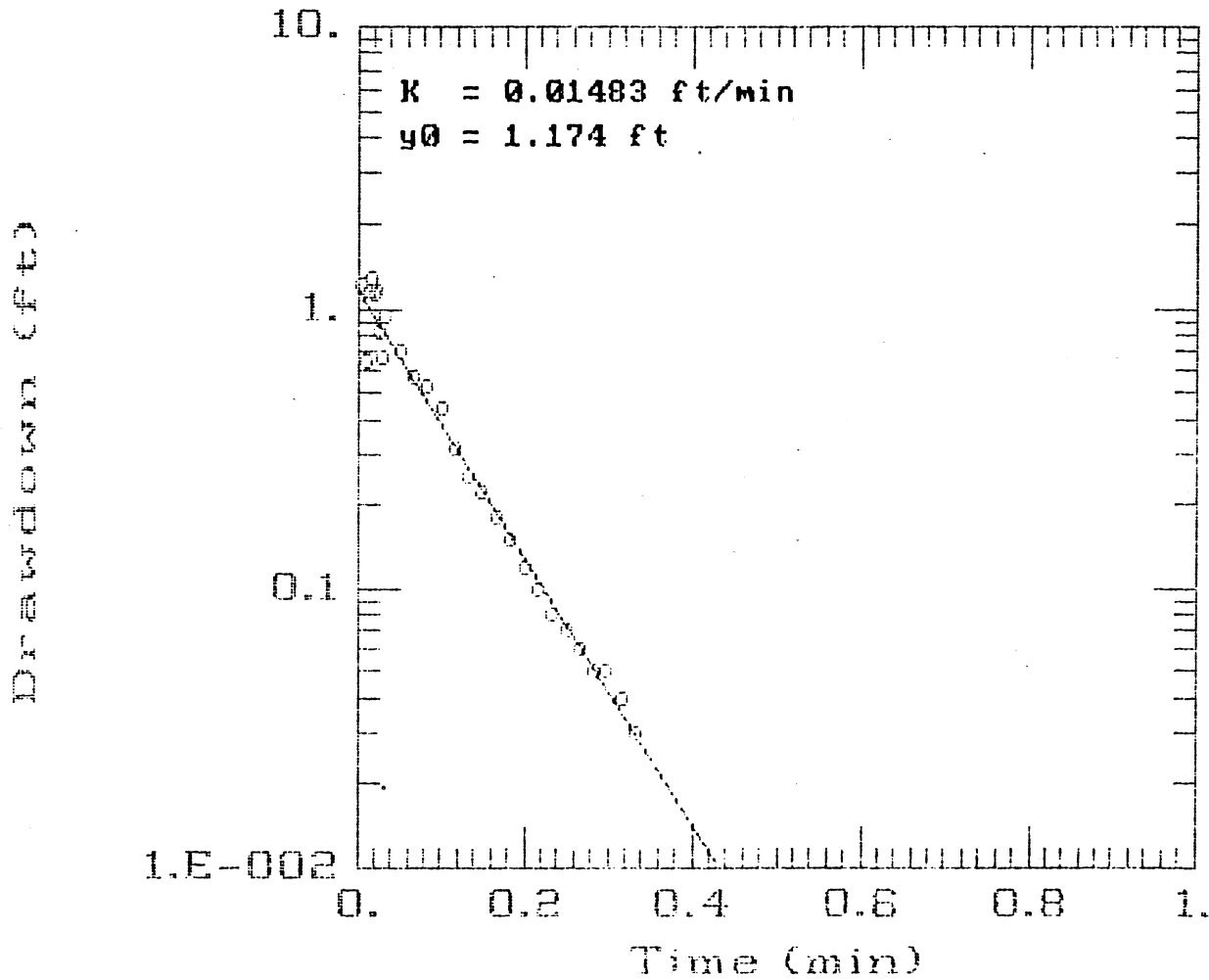
Aqt5a DP4 Elev 1015.3-1018.12




AQTESOLV

 GERAGHTY
& MILLER, INC.
Modeling Group

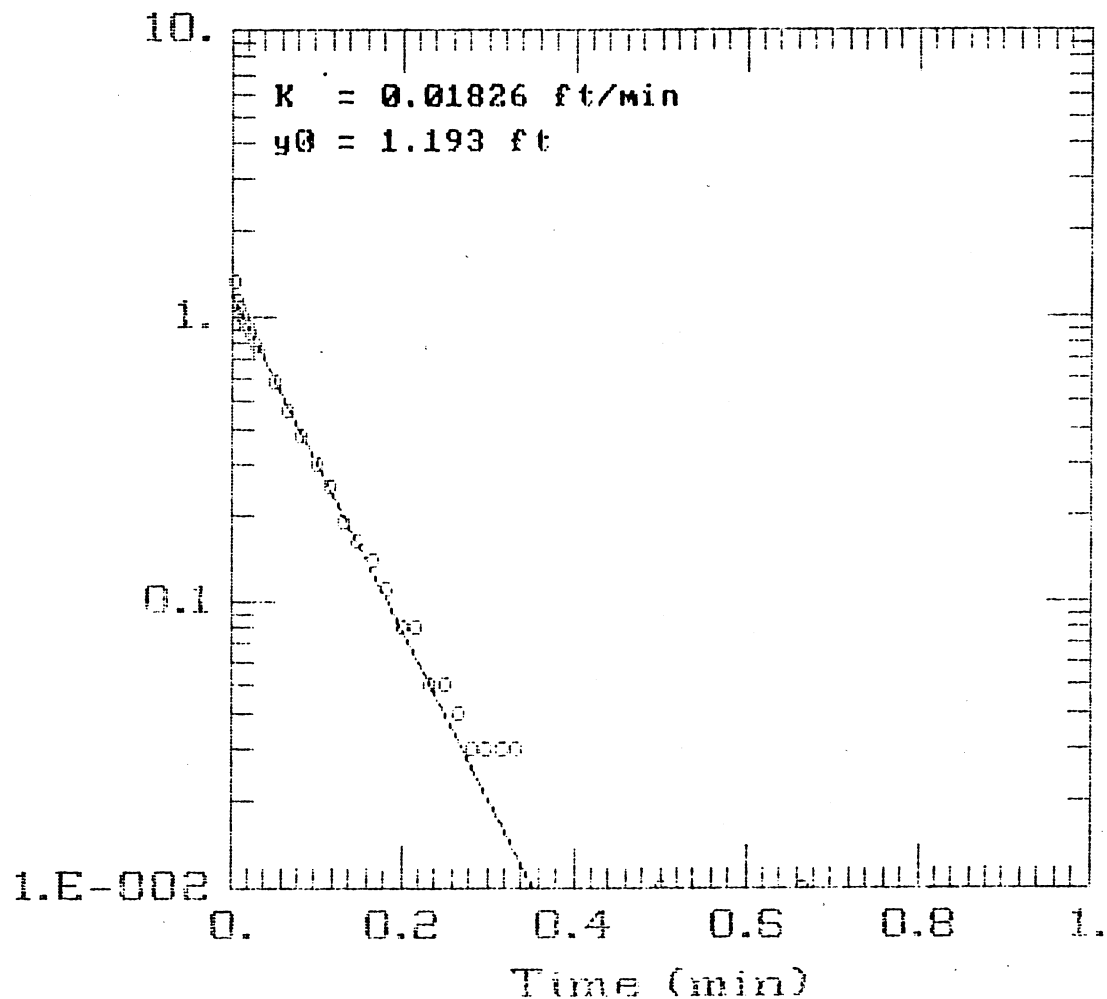
Aqt6a VB2 Elev 1029.4-1032.4





AQTESOLV

 GERAGHTY
& MILLER, INC.
Modeling Group

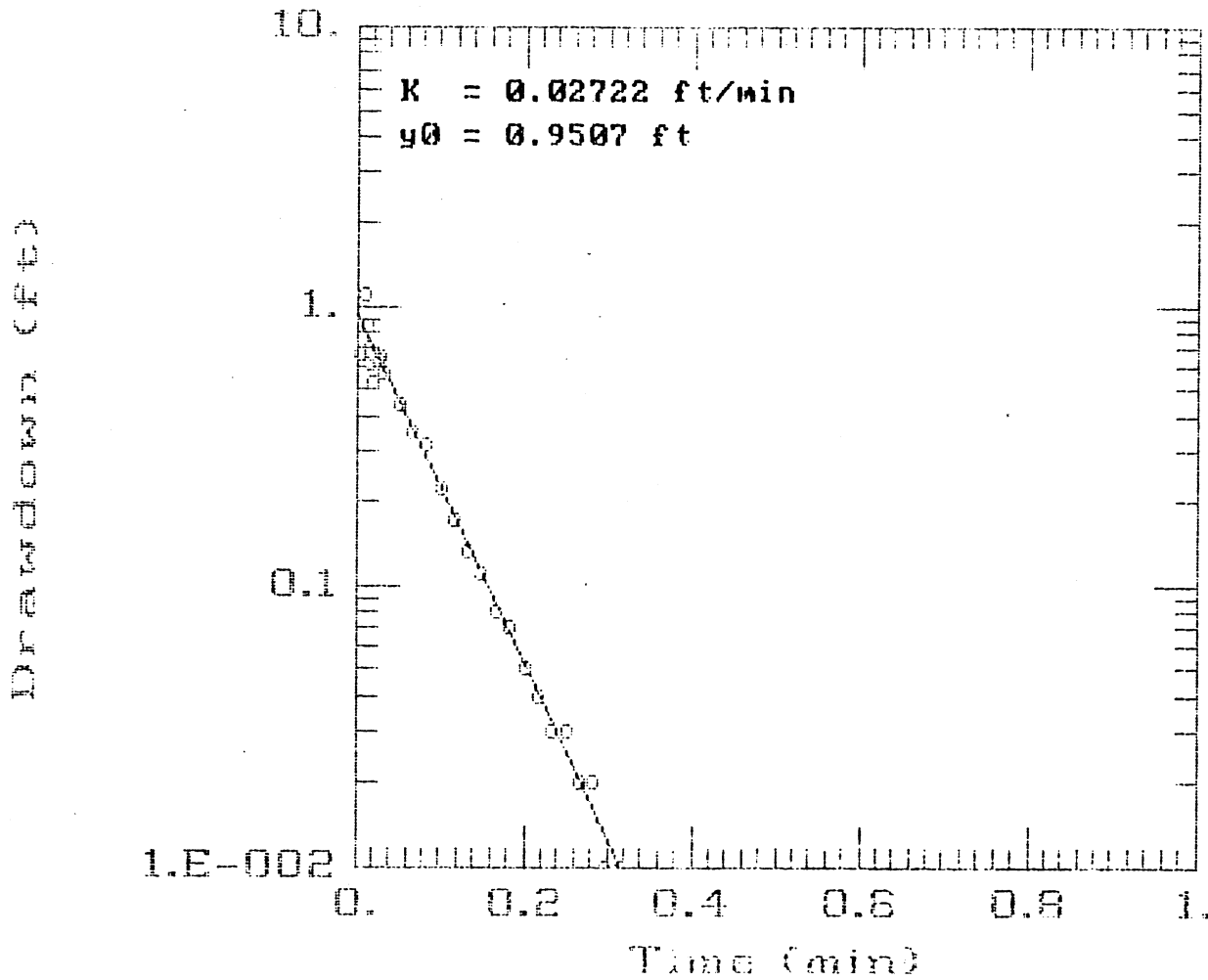
Aqt7a VB2 Elev 1029.4-1032.4




AQTESOLV

 GERAGHTY
& MILLER, INC.
 Modeling Group

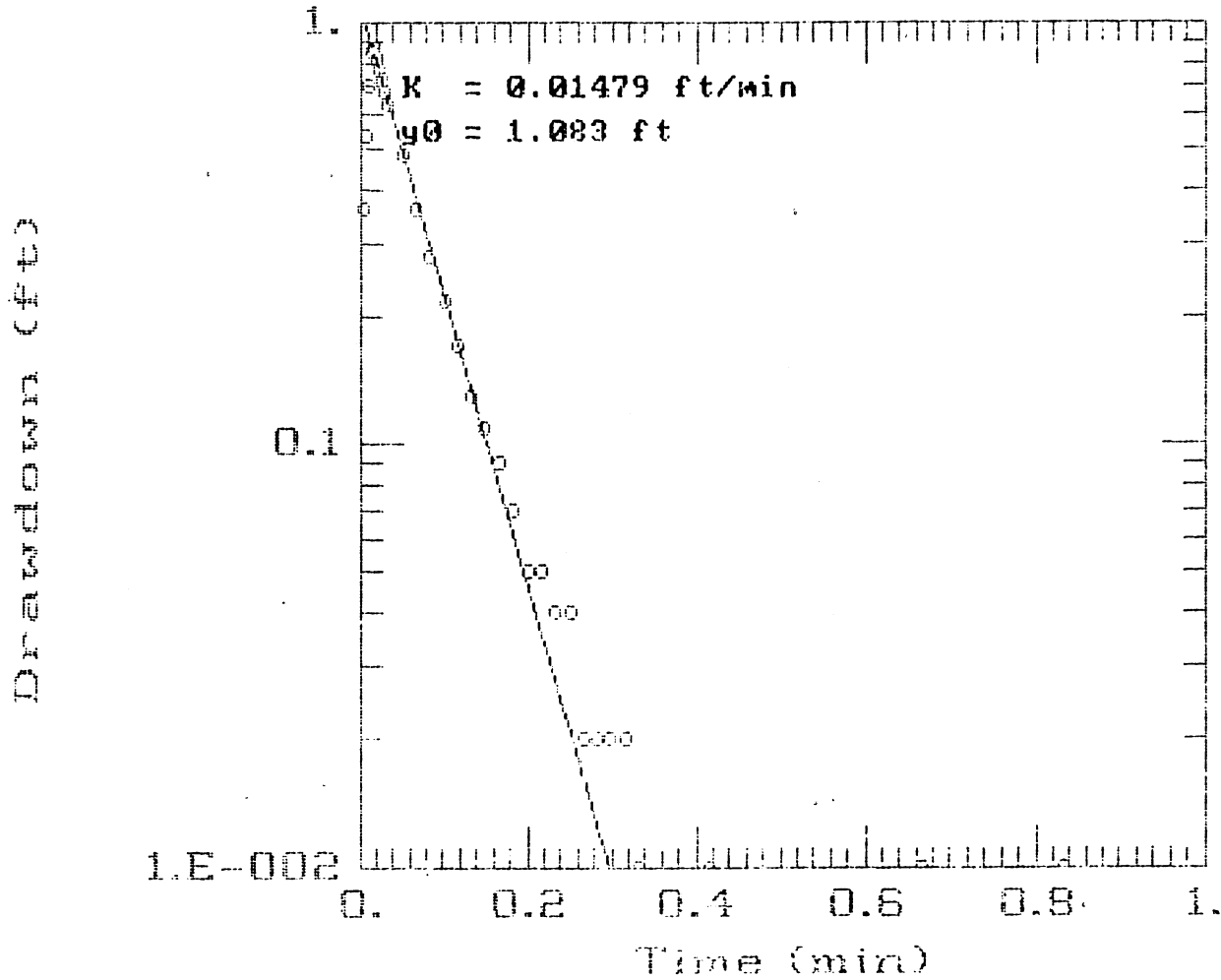
Aqt8a IW2 Elev 1012.2-1018.8



AQTESOLV

 GERAGHTY
& MILLER, INC.
Modeling Group

Aqt9a IW2 Elev 1012.2-1018.8



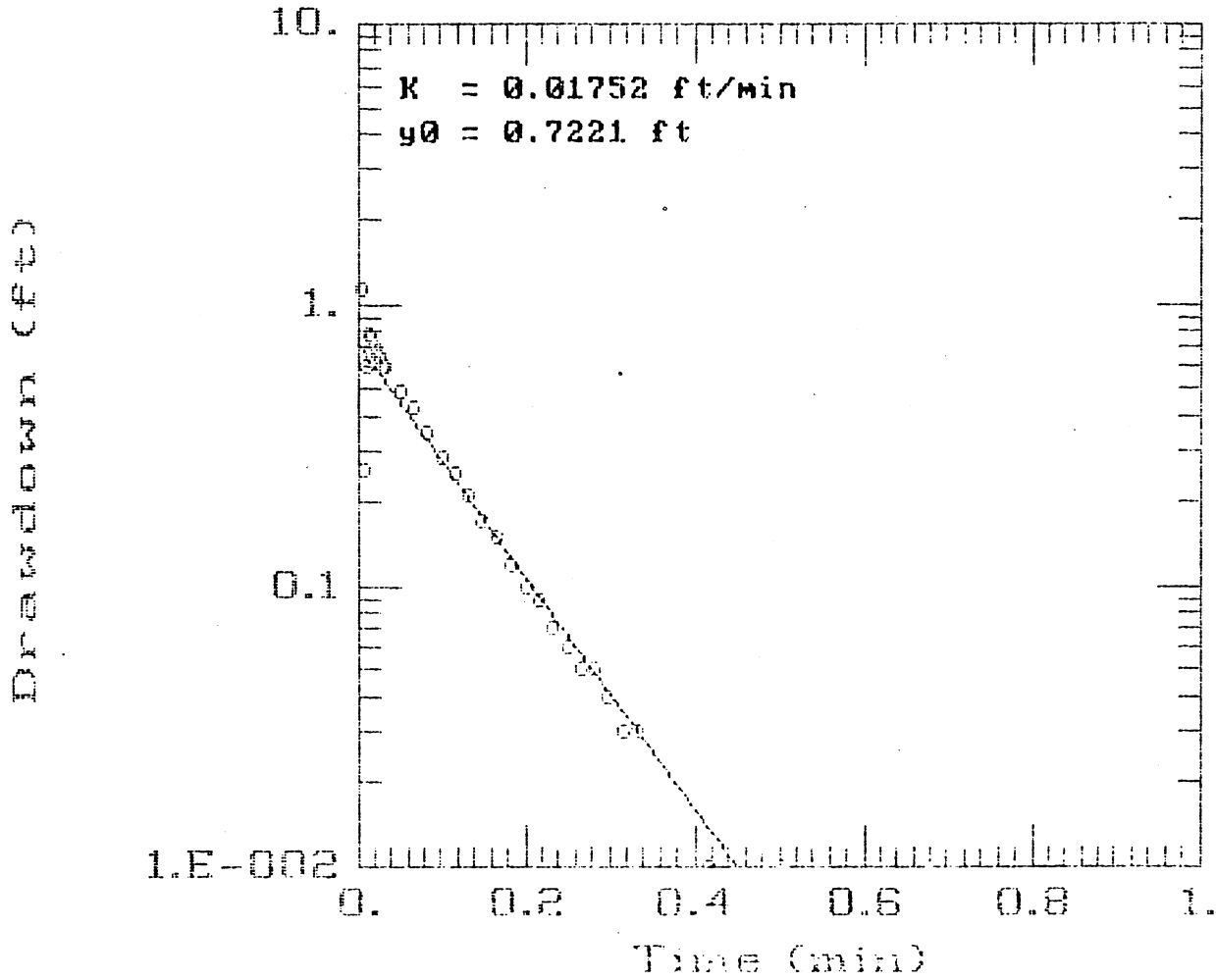
AQTESOLV




GERAGHTY
& MILLER, INC.

Modeling Group

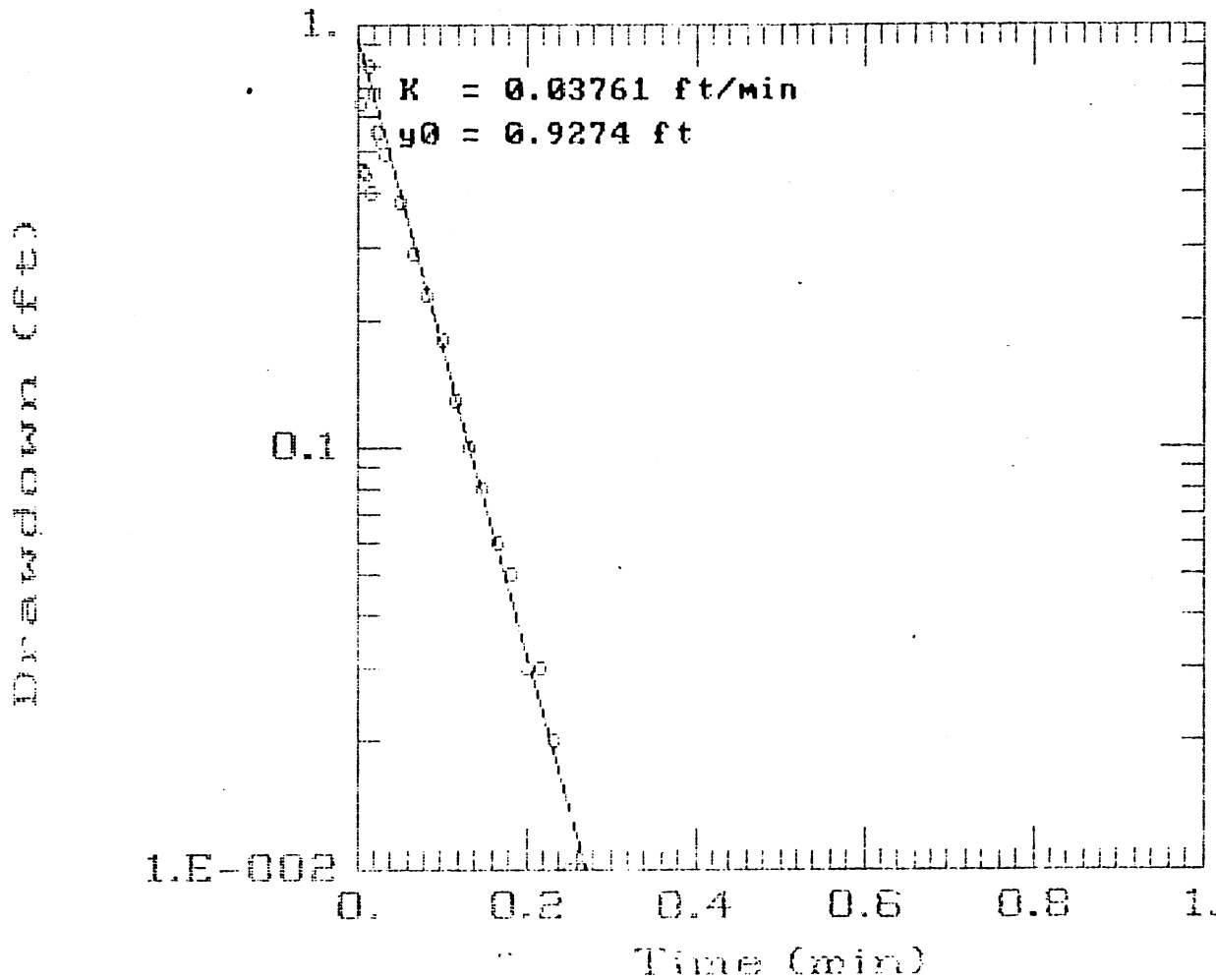
Aqt2b IW4 Elev 1012.9-1019.8





AQTESOLV

 GERAGHTY
& MILLER, INC.
Modeling Group

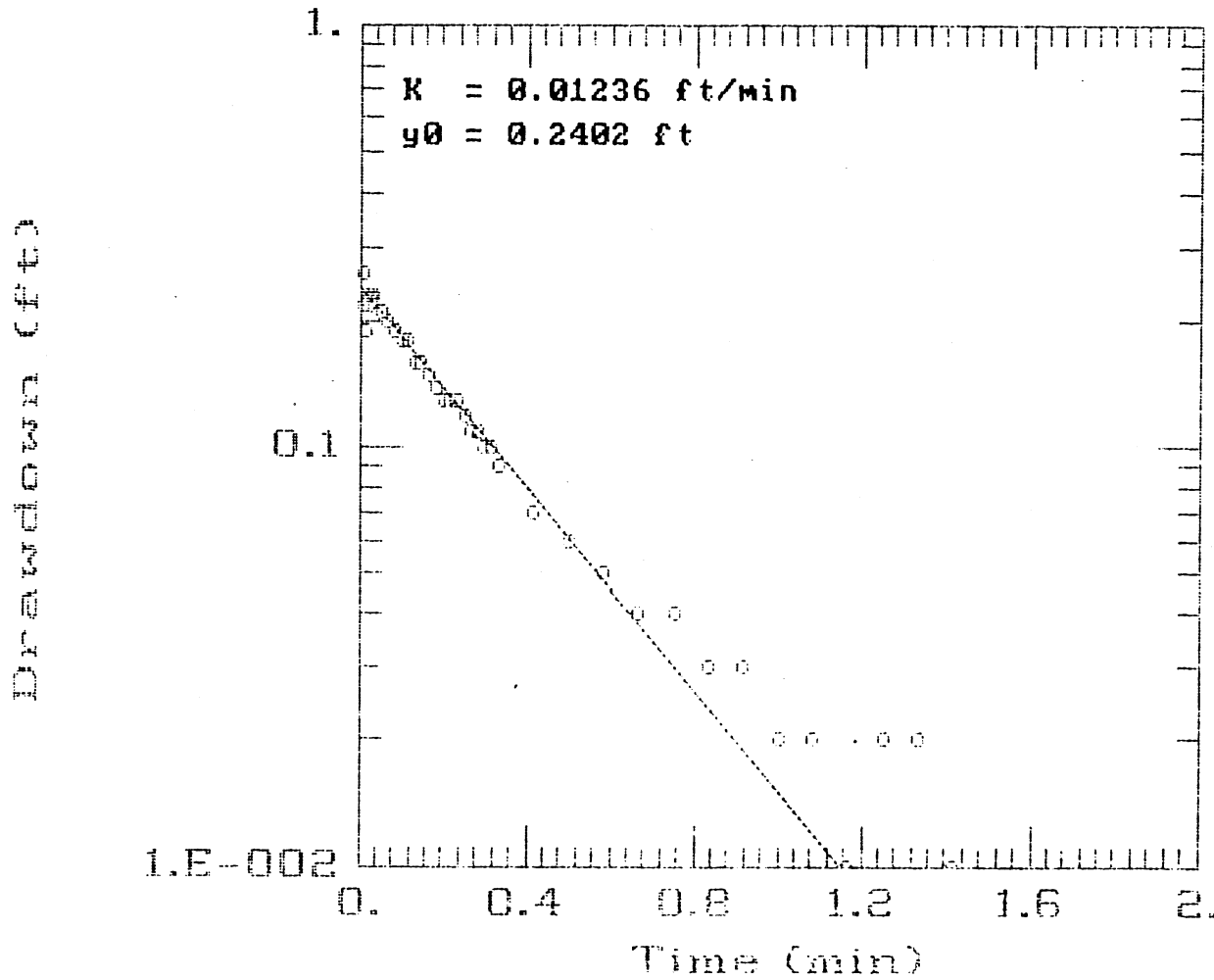
Aqt3b IW9 Elev. 1024.4-1029.1





AQTESOLV

 GERAGHTY
& MILLER, INC.
 Modeling Group

Aqt4b IW7 Elev 1033.4-1034.8

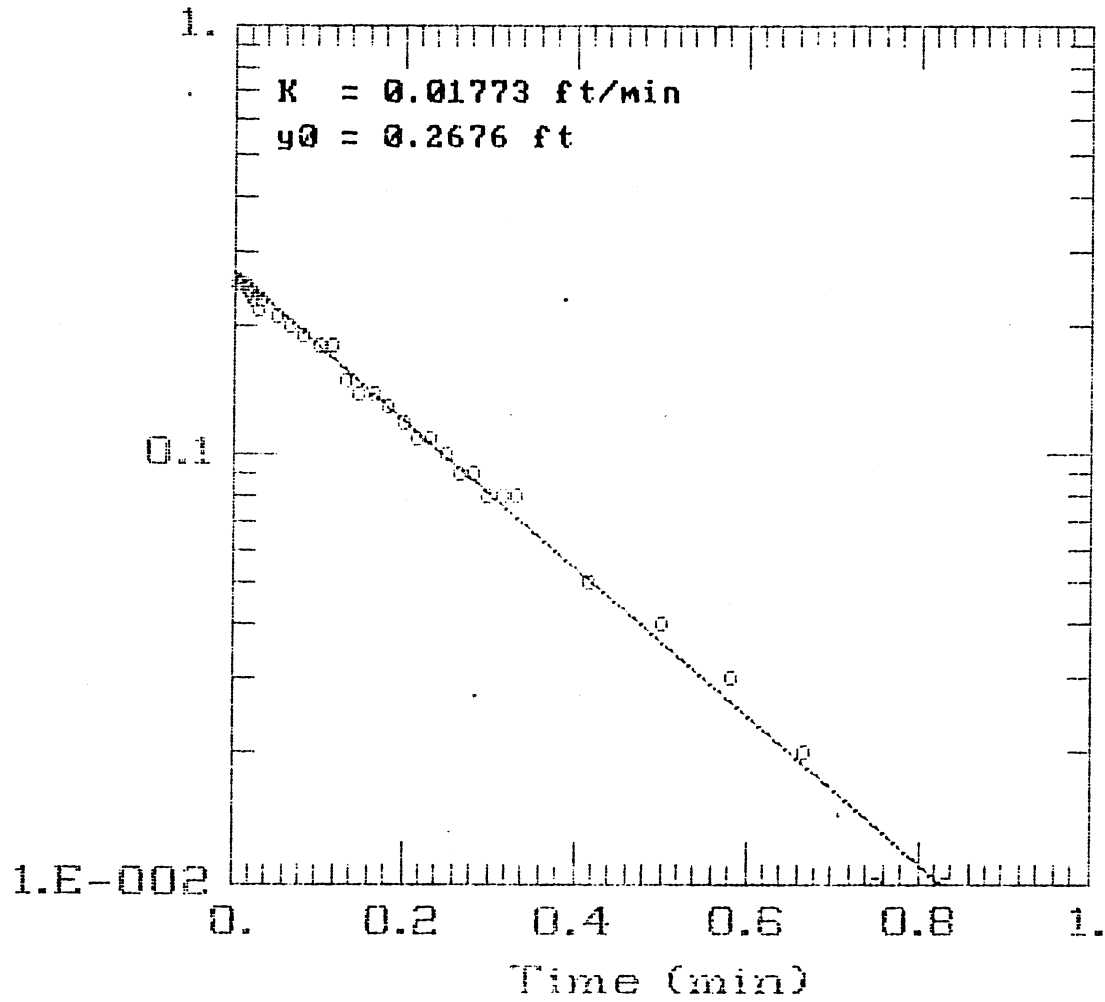


AQTESOLV


 GERAGHTY
& MILLER, INC.
 Modeling Group

Aqt5b IW7 Elev 1033.4-1034.8

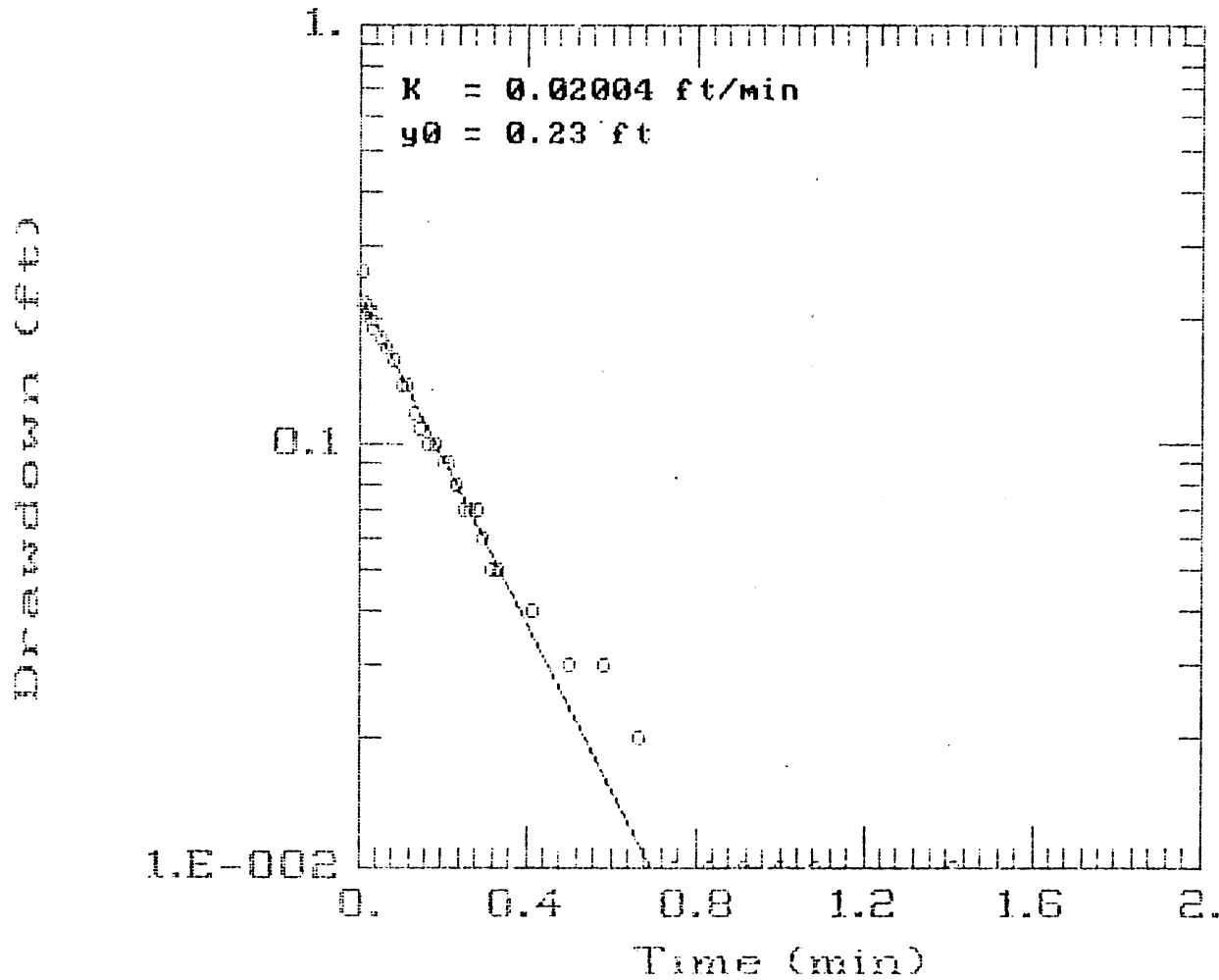
Drawdown (ft)





AQTESOLV

 GERAGHTY
& MILLER, INC.
Modeling Group

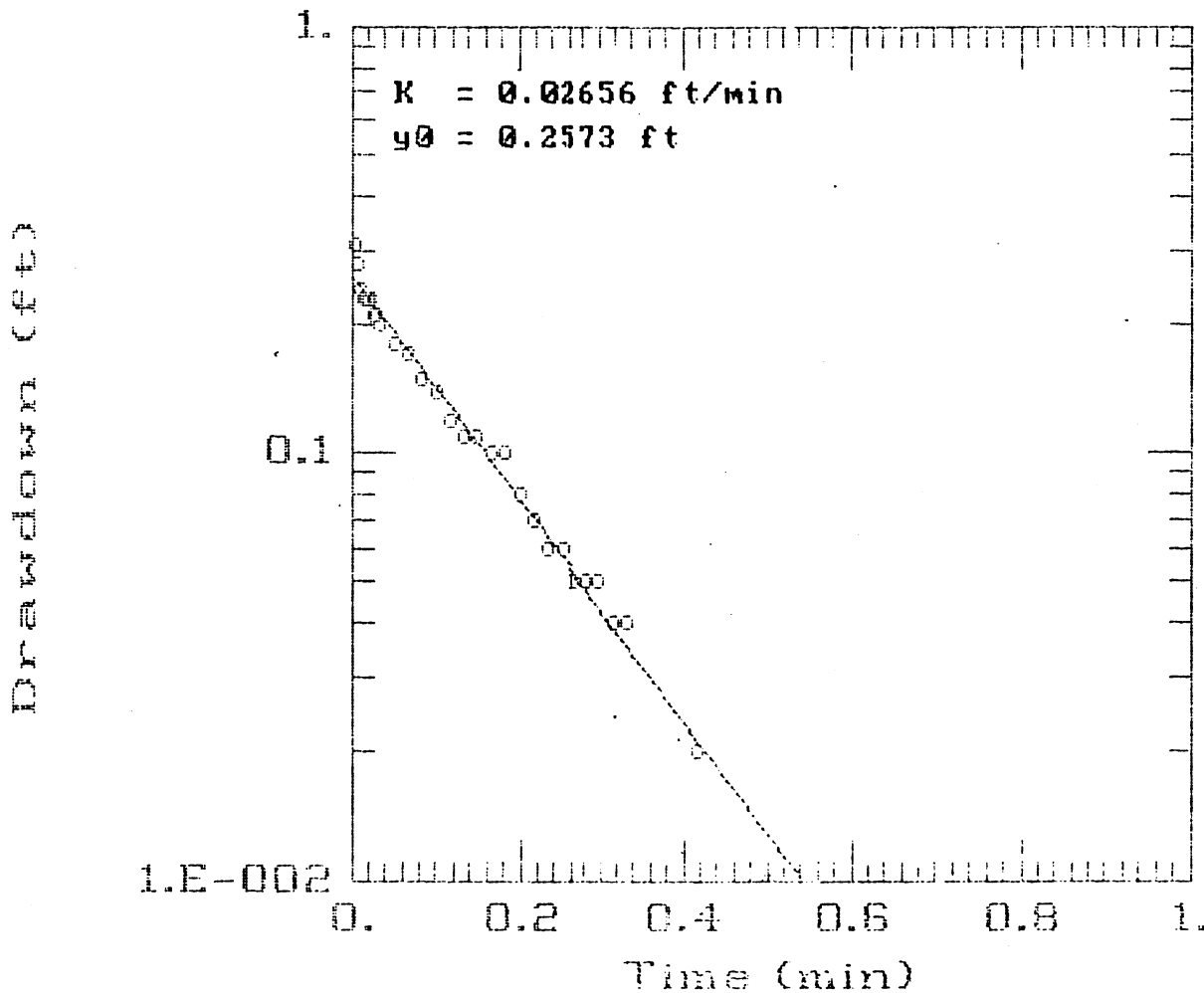
Aqt6b IW8 Elev 1033.5-1034.9




AQTESOLV

 GERAGHTY
& MILLER, INC.
 Modeling Group

Aqt7b IW8 Elev 1033.5-1034.9

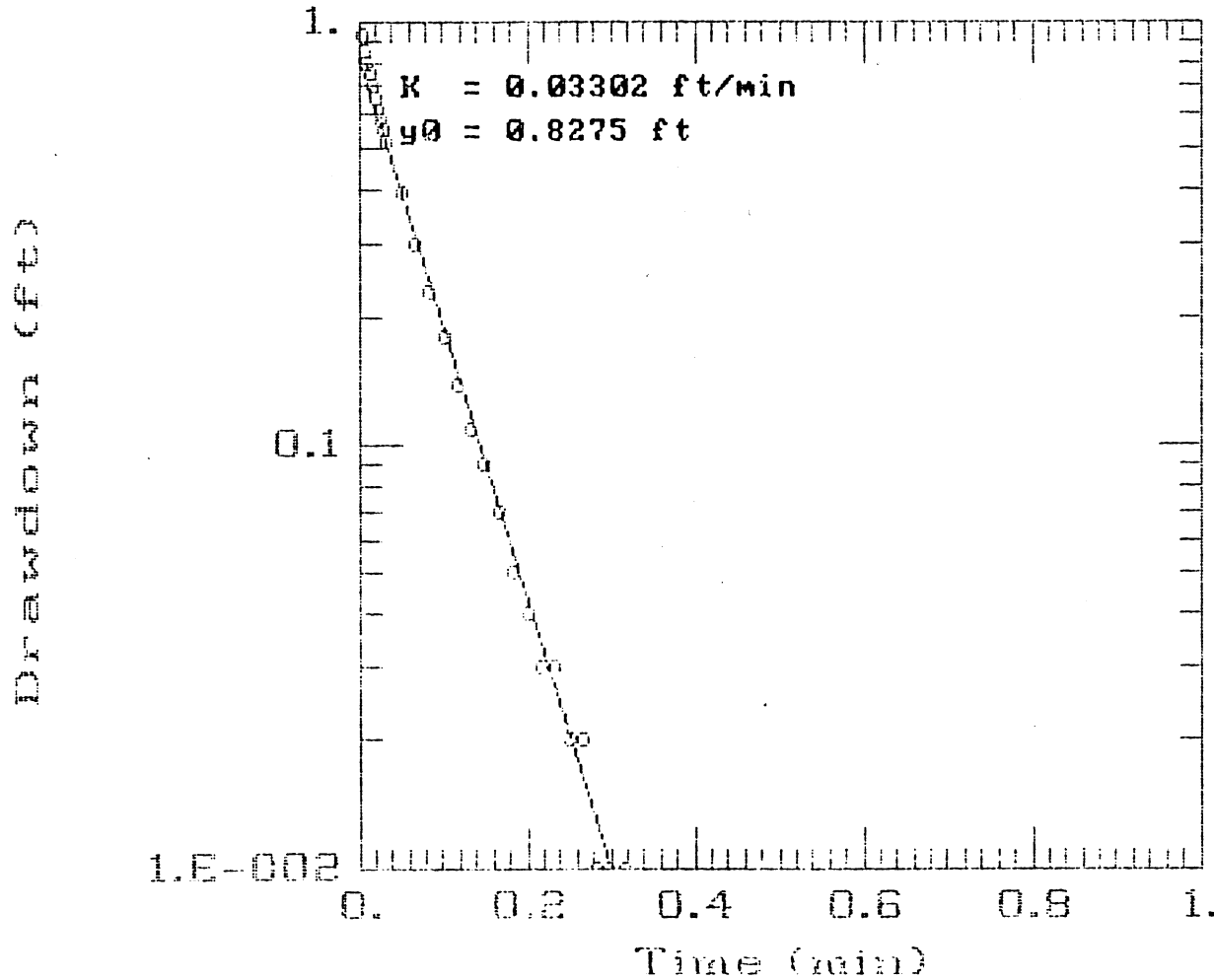


AQTESOLV


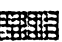
 GERAGHTY
& MILLER, INC.

Modeling Group

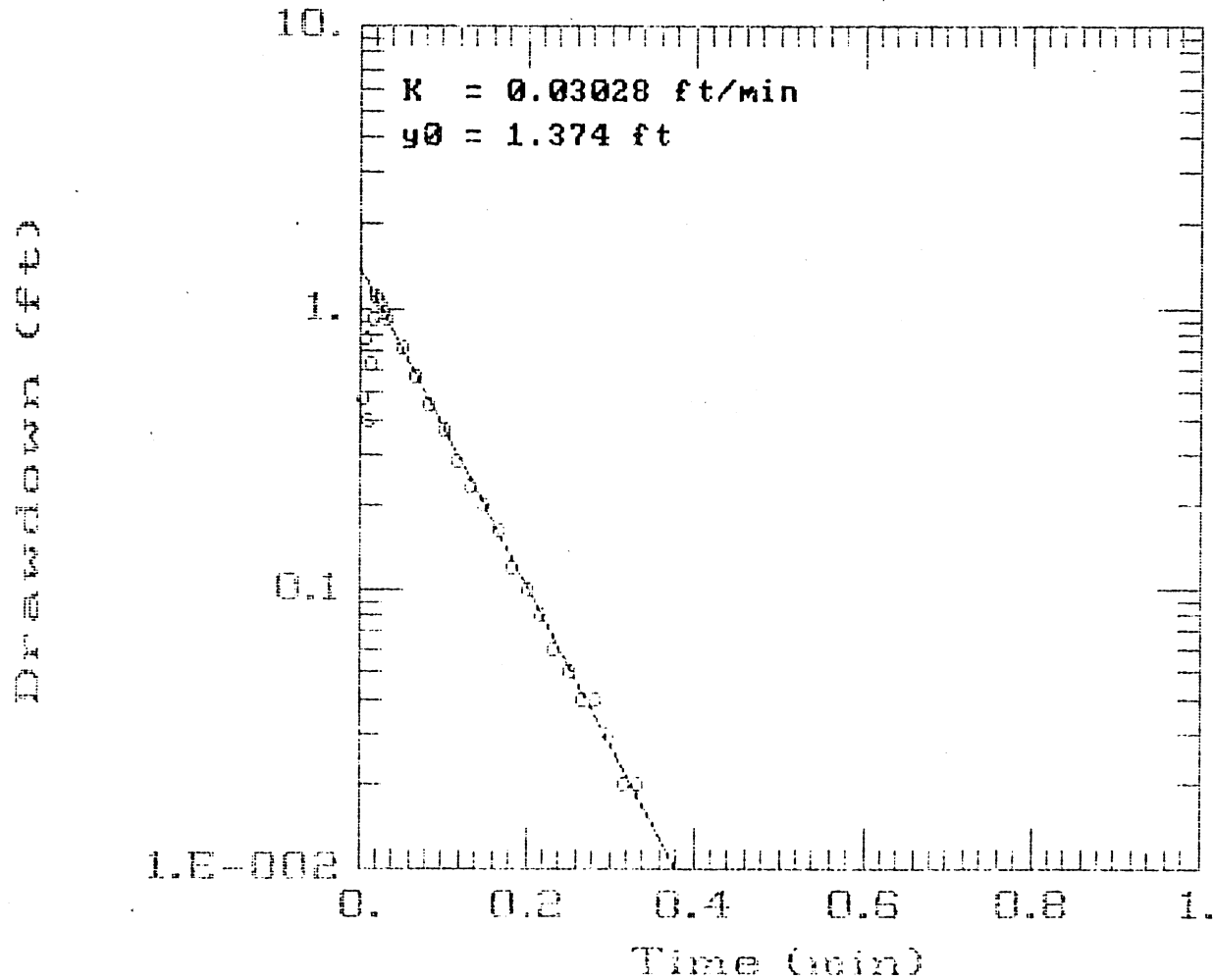
Aqt8b IW9 Elev 1024.4-1029.1




AQTESOLV

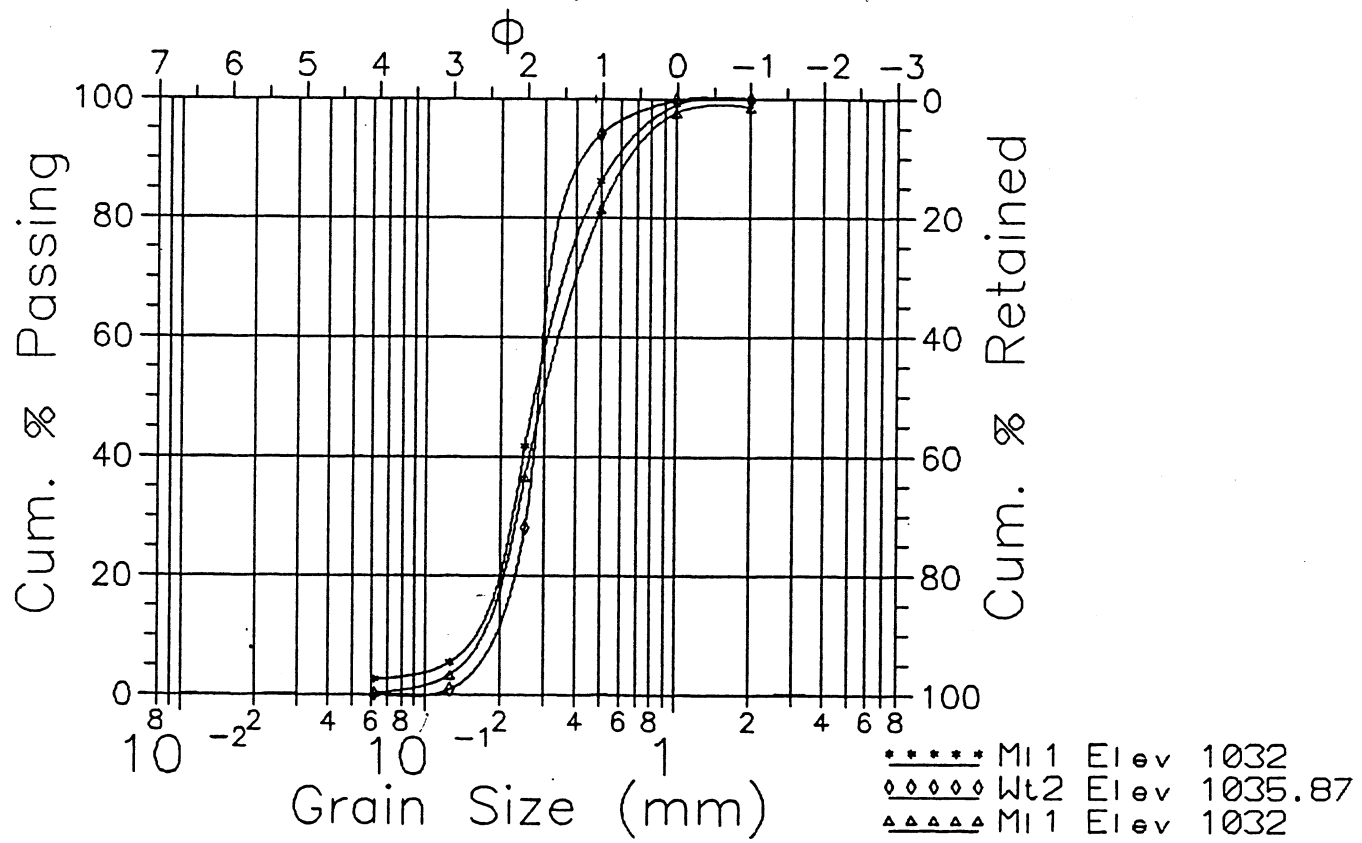
 GERAGHTY
& MILLER, INC.
 Modeling Group

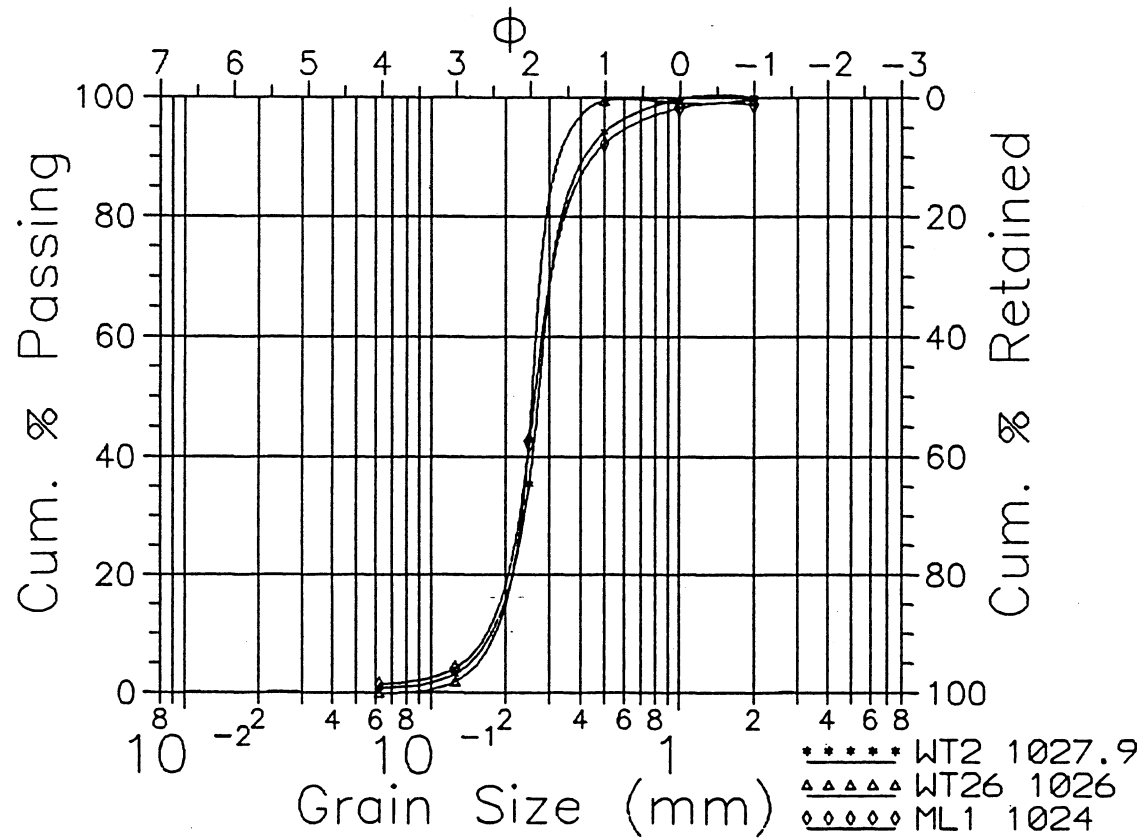
Aqt9b DP3 Elev 1015.7-1018.4

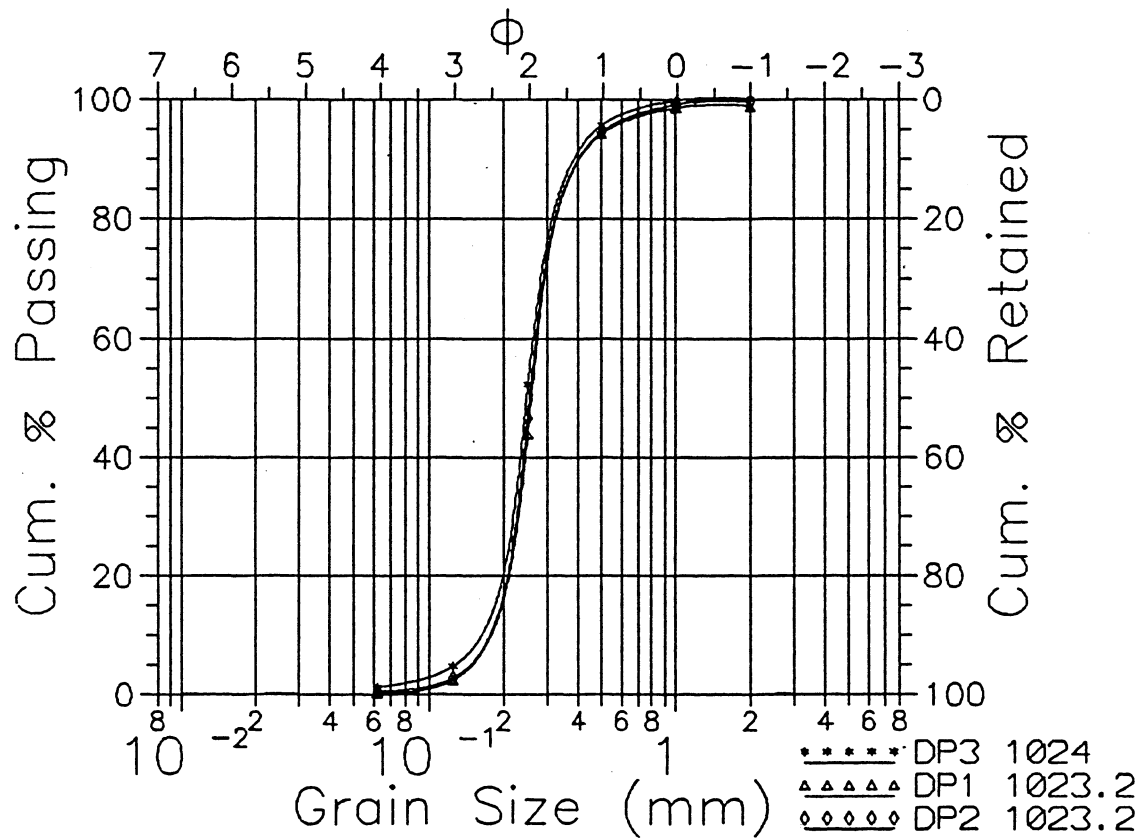


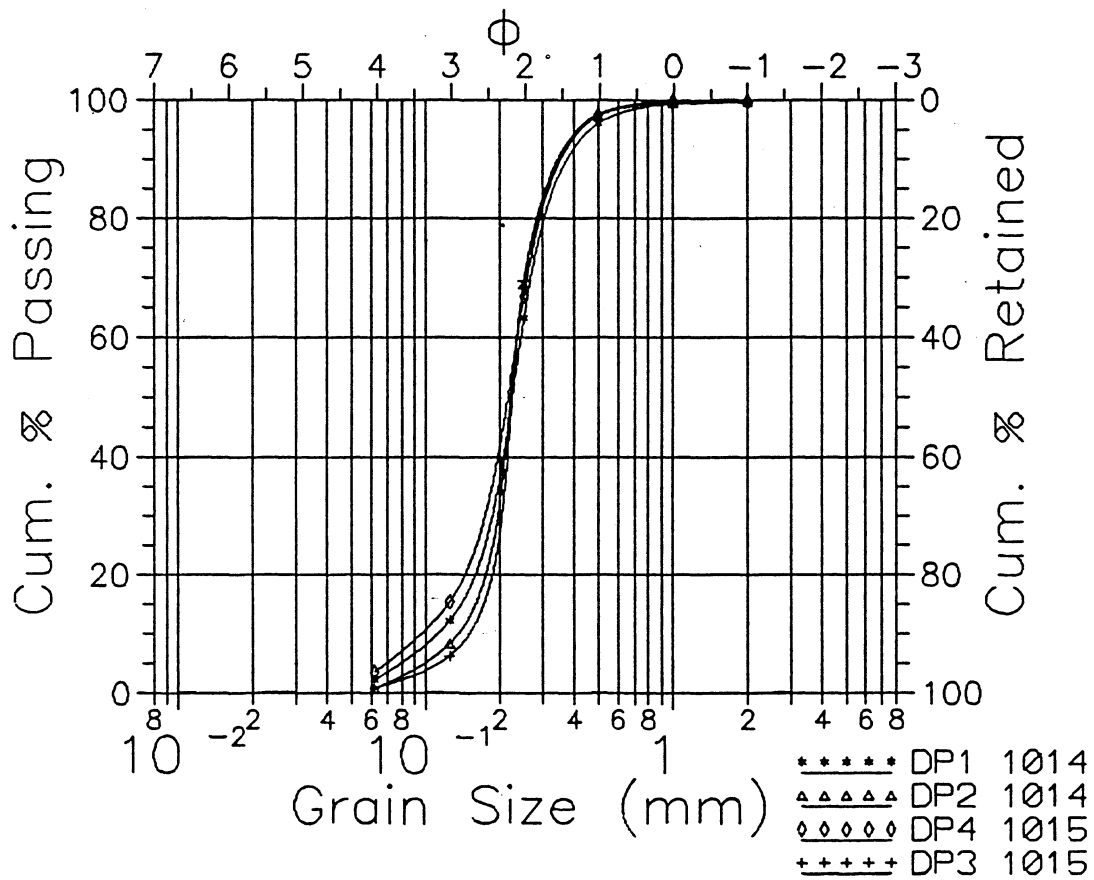
AQTESOLV

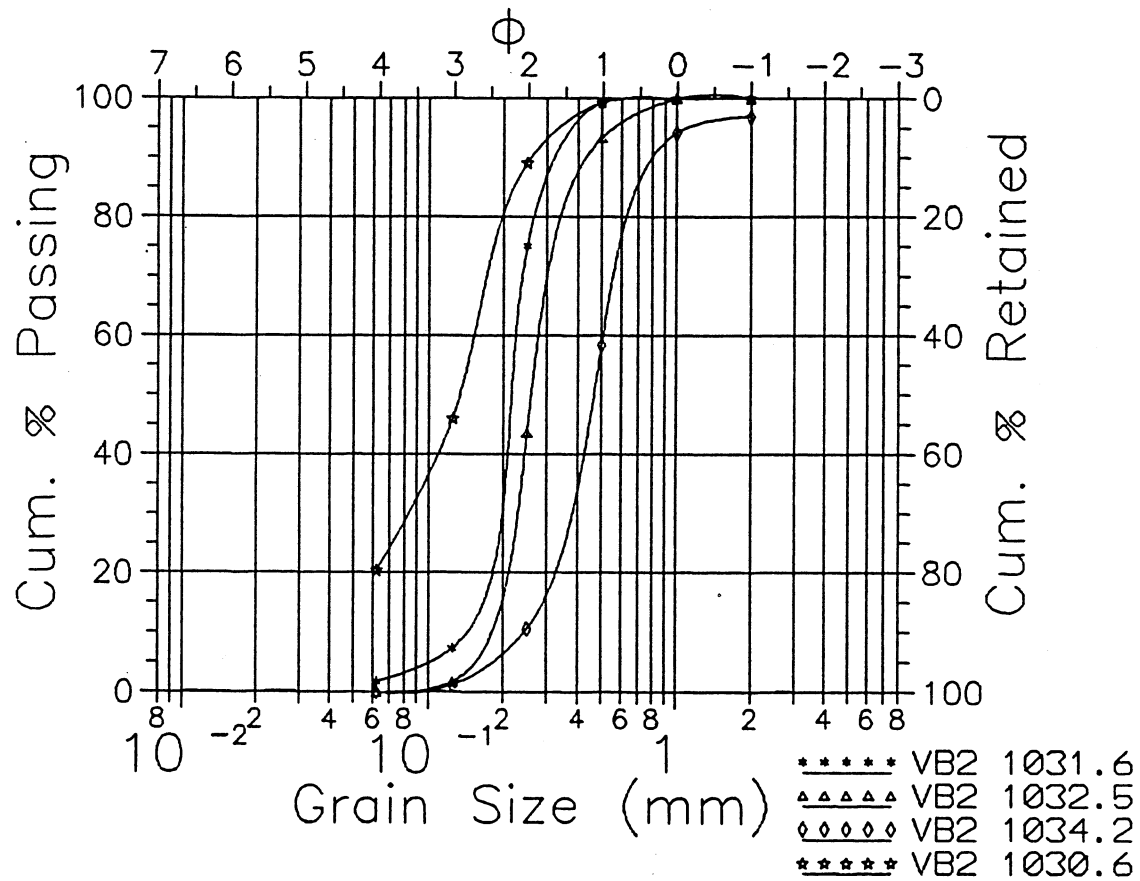
 GERAGHTY
& MILLER, INC.
Modeling Group

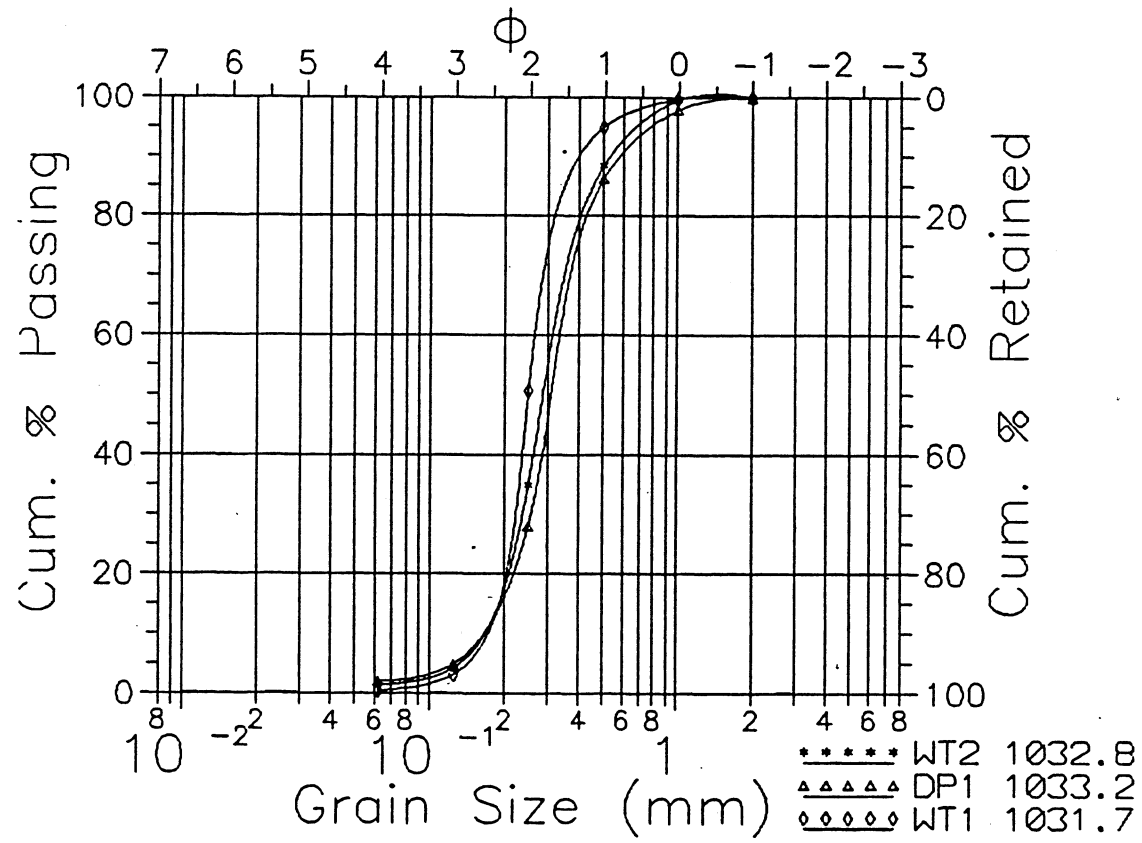












APPENDIX B - Chemical Analyses

SUMMARY OF BACKGROUND CHEMICAL ANALYSES

Sample Point	Elev. fasl	Date Sampled	Spec. Cond. micromhos/cm	Temp. C	pH	DO ppm	Ca ppm	Mg ppm	Na ppm
m17-10	1002.6	6/7/91	135	12	7.53	0.8	31.98	9.73	1.28
m17-11	1005.6	6/7/91	140	12	7.65	0.8	37.41	11.96	1.31
m17-12	1008.6	6/7/91	140	12	7.69	0.8	58.03	21.86	1.28
m17-13	1011.6	6/7/91	140	12	7.66	0.7	51.00	18.75	0.96
m17-14	1014.6	6/7/91	140	12	7.5	1.2	35.34	8.53	1.51
m17-15	1017.6	6/7/91	165	10	7.37	1.0	48.27	10.93	1.25
m17-16	1020.6	6/7/91	165	11	7.16	1.6	40.28	11.65	1.33
m17-17	1023.6	6/6/91	170	12	7.46	1.0	39.49	17.60	1.48
m17-18	1026.6	6/6/91	130	11.5	7.94	0.5	25.39	11.92	0.69
m17-19	1029.6	6/6/91	220	11	7.88	0.5	46.46	21.17	2.53
m17-20	1032.6	6/6/91	250	11.5	7.54	0.5	60.81	24.83	1.93
m17-21	1035.6	6/6/91	320	11	7.18	2.6	111.6	43.88	<.6
m18-11	1001.7	5/28/91	175	13.5	7.78	1.0	37.41	9.76	1.16
m18-12	1004.7	5/28/91	180	15	7.79	2.4?	58.03	10.08	1.14
m18-13	1007.7	5/29/91	160	12.5	7.48	-	51.00	9.78	1.09
m18-14	1010.7	5/29/91	160	12.5	7.49	-	35.23	9.81	1.23
m18-15	1013.7	5/29/91	155	13	7.55	1.0	34.59	9.59	1.18
m18-16	1016.7	5/29/91	190	14	7.64	1.2	40.75	11.43	1.32
m18-17	1019.7	5/29/91	175	13	7.58	1.4	39.71	10.65	1.39
m18-18	1022.7	5/29/91	145	13	7.24	1.2	27.82	7.37	1.54
m18-19	1025.7	5/29/91	155	13	7.48	1.0	31.73	10.61	0.68
m18-20	1028.7	5/29/91	160	14	7.14	2?	27.86	12.62	1.01
m18-21	1031.7	5/29/91	290	18	7.15	1.2	48.70	22.80	1.22
m19-11	1001.2	9/7/90	238	25	8.05	0.3	42.15	9.76	1.16
m19-12	1004.2	9/7/90	182	16	8.02	0.3	42.15	10.08	1.14
m19-13	1007.2	9/7/90	180	16	8.06	0.25	37.55	9.78	1.09
m19-14	1010.2	9/7/90	170	16.5	8.06	0.25	35.77	9.81	1.23
m19-15	1013.2	9/7/90	162	16	8.05	0.25	36.68	9.59	1.18
m19-16	1016.2	9/7/90	187	17	8.00	0.25	47.15	11.43	1.32
m19-17	1019.2	9/7/90	186	17	8.00	0.2	51.27	10.65	1.39
m19-18	1022.2	9/7/90	190	17	7.94	0.2	62.39	7.37	1.54
m19-19	1025.2	9/7/90	162	16.5	7.81	0.2	44.94	10.61	0.68
m19-20	1028.2	9/7/90	196	17	7.52	0.25	90.79	12.62	1.01
m19-21	1031.2	9/7/90	212	18	7.38	0.2	49.28	22.80	1.22

Sample Point	Elev. fasl	Date Sampled	Spec. Cond. micromhos/cm	Temp. C	pH	DO ppm	Ca ppm	Mg ppm	Na ppm
mm7-1	1034.0	5/28/91	360	18.6	7.23	1.9	56.43	25.45	1.025
mm7-2	1035.0	5/28/91	300	21.6	7.06	3.2	44.53	21.07	1.125
mm20-1	1024.2	5/29/91	145	16.2	7.04	1.4	26.84	7.489	1.643
mm20-2	1026.0	5/29/91	150	14.5	7.36	1.0	30.13	8.445	1.153
mm20-3	1027.8	5/29/91	155	12.9	7.45	1.2	30.3	9.878	2.595
mm20-4	1028.3	5/29/91	165	13.6	7.40	2.0	31.31	10.85	0.894
mm20-5	1030.0	5/29/91	165	13.6	7.21	1.4	26.71	12.61	1.118
mm20-6	1031.8	5/29/91	190	13.6	7.27	1.0	34.98	15.32	1.13
mm38-1	1023.3	5/29/91	165	13	7.61	2.0	37.3	10.24	<.6
mm38-2	1024.8	5/29/91	160	13	7.52	1.8	36.1	12.12	<.6
mm38-3	1026.3	5/29/91	165	13	7.33	1.6	31.67	14.52	<.6
mm38-4	1028.0	5/29/91	165	13	7.36	1.1	34.08	14.94	<.6
mm38-5	1029.5	5/29/91	210	13	7.43	1.0	41.81	18.94	<.6
mm38-6	1031.0	5/29/91	310	13	7.35	1.0	59.21	27.85	<.6

Sample Point	Elev. fasl	Date Sampled	Cl ppm	S ppm	Alkalinity mg/L CaCO3	Fe ppm	Mn ppm
m17-10	1002.6	6/7/91	-	8.56	80	0.90	.086
m17-11	1005.6	6/7/91	-	8.19	80	1.31	.103
m17-12	1008.6	6/7/91	-	8.47	75	3.43	.177
m17-13	1011.6	6/7/91	-	8.26	70	3.12	.162
m17-14	1014.6	6/7/91	-	8.83	65	2.11	.064
m17-15	1017.6	6/7/91	-	11.12	95	5.25	.084
m17-16	1020.6	6/7/91	-	8.43	85	4.99	.070
m17-17	1023.6	6/6/91	-	8.26	90	5.82	.106
m17-18	1026.6	6/6/91	-	9.06	70	1.01	.029
m17-19	1029.6	6/6/91	-	13.96	105	1.21	.048
m17-20	1032.6	6/6/91	-	14.69	155	1.39	.057
m17-21	1035.6	6/6/91	-	15.69	180	4.70	.216
m18-11	1001.7	5/28/91	0.33	7.16	118	0.83	.065
m18-12	1004.7	5/28/91	0.33	6.98	103.5	0.96	.083
m18-13	1007.7	5/29/91	0.35	7.00	110.5	0.86	.080
m18-14	1010.7	5/29/91	0.21	7.02	96.5	0.89	.081
m18-15	1013.7	5/29/91	0.34	6.83	96.5	0.87	.083
m18-16	1016.7	5/29/91	0.19	8.40	135.5	0.98	.064
m18-17	1019.7	5/29/91	0.19	8.21	114	0.97	.071
m18-18	1022.7	5/29/91	0.73	6.98	78.5	3.68	.045
m18-19	1025.7	5/29/91	0.15	5.09	100	1.08	.037
m18-20	1028.7	5/29/91	0.15	7.75	96.5	3.91	.116
m18-21	1031.7	5/29/91	0.40	31.03	114	3.41	.111
m19-11	1001.2	9/7/90	1.0	6.70	-	1.04	.122
m19-12	1004.2	9/7/90	1.5	6.27	100	1.23	.136
m19-13	1007.2	9/7/90	1.5	6.16	-	0.99	.122
m19-14	1010.2	9/7/90	2.0	5.86	-	1.12	.139
m19-15	1013.2	9/7/90	1.0	5.68	-	1.25	.161
m19-16	1016.2	9/7/90	4.0	6.19	96	2.03	.167
m19-17	1019.2	9/7/90	2.5	6.13	-	2.30	.185
m19-18	1022.2	9/7/90	0.5	6.19	104	4.00	.210
m19-19	1025.2	9/7/90	1.5	5.31	-	2.05	.266
m19-20	1028.2	9/7/90	2.5	6.72	-	9.21	.515
m19-21	1031.2	9/7/90	0.5	10.41	107	3.81	.246

Sample Point	Elev. fasl	Date Sampled	Cl ppm	S ppm	Alkalinity mg/L CaCO3	Fe ppm	Mn ppm
mm7-1	1034.0	5/28/91	0.76	34.57	139.5	0.80	.073
mm7-2	1035.0	5/28/91	0.59	6.95	135.5	0.07	.062
mm20-1	1024.2	5/29/91	0.80	7.18	64.5	5.66	.061
mm20-2	1026.0	5/29/91	0.51	5.61	89.5	1.86	.032
mm20-3	1027.8	5/29/91	0.12	5.03	82	0.98	.033
mm20-4	1028.3	5/29/91	0.43	6.49	85.5	1.38	.046
mm20-5	1030.0	5/29/91	0.48	7.54	85.5	3.51	.126
mm20-6	1031.8	5/29/91	0.45	14.88	103.5	3.40	.072
mm38-1	1023.3	5/29/91	0.43	6.31	85.5	1.04	.036
mm38-2	1024.8	5/29/91	0.18	6.53	93	1.28	.045
mm38-3	1026.3	5/29/91	0.33	8.87	89	3.71	.138
mm38-4	1028.0	5/29/91	0.36	9.39	78.5	4.39	.104
mm38-5	1029.5	5/29/91	0.57	17.20	93	3.86	.073
mm38-6	1031.0	5/29/91	0.81	40.23	132	2.04	.149

APPENDIX C - Bromide and Nitrate Concentrations, 1991 Experiment

Laboratory Measurements of Concentration, 1991 Tracer Experiment

Tracer injection began at Julian day 169.485

Analyses by ion-chromatography (IC, Br and NO3-N) or specific ion electrode (Br only).

Sample Point	Julian Day	Br ppm	NO3-N ppm	Method	Notes
inj soln	169.5210	47.80024	12.31182	IC	Sampled from tracer tank
inj soln	169.5937	47.45256	12.39225	IC	Sampled from tracer tank
inj soln	169.6493	43.91852	11.39302	IC	Sampled from tracer tank
mm57-1	169.6888	0	0	IC	
mm57-1	169.775	0	0	IC	
mm57-1	170.2465	0	0	IC	
mm57-1	170.4104	0	0	IC	
mm57-1	170.535	0	0	IC	
mm57-1	170.6284	0.842930	0.378318	IC	
mm57-1	170.7083	2.927931	0.818756	IC	
mm57-1	171.2409	40.87647	9.807459	IC	
mm57-1	172.3423	3.272806	1.346858	IC	
mm57-1	172.7777	1.449542	0	IC	
mm57-1	173.4791	0.158477	0	IC	
mm57-1	174.5	0.117397	0	IC	
mm57-1	175.2986	0	0	IC	
mm57-1	176.2916	0	0.038240	IC	
mm57-1	177.3513	0	0	IC	
mm57-2	169.6881	0	0	IC	
mm57-2	169.7729	0.720057	0	IC	
mm57-2	169.9444	5.573539	1.651414	IC	
mm57-2	170.2472	22.06155	5.215494	IC	
mm57-2	170.4111	34.85570	8.305030	IC	
mm57-2	170.5361	38.70094	8.928987	IC	
mm57-2	170.7090	44.05581	10.72538	IC	
mm57-2	171.2229	43.96750	10.61424	IC	
mm57-2	172.3430	45.57831	10.37007	IC	
mm57-2	172.7784	44.69437	9.638496	IC	
mm57-2	173.4798	40.30034	7.689378	IC	
mm57-2	174.5013	9.509899	0.554058	IC	
mm57-2	175.2993	3.059215	0	IC	
mm57-2	176.2923	1.685581	0	IC	
mm57-2	177.3520	0.718813	0	IC	
mm57-3	169.6875	3.332395	0.809564	IC	
mm57-3	169.7770	8.353540	1.955428	IC	
mm57-3	169.9444	23.35172	5.692978	IC	
mm57-3	170.2479	37.87376	9.007731	IC	

Sample Point	Julian Day	Br ppm	NO3-N ppm	Method	Notes
mm57-3	170.4118	40.17379	9.744539	IC	
mm57-3	170.7104	45.96418	11.16582	IC	
mm57-3	171.2236	46.80893	11.36340	IC	
mm57-3	171.7513	47.76317	12.12642	IC	
mm57-3	172.3437	33.75781	8.244899	IC	
mm57-3	172.7791	17.42834	3.987935	IC	
mm57-3	173.0048	10.19325	2.248148	IC	
mm57-3	173.4805	7.509396	1.670228	IC	
mm57-3	174.5020	3.249181	0.707228	IC	
mm57-3	175.3	0.824011	0	IC	
mm57-3	176.2930	0	0	IC	
mm57-3	177.3527	0	0	IC	
mm57-4	169.6868	0	0.136654	IC	
mm57-4	169.7784	0	0	IC	
mm57-4	170.2486	18.00674	4.265817	IC	
mm57-4	170.4131	32.68622	7.825781	IC	
mm57-4	170.7111	45.62244	11.15229	IC	
mm57-4	171.2243	46.40960	11.23109	IC	
mm57-4	172.3444	50.33178	16.53112	IC	
mm57-4	172.7798	47.54058	8.862108	IC	
mm57-4	173.4812	4.957426	0.276735	IC	
mm57-4	174.5027	0.180483	0.092765	IC	
mm57-4	175.3006	0	0	IC	
mm57-4	176.2937	0	0.036606	IC	
mm57-4	177.3548	0	0	IC	
mm57-5	169.6854	0	0.910272	IC	
mm57-5	169.7597	0	1.276247	IC	
mm57-5	169.9444	2.378842	2.730458	IC	
mm57-5	170.2493	42.25879	10.45253	IC	
mm57-5	170.4145	47.62681	11.31341	IC	
mm57-5	170.7118	47.02012	11.33341	IC	
mm57-5	171.225	47.16987	11.44454	IC	
mm57-5	171.7527	48.68127	10.98524	IC	
mm57-5	172.3451	31.58325	7.673608	IC	
mm57-5	172.7805	7.436641	1.672638	IC	
mm57-5	173.0055	1.563688	0.347459	IC	
mm57-5	173.4819	0	0	IC	
mm57-5	174.5034	0	0	IC	
mm57-5	175.3013	0	0	IC	
mm57-5	176.2944	0	0	IC	
mm57-5	177.3555	0	0	IC	
mm57-6	169.6840	0	0	IC	
mm57-6	169.7618	0	0	IC	
mm57-6	170.25	1.130914	0.414776	IC	
mm57-6	170.4152	9.255888	2.184173	IC	

Sample Point	Julian Day	Br ppm	NO3-N ppm	Method	Notes
mm57-6	170.7125	29.34561	6.956665	IC	
mm57-6	171.2256	36.79479	8.748408	IC	
mm57-6	172.3458	45.46827	7.254042	IC	
mm57-6	172.7812	41.75279	6.343794	IC	
mm57-6	173.4826	14.45666	0.446271	IC	
mm57-6	174.5041	9.803323	0.504995	IC	
mm57-6	175.3020	3.142138	0	IC	
mm57-6	176.2951	1.411191	0	IC	
mm57-6	177.3576	0.441726	0	IC	
mm57-7	169.6819	0	0	IC	
mm57-7	169.7652	0	0	IC	
mm57-7	170.2506	0	0	IC	
mm57-7	170.4166	0	0	IC	
mm57-7	170.6291	0	0	IC	
mm57-7	170.7138	0	0	IC	
mm57-7	171.2263	1.150113	0.444178	IC	
mm57-7	171.7541	7.424515	1.603939	IC	
mm57-7	172.3465	19.97477	4.510414	IC	
mm57-7	172.7819	25.97706	5.924782	IC	
mm57-7	173.4833	25.50415	5.636123	IC	
mm57-7	174.5055	15.29419	3.121356	IC	
mm57-7	175.3027	6.785385	0.471022	IC	
mm57-7	176.2958	0.545549	0	IC	
mm57-7	177.3590	0	0.056565	IC	
mm58-1	169.8062	0	0	IC	
mm58-1	170.5402	0	0	IC	
mm58-1	170.6326	0	0	IC	
mm58-1	171.4034	0	0	IC	
mm58-1	171.4583	0	0.031313	IC	
mm58-1	171.4861	0	0	IC	
mm58-1	171.5833	0	0.032698	IC	
mm58-1	171.6666	0	0.009247	IC	
mm58-1	171.7569	0	0.016910	IC	
mm58-1	171.8333	0	0	IC	
mm58-1	172	0	0.007031	IC	
mm58-1	172.2083	0	0.033344	IC	
mm58-1	172.3333	0	0.018387	IC	
mm58-1	172.5833	0	0.048300	IC	
mm58-1	172.7708	1.917797	0	IC	
mm58-1	173	9.872473	1.010204	IC	
mm58-1	173.2673	28.24590	3.804822	IC	
mm58-1	173.4687	37.95950	6.844908	IC	
mm58-1	173.6631	42.48009	15.21499	IC	
mm58-1	173.9583	25.27920	13.31396	IC	
mm58-1	174.3451	10.97018	0	IC	
mm58-1	174.5083	8.292841	0.501855	IC	

Sample Point	Julian Day	Br ppm	NO3-N ppm	Method	Notes
mm58-1	174.7138	6.619159		0 IC	
mm58-1	174.9583	4.000169		0 IC	
mm58-1	175.2916	4.066073		0 IC	
mm58-1	175.5	1.637930		0 IC	
mm58-1	175.7083	1.414818		0 IC	
mm58-1	175.9583	0		0 IC	
mm58-1	176.3020	0		0 IC	
mm58-1	176.4791	0	0.123442	IC	
mm58-1	176.7013	0	0.153989	IC	
mm58-1	176.9513	0		0 IC	
mm58-1	177.3437	0		0 IC	
mm58-1	177.5416	0		0 IC	
mm58-1	177.7694	0		0 IC	
mm58-1	177.9083	0		0 IC	
mm58-1	178.4270	0		0 IC	
mm58-1	178.6145	0		0 IC	
mm58-1	179.4305	0		0 IC	
mm58-1	180.2833	0		0 IC	
mm58-1	181.5611	0		0 IC	
mm58-1	182.4479	0		0 IC	
mm58-2	169.8076	0		0 IC	
mm58-2	170.5416	0		0 IC	
mm58-2	170.6333	0		0 IC	
mm58-2	171.4	0		0 IC	
mm58-2	171.4875	1.080997	0.452410	IC	
mm58-2	171.5840	1.068762	0.098731	IC	
mm58-2	171.6673	4.633243	0.444960	IC	
mm58-2	171.7576	3.438581	0.287738	IC	
mm58-2	171.8340	6.222874	0.842273	IC	
mm58-2	172.0006	2.502356	0.112921	IC	
mm58-2	172.2090	4.248025	0.433041	IC	
mm58-2	172.3340	4.525967	0.535774	IC	
mm58-2	172.4590	3.989588	0.322361	IC	
mm58-2	172.5840	9.041300	1.466053	IC	
mm58-2	172.7715	12.13279	2.172701	IC	
mm58-2	173.0006	36.61604	8.934957	IC	
mm58-2	173.2680	23.05053	4.872722	IC	
mm58-2	173.4694	27.48297	6.114039	IC	
mm58-2	173.6638	29.17500	6.702061	IC	
mm58-2	173.9590	31.25713	7.065886	IC	
mm58-2	174.3458	32.13484	7.338329	IC	
mm58-2	174.5090	34.85574	8.886711	IC	
mm58-2	174.9590	38.58601	9.986131	IC	
mm58-2	175.2923	41.35191	9.995299	IC	
mm58-2	175.5006	38.06426	10.59685	IC	
mm58-2	175.7090	37.84971	10.13427	IC	
mm58-2	175.9590	38.82752	10.50144	IC	

Sample Point	Julian Day	Br ppm	NO3-N ppm	Method	Notes
mm58-2	176.3027	35.84073	8.623350	IC	
mm58-2	176.4798	30.57446	7.145916	IC	
mm58-2	176.7041	26.21029	5.838759	IC	
mm58-2	176.9520	18.93067	3.552761	IC	
mm58-2	177.3444	11.08469	1.681851	IC	
mm58-2	177.5423	8.447546	1.193475	IC	
mm58-2	177.7701	5.934068	0.845320	IC	
mm58-2	177.9097	4.145626	0.494908	IC	
mm58-2	178.4277	3.12232	0.298838	IC	
mm58-2	178.6152	3.482427	0.255619	IC	
mm58-2	179.4312	1.765551		0 IC	
mm58-2	180.2701	1.118085		0 IC	
mm58-2	181.5618	0.350583		0 IC	
mm58-2	182.4486	0.143248		0 IC	
mm58-3	169.8083		0	0 IC	
mm58-3	170.5423		0	0 IC	
mm58-3	170.6340		0	0 IC	
mm58-3	171.2340	2.455638	1.076315	IC	
mm58-3	171.4215	8.606966	2.100084	IC	
mm58-3	171.4875	10.78796	2.589917	IC	
mm58-3	171.5847	16.36126	3.842702	IC	
mm58-3	171.6680	15.20122	3.581161	IC	
mm58-3	171.7583	20.43151	4.736399	IC	
mm58-3	171.8347	19.59482	4.706870	IC	
mm58-3	172.0013	25.71029	6.266472	IC	
mm58-3	172.2097	28.24864	6.866086	IC	
mm58-3	172.3347	29.23083	6.864279	IC	
mm58-3	172.4597	30.95270	7.483178	IC	
mm58-3	172.5847	30.88399	7.466907	IC	
mm58-3	172.7722	32.39164	7.880309	IC	
mm58-3	173.0013	34.14988	8.316009	IC	
mm58-3	173.2687	36.26382	8.818601	IC	
mm58-3	173.4701	36.02939	8.895135	IC	
mm58-3	173.6645	36.35679	8.977092	IC	
mm58-3	173.9597	33.95587	8.217178	IC	
mm58-3	174.3465	23.47914	5.397482	IC	
mm58-3	174.5097	22.28272	5.135941	IC	
mm58-3	174.7152	20.89167	4.768266	IC	
mm58-3	174.9597	16.47910	3.610659	IC	
mm58-3	175.2930	15.25741	3.298881	IC	
mm58-3	175.5013	16.42686	3.607102	IC	
mm58-3	175.7097	15.30161	3.335038	IC	
mm58-3	175.9597	13.56150	2.943834	IC	
mm58-3	176.3034	12.83411	2.731043	IC	
mm58-3	176.4805	12.66131	2.704963	IC	
mm58-3	176.7055	11.92186	2.476168	IC	
mm58-3	176.9534	10.86092	2.266933	IC	

Sample Point	Julian Day	Br ppm	NO3-N ppm	Method	Notes
mm58-3	177.3451	9.671377	1.919591	IC	
mm58-3	177.5430	9.128848	1.850834	IC	
mm58-3	177.7708	9.185110	1.882842	IC	
mm58-3	177.9111	9.956707	2.065404	IC	
mm58-3	178.4284	7.111446	1.445998	IC	
mm58-3	178.6159	6.536767	1.320931	IC	
mm58-3	179.4319	3.080660	0.559862	IC	
mm58-3	180.2847	1.099426	0	IC	
mm58-3	181.5625	0	0	IC	
mm58-3	182.4493	0	0	IC	
mm58-4	169.7256	0	0	IC	
mm58-4	171.4013	0	0	IC	
mm58-4	171.4881	0	0	IC	
mm58-4	171.5854	0	0	IC	
mm58-4	171.6687	0.394387	0	IC	
mm58-4	171.7590	0.583887	0	IC	
mm58-4	171.8354	1.194496	0	IC	
mm58-4	172.0020	2.280960	0.182509	IC	
mm58-4	172.2104	2.217794	0.233404	IC	
mm58-4	172.3354	3.089491	0.395449	IC	
mm58-4	172.4604	3.135813	0.395449	IC	
mm58-4	172.5854	5.211886	0.795590	IC	
mm58-4	172.7729	7.258480	1.247795	IC	
mm58-4	173.0020	11.80646	2.305477	IC	
mm58-4	173.2694	21.61833	4.672391	IC	
mm58-4	173.4708	25.91882	5.701464	IC	
mm58-4	173.4708	25.79574	5.824843	IC	
mm58-4	173.6652	27.51146	6.251160	IC	
mm58-4	173.9604	31.59125	7.233131	IC	
mm58-4	174.3472	38.04037	8.909848	IC	
mm58-4	174.5104	39.84682	9.668486	IC	
mm58-4	174.7159	41.74054	9.805478	IC	
mm58-4	174.9604	42.83576	10.56008	IC	
mm58-4	175.2937	43.25028	10.97336	IC	
mm58-4	175.5020	43.11501	10.14911	IC	
mm58-4	175.7104	41.38710	9.574088	IC	
mm58-4	175.9604	39.00032	8.924813	IC	
mm58-4	176.3041	28.48450	6.181513	IC	
mm58-4	176.4812	22.41500	4.626823	IC	
mm58-4	176.7069	19.86240	4.036835	IC	
mm58-4	176.9541	15.80007	3.243661	IC	
mm58-4	177.3465	12.85040	2.396381	IC	
mm58-4	177.5437	8.718258	1.607236	IC	
mm58-4	177.7722	6.353290	1.194532	IC	
mm58-4	177.9125	3.979595	0.713332	IC	
mm58-4	178.4291	2.190597	0.332286	IC	
mm58-4	178.6166	1.470634	0.197596	IC	

Sample Point	Julian Day	Br ppm	NO3-N ppm	Method	Notes
mm58-4	179.4326	0.414689		0 IC	
mm58-4	180.2854	0		0 IC	
mm58-4	181.5631	0		0 IC	
mm58-4	182.45	0		0 IC	
mm58-5	169.8104	0		0 IC	
mm58-5	171.4020	2.812122	0.912011	IC	
mm58-5	171.4888	8.311303	2.130074	IC	
mm58-5	171.5861	10.40747	2.500047	IC	
mm58-5	171.6694	13.51169	3.483536	IC	
mm58-5	171.7597	13.48339	3.595624	IC	
mm58-5	171.8361	14.91020	4.039761	IC	
mm58-5	172.0027	16.11066	4.430264	IC	
mm58-5	172.2111	24.91403	6.595507	IC	
mm58-5	172.3361	29.90179	7.994206	IC	
mm58-5	172.4611	31.28818	8.083998	IC	
mm58-5	172.5861	40.29769	10.39146	IC	
mm58-5	172.7736	44.63874	11.48523	IC	
mm58-5	173.0027	46.46166	11.95708	IC	
mm58-5	173.2708	46.97903	12.11075	IC	
mm58-5	173.4715	45.41480	11.60093	IC	
mm58-5	173.6659	46.47379	11.99806	IC	
mm58-5	173.9611	43.59188	11.10979	IC	
mm58-5	174.3479	38.89513	9.709888	IC	
mm58-5	174.5111	30.50809	7.197532	IC	
mm58-5	174.7166	24.20712	5.577347	IC	
mm58-5	174.9611	20.02362	4.610007	IC	
mm58-5	175.2944	9.530721	2.048807	IC	
mm58-5	175.5027	4.692170	0.970626	IC	
mm58-5	175.7111	2.425607	0.487549	IC	
mm58-5	175.9611	1.236063	0.257568	IC	
mm58-5	176.3048	0.753815		0 IC	
mm58-5	176.4854	0.749796		0 IC	
mm58-5	176.7076	0		0 IC	
mm58-5	176.9548	0		0 IC	
mm58-5	177.3472	0		0 IC	
mm58-5	177.5444	0		0 IC	
mm58-5	177.7736	0		0 IC	
mm58-5	177.9138	0		0 IC	
mm58-5	178.4298	0		0 IC	
mm58-5	178.6173	0		0 IC	
mm58-5	179.4333	0		0 IC	
mm58-5	180.2861	0		0 IC	
mm58-5	181.5638	0		0 IC	
mm58-5	182.4506	0		0 IC	
mm58-6	170.8118	0		0 IC	
mm58-6	171.4027	0		0 IC	

Sample Point	Julian Day	Br ppm	NO3-N ppm	Method	Notes
mm58-6	171.4895	0	0	IC	
mm58-6	171.5868	0	0.09872	IC	
mm58-6	171.6701	0	0.23129	IC	
mm58-6	171.7604	0	0.248095	IC	
mm58-6	171.8368	0	0.24685	IC	
mm58-6	172.0035	0.276999	0.200793	IC	
mm58-6	172.2118	3.460986	0.162827	IC	
mm58-6	172.3368	7.452025	0.966961	IC	
mm58-6	172.4618	11.50203	1.498486	IC	
mm58-6	172.5868	15.99425	2.779375	IC	
mm58-6	172.7743	18.50261	1.804077	IC	
mm58-6	173.0035	16.36645	2.713401	IC	
mm58-6	173.2701	21.53306	3.042648	IC	
mm58-6	173.4722	26.67019	5.09344	IC	
mm58-6	173.6667	30.0716	5.455051	IC	
mm58-6	173.9618	36.74176	7.142987	IC	
mm58-6	174.3486	43.30136	8.331761	IC	
mm58-6	174.5118	44.56906	8.820341	IC	
mm58-6	174.7174	44.15632	8.660386	IC	
mm58-6	174.9618	42.42797	7.881147	IC	
mm58-6	175.2951	40.85809	8.361636	IC	
mm58-6	175.5035	39.13343	6.775151	IC	
mm58-6	175.7118	37.3019	6.439058	IC	
mm58-6	175.9618	36.458	5.541564	IC	
mm58-6	176.3056	26.07687	3.382476	IC	
mm58-6	176.4826	21.73943	2.831034	IC	
mm58-6	176.7083	17.92159	2.063621	IC	
mm58-6	176.9563	14.52018	1.483549	IC	
mm58-6	177.3479	11.30303	0.880448	IC	
mm58-6	177.5451	9.626275	0.699331	IC	
mm58-6	177.7743	7.67682	0.101832	IC	
mm58-6	177.9153	5.399385	0.114902	IC	
mm58-6	178.4306	5.321997	0	IC	
mm58-6	178.6181	5.145109	0.316558	IC	
mm58-6	179.434	3.523634	0	IC	
mm58-6	180.2868	2.211713	0.162204	IC	
mm58-6	181.5646	0.977181	0.198303	IC	
mm58-6	182.4514	0.549702	0.151624	IC	
mm58-7	169.7569	0	0	IC	
mm58-7	171.6708	0	0	IC	
mm58-7	171.8375	0	0.333363	IC	
mm58-7	172.2125	0	0.159092	IC	
mm58-7	172.4625	0	1.194758	IC	
mm58-7	172.775	0	0.440415	IC	
mm58-7	173.0042	0	0.200793	IC	
mm58-7	173.2715	0	0.245605	IC	
mm58-7	173.4799	0	0.216975	IC	

Sample Point	Julian Day	Br ppm	NO3-N ppm	Method	Notes
mm58-7	173.6674	0	0.33523	IC	
mm58-7	173.9625	0	0.294152	IC	
mm58-7	174.3493	0	0	IC	
mm58-7	174.5125	0.803978	0	IC	
mm58-7	174.7181	1.419402	0	IC	
mm58-7	174.9625	1.835826	0	IC	
mm58-7	175.2958	4.824499	0.204527	IC	
mm58-7	175.5042	6.958212	0.257431	IC	
mm58-7	175.7125	9.519405	1.005549	IC	
mm58-7	175.9625	10.75394	0.755969	IC	
mm58-7	176.3063	12.90608	0.241248	IC	
mm58-7	176.4833	13.58046	2.004493	IC	
mm58-7	176.7090	15.65686	1.244905	IC	
mm58-7	176.9569	16.91589	0	IC	
mm58-7	177.3486	20.74959	1.043920	IC	
mm58-7	177.5458	21.03106	1.984065	IC	
mm58-7	177.775	21.92771	1.738203	IC	
mm58-7	177.9166	19.39483	1.181411	IC	
mm58-7	178.4312	19.88395	1.075900	IC	
mm58-7	178.6187	19.00718	1.430949	IC	
mm58-7	179.4347	18.77897	0.692782	IC	
mm58-7	180.2875	13.48838	0	IC	
mm58-7	181.5673	6.066714	0	IC	
mm58-7	182.4520	2.335824	0	IC	
mm58-8	169.8	0	0	IC	
mm58-8	171.4041	0	0	IC	
mm59-1	169.8590	0	0	IC	
mm59-1	170.6305	0	0	IC	
mm59-1	171.4965	0	0	IC	
mm59-1	171.5902	0	0	IC	
mm59-1	171.6736	0	0	IC	
mm59-1	171.7638	0	0	IC	
mm59-1	171.8402	0	0	IC	
mm59-1	172.0069	0	0	IC	
mm59-1	172.2152	0	0	IC	
mm59-1	172.3388	0	0	IC	
mm59-1	172.4652	0	0	IC	
mm59-1	172.5888	0	0	IC	
mm59-1	176.2972	0	0	IC	
mm59-2	169.8611	0	0	IC	
mm59-2	170.4833	0	0	IC	
mm59-2	170.5388	0	0	IC	
mm59-2	170.6312	0	0	IC	
mm59-2	171.4972	0	0	IC	
mm59-2	171.5909	0	0	IC	

Sample Point	Julian Day	Br ppm	NO3-N ppm	Method	Notes
mm59-2	171.6743	0		0 IC	
mm59-2	171.7645	0		0 IC	
mm59-2	171.8409	0		0 IC	
mm59-2	172.0076	0		0 IC	
mm59-2	172.2159	0		0 IC	
mm59-2	172.3395	0		0 IC	
mm59-2	172.4659	0		0 IC	
mm59-2	172.5895	0		0 IC	
mm59-2	176.2979	0.970663		0 IC	
mm59-2	177.3631	0		0 IC	
mm59-2	177.3638	0.902562		0 IC	
mm59-3	169.8631	0		0 IC	
mm59-3	170.4840	0		0 IC	
mm59-3	170.5395	0		0 IC	
mm59-3	171.4979	0		0 IC	
mm59-3	171.5916	0		0 IC	
mm59-3	171.675	0		0 IC	
mm59-3	171.7652	0		0 IC	
mm59-3	171.8416	0		0 IC	
mm59-3	172.0083	0		0 IC	
mm59-3	172.2166	0		0 IC	
mm59-3	172.3402	0		0 IC	
mm59-3	172.4666	0		0 IC	
mm59-3	172.5902	0.425852		0 IC	
mm59-3	176.2986	4.504368	0.159799	IC	
mm59-3	177.3652	0.690691		0 IC	
mm59-4	169.8659	0		0 IC	
mm59-4	170.4847	0		0 IC	
mm59-4	171.4986	0.422438	0.330116	IC	
mm59-4	171.6756	0.361534	0.145809	IC	
mm59-4	171.8423	0.558271		0 IC	
mm59-4	172.2173	0.645290		0 IC	
mm59-4	172.4673	0.282082		0 IC	
mm59-4	176.2993	2.287290		0 IC	
mm59-4	177.3659	0.259382		0 IC	
mm59-5	170.4854	0		0 IC	
mm59-5	171.6763	0		0 IC	
mm59-5	171.8430	0.244248		0 IC	
mm59-5	172.2180	0.985797		0 IC	
mm59-5	172.4680	0.872294		0 IC	
mm59-5	176.3	0.577188		0 IC	
mm59-5	177.3673	0		0 IC	
mm59-6	169.8701	0		0 IC	
mm59-6	171.6770	0		0 IC	

Sample Point	Julian Day	Br ppm	NO3-N ppm	Method	Notes
mm59-6	171.8437	0		0 IC	
mm59-6	172.2187	0		0 IC	
mm59-6	172.4687	0		0 IC	
mm59-6	176.3006	0		0 IC	
mm59-6	177.3687	0		0 IC	
mm59-7	169.8722	0		0 IC	
mm59-7	170.4868	0		0 IC	
mm59-7	171.6777	0		0 IC	
mm59-7	171.8444	0		0 IC	
mm59-7	172.2194	0		0 IC	
mm59-7	172.4694	0		0 IC	
mm59-7	176.3013	0		0 IC	
mm59-7	177.3694	0		0 IC	
mm60-1	171.7674	0		0 IC	
mm60-1	172.3486	0		0 IC	
mm60-1	172.4715	0		0 IC	
mm60-1	172.5924	0		0 IC	
mm60-1	176.3083	0		0 IC	
mm60-1	177.3729	0		0 IC	
mm60-2	171.7681	0		0 IC	
mm60-2	172.3493	0		0 IC	
mm60-2	172.4722	0		0 IC	
mm60-2	172.5931	0		0 IC	
mm60-2	176.309	0		0 IC	
mm60-2	177.3743	0		0 IC	
mm60-3	169.8298	0		0 IC	
mm60-3	171.7688	0		0 IC	
mm60-3	172.35	0		0 IC	
mm60-3	172.4729	0		0 IC	
mm60-3	172.5938	0		0 IC	
mm60-3	176.3097	0		0 IC	
mm60-3	177.375	0		0 IC	
mm60-4	169.8312	0		0 IC	
mm60-4	171.7694	0		0 IC	
mm60-4	172.3507	0		0 IC	
mm60-4	172.5944	0		0 IC	
mm60-4	176.3104	0		0 IC	
mm60-4	177.3764	0		0 IC	
mm60-5	171.7701	0		0 IC	
mm60-5	172.3513	0		0 IC	
mm60-5	172.5951	0		0 IC	
mm60-5	176.3111	0		0 IC	

Sample Point	Julian Day	Br ppm	NO3-N ppm	Method	Notes
mm60-5	177.3770	0	0	IC	
mm60-5	196.7180	0	0	IC	
mm60-5	200.8312	0	0	IC	
mm60-5	201.5916	0	0	IC	
mm60-5	202.7833	0	0	IC	
mm60-5	204.4611	0	0	IC	
mm60-5	207.6389	0	0	IC	
mm60-5	209.6458	0	0	IC	
mm60-5	213.6806	0	0	IC	
mm60-5	217.7986	0	0	IC	
mm60-5	252.6020	0	0.002275	IC	
mm60-5	256.4513	0	0.069352	IC	
mm60-5	262.4361	0	0.008015	IC	
mm60-5	265.5583	0	0.033298	IC	
mm60-5	270.4541	0	0.058387	IC	
mm60-6	169.8354	0	2.392033	IC	Background nitrate
mm60-6	170.2597	0	2.169696	IC	
mm60-6	171.7708	0	1.052772	IC	
mm60-6	172.3520	0	0.981701	IC	
mm60-6	172.5958	0	2.227854	IC	
mm60-6	176.3118	0	2.491491	IC	
mm60-6	177.3784	0	1.928044	IC	
mm60-6	177.3784	0	2.053536	IC	
mm60-6	196.7187	0	2.201202	IC	
mm60-6	197.7916	0	2.095969	IC	
mm60-6	198.4916	0	2.198403	IC	
mm60-6	199.2972	0	1.681195	IC	
mm60-6	200.5138	0	1.291050	IC	
mm60-6	200.8319	0	1.160069	IC	
mm60-6	201.5923	0	1.369975	IC	
mm60-6	202.7840	0	1.456736	IC	
mm60-6	204.4618	0	0.862842	IC	
mm60-6	207.6424	0	0.449184	IC	
mm60-6	209.6465	0	0.449184	IC	
mm60-6	213.6813	0	0.20393	IC	
mm60-6	217.7993	0	0.178469	IC	
mm60-6	252.6027	0	0.001695	IC	
mm60-6	256.4520	0	0.026461	IC	
mm60-6	262.4368	0	0.027945	IC	
mm60-6	265.5590	0	0.017367	IC	
mm60-6	270.4548	0	0.037813	IC	
mm60-7	171.7715	0	0.413364	IC	Background nitrate
mm60-7	172.3527	0	0.522515	IC	
mm60-7	172.5965	0.384247	0.708911	IC	
mm60-7	176.3125	0	1.622981	IC	
mm60-7	177.3798	0	1.915170	IC	

Sample Point	Julian Day	Br ppm	NO3-N ppm	Method	Notes
mm60-7	196.7194	0	2.982052	IC	
mm60-7	197.7923	0	3.059297	IC	
mm60-7	198.4923	0	3.289914	IC	
mm60-7	199.2979	0	3.139341	IC	
mm60-7	200.5145	0	3.062656	IC	
mm60-7	200.8326	0	2.794536	IC	
mm60-7	201.5930	0	2.832039	IC	
mm60-7	202.7847	0	2.893052	IC	
mm60-7	204.4625	0	2.781102	IC	
mm60-7	207.6444	0	1.804839	IC	
mm60-7	209.6472	0	1.654672	IC	
mm60-7	213.6819	0	1.325241	IC	
mm60-7	217.8	0	0.886174	IC	
mm60-7	252.6034	0	0.048261	IC	
mm60-7	256.4527	0	0.026268	IC	
mm60-7	262.4375	0	0.026784	IC	
mm60-7	265.5597	0	0.034136	IC	
mm60-7	270.4562	0	0.006274	IC	
mm61-1	179.4361	0	0.020342	IC	
mm61-1	181.5972	0	0	IC	
mm61-1	182.4131	0	0	IC	
mm61-1	188.5180	0	0	IC	
mm61-2	179.4368	0	0.013448	IC	
mm61-2	181.5979	6.319756	0	IC	
mm61-2	182.4138	13.64992	0	IC	
mm61-2	188.5187	0	0	IC	
mm61-3	179.4375	0	0	IC	
mm61-3	181.5986	0.094733	0	IC	
mm61-3	182.4145	1.438280	0	IC	
mm61-3	188.5194	0.781952	0	IC	
mm61-4	179.4381	0	0	IC	
mm61-4	181.5993	0	0	IC	
mm61-4	182.4152	0.438337	0.150460	IC	
mm61-4	188.5201	21.28144	0	IC	
mm61-4	188.7006	19.77808	0	IC	
mm61-4	188.7708	18.64108	0	IC	
mm61-4	189.3923	16.51191	0	IC	
mm61-4	189.4986	14.02757	0	IC	
mm61-4	189.7465	10.81900	0	IC	
mm61-4	190.5083	2.532028	0	IC	
mm61-4	190.7187	2.690042	0	IC	
mm61-4	190.9652	1.878024	0	IC	
mm61-4	191.2986	1.153791	0	IC	
mm61-4	191.4993	0.881655	0	IC	

Sample Point	Julian Day	Br ppm	NO3-N ppm	Method	Notes
mm61-4	191.7569	0.706083		0 IC	
mm61-4	191.9645	0.662190		0 IC	
mm61-4	192.2979	0.561237		0 IC	
mm61-4	192.5062	0.556847		0 IC	
mm61-4	192.7145	0.561237		0 IC	
mm61-4	192.9645	0.530512		0 IC	
mm61-4	193.2979	0.482229		0 IC	
mm61-4	193.5062	0.482229		0 IC	
mm61-4	193.7145	0.517344		0 IC	
mm61-4	193.9645	0.486619		0 IC	
mm61-4	194.2979	0.469062		0 IC	
mm61-4	194.9090	0.425169		0 IC	
mm61-4	195.2979	0.420779		0 IC	
mm61-4	195.7145	0.425169		0 IC	
mm61-4	196.7152	0.623176		0 IC	
mm61-4	197.7930	0		0 IC	
mm61-5	179.4388		0 0.010576	IC	
mm61-6	179.4395		0	0 IC	
mm61-7	179.4402		0 0.010288	IC	
mm62-1	178.5138		0 0.158035	IC	
mm62-1	179.4423		0 0.165288	IC	
mm62-1	181.6041		0 0.160936	IC	
mm62-1	182.4159		0	0 IC	
mm62-1	188.5138		0 0.160452	IC	
mm62-2	178.5145		0 0.160392	IC	
mm62-2	179.4430		0 0.166799	IC	
mm62-2	181.6048		0 0.159667	IC	
mm62-2	182.4166		0	0 IC	
mm62-2	188.5145		0 0.160090	IC	
mm62-3	178.5152		0 0.158277	IC	
mm62-3	179.4437		0 0.167645	IC	
mm62-3	181.6055		0 0.167766	IC	
mm62-3	182.4173	2.216633		0 IC	
mm62-3	188.5152		0 0.160936	IC	
mm62-4	182.4180		0	0 IC	
mm62-4	208.5159		0 0.016626	IC	
mm62-4	209.4444		0 0.072839	IC	
mm62-4	211.6062		0 0.031488	IC	
mm62-4	219.5159	0.403920		0 IC	
mm62-5	178.5166		0	0 IC	

Sample Point	Julian Day	Br ppm	NO3-N ppm	Method	Notes
mm62-5	179.4451	0		0 IC	
mm62-5	181.6076	0		0 IC	
mm62-5	182.4187	0		0 IC	
mm62-5	188.5166	0.688526		0 IC	
mm62-5	189.4965	1.245966		0 IC	
mm62-5	189.7472	1.522491		0 IC	
mm62-5	190.5062	1.026501		0 IC	
mm62-5	190.7180	1.228409		0 IC	
mm62-5	190.9645	1.030891		0 IC	
mm62-5	191.2979	1.066005		0 IC	
mm62-5	191.4986	0.991387		0 IC	
mm62-5	191.7562	1.048448		0 IC	
mm62-5	191.9638	1.000166		0 IC	
mm62-5	192.2972	2.571532		0 IC	
mm62-5	192.5055	1.079173		0 IC	
mm62-5	192.7138	2.685653		0 IC	
mm62-5	192.9638	0.916769		0 IC	
mm62-5	193.2972	0.938716		0 IC	
mm62-5	193.5055	1.044059		0 IC	
mm62-5	193.7138	1.004555		0 IC	
mm62-5	193.9638	1.039669		0 IC	
mm62-5	194.2972	1.195624		0 IC	
mm62-5	194.9083	1.233507		0 IC	
mm62-5	195.2972	1.258762		0 IC	
mm62-5	195.7138	1.262971		0 IC	
mm62-5	227.7159	1.005261		0 IC	
mm62-5	228.325	0.914356		0 IC	
mm62-5	228.7944	0.812188		0 IC	
mm63-1	219.7083	0	0.020457	IC	
mm63-2	219.7090	0	0.037829	IC	
mm63-3	219.7097	0	0.026336	IC	
mm63-4	188.7104	0		0 IC	
mm63-5	188.7111	0		0 IC	
mm63-6	219.7118	0	0.035187	IC	
mm63-7	219.7125	0	0.036244	IC	
mm64-1	188.5833	0		0 IC	
mm64-1	188.6979	0		0 IC	
mm64-1	188.7715	0		0 IC	
mm64-1	189.375	0		0 IC	
mm64-1	189.75	0		0 IC	
mm64-1	190.5	0		0 IC	
mm64-1	190.7118	0		0 IC	
mm64-1	190.9583	0		0 IC	
mm64-1	191.2917	0		0 IC	
mm64-1	191.4931	0		0 IC	
mm64-1	191.75	0		0 IC	

Sample Point	Julian Day	Br ppm	NO3-N ppm	Method	Notes
mm64-1	191.9583	0		0 IC	
mm64-1	192.2917	0		0 IC	
mm64-1	192.5	0		0 IC	
mm64-1	192.7083	0		0 IC	
mm64-1	192.9583	0		0 IC	
mm64-1	193.2917	0		0 IC	
mm64-1	193.5	0		0 IC	
mm64-1	193.7083	0		0 IC	
mm64-1	193.9583	0		0 IC	
mm64-1	194.2917	0		0 IC	
mm64-1	194.9028	0		0 IC	
mm64-1	195.2917	0		0 IC	
mm64-1	195.7083	0		0 IC	
mm64-1	196.5833	0		0 IC	
mm64-1	197.3021	0		0 IC	
mm64-1	197.5625	0		0 IC	
mm64-1	197.7951	0		0 IC	
mm64-1	198.4861	0		0 IC	
mm64-1	198.7083	0		0 IC	
mm64-1	199.2917	0		0 IC	
mm64-1	199.6667	0		0 IC	
mm64-1	200.4931	0		0 IC	
mm64-1	201.6049	0		0 IC	
mm64-1	202.7639	0		0 IC	
mm64-1	204.4792	0		0 IC	
mm64-1	207.6743	0		0 IC	
mm64-1	207.6743	0		0 IC	
mm64-1	209.6319	0		0 IC	
mm64-1	209.6319	0		0 IC	
mm64-1	213.6666	0		0 IC	
mm64-1	217.7638	0		0 IC	
mm64-2	188.5840	0		0 IC	
mm64-2	188.6986	0		0 IC	
mm64-2	188.7722	0		0 IC	
mm64-2	189.3756	0.371048		- elect	
mm64-2	189.7506	0.431210		- elect	
mm64-2	190.5006	0.646555		- elect	
mm64-2	190.7125	1.756800		- elect	
mm64-2	190.9590	1.126631		- elect	
mm64-2	191.2923	2.419653		- elect	
mm64-2	191.4937	1.839009		- elect	
mm64-2	191.7506	2.933968		- elect	
mm64-2	191.9590	2.244520		- elect	
mm64-2	192.2923	25.95307		- elect	
mm64-2	192.5006	3.454533		- elect	
mm64-2	192.7090	4.243911		- elect	
mm64-2	192.9590	3.420844		- elect	

Sample Point	Julian Day	Br ppm	NO3-N ppm	Method	Notes
mm64-2	193.9590	3.031392		- elect	
mm64-2	194.2923	2.608452		- elect	
mm64-2	194.9034	2.068504		- elect	
mm64-2	195.2923	1.863369		- elect	
mm64-2	195.7090	1.301404		- elect	
mm64-2	196.5840	0.788912		- elect	
mm64-2	196.8402	0.588498		- elect	
mm64-2	197.3027	0.604208		- elect	
mm64-2	197.5631	0.417839		- elect	
mm64-2	197.7958	0.400329		- elect	
mm64-2	198.4868	0.322127		- elect	
mm64-2	198.7090	0.342925		- elect	
mm64-2	199.2923	0.334009		- elect	
mm64-2	199.6673	0.373580		- elect	
mm64-2	200.4937	0.376049		- elect	
mm64-2	201.6055	0.353241		- elect	
mm64-2	202.7645	0.311692		- elect	
mm64-2	204.4798	0.263504		- elect	
mm64-2	207.6770	0.276847		- elect	
mm64-2	209.6326	0.285175		- elect	
mm64-2	213.6673	0.265245		- elect	
mm64-2	217.7645	0.306602		- elect	
mm64-3	188.5847	0		0 IC	
mm64-3	188.6993	0		0 IC	
mm64-3	188.7729	0		0 IC	
mm64-3	189.3763	0		0 IC	
mm64-3	189.7513	0		0 IC	
mm64-3	190.5013	0		0 IC	
mm64-3	190.7131	0		0 IC	
mm64-3	190.9597	0		0 IC	
mm64-3	191.2930	0		0 IC	
mm64-3	191.4944	0		0 IC	
mm64-3	191.7513	0		0 IC	
mm64-3	191.9597	0		0 IC	
mm64-3	192.2930	0.665268		0 IC	
mm64-3	192.5013	0.690523		0 IC	
mm64-3	192.7097	0.293451		0 IC	
mm64-3	192.9597	0.269071		0 IC	
mm64-3	193.2930	2.950964		0 IC	
mm64-3	193.5013	0.742059		0 IC	
mm64-3	193.7097	1.161410		0 IC	
mm64-3	193.9597	2.209786		0 IC	
mm64-3	194.2930	1.917216		0 IC	
mm64-3	194.9041	3.614123		0 IC	
mm64-3	195.2930	5.067222		0 IC	
mm64-3	195.7097	6.627596		0 IC	
mm64-3	196.5854	9.280233		0 IC	

Sample Point	Julian Day	Br ppm	NO3-N ppm	Method	Notes
mm64-3	196.8409	9.958020		0 IC	
mm64-3	197.3034	10.79184		0 IC	
mm64-3	197.5638	10.83573		0 IC	
mm64-3	197.7965	11.14780		0 IC	
mm64-3	198.4875	10.80647		0 IC	
mm64-3	198.7097	10.45051		0 IC	
mm64-3	199.2930	10.72357		0 IC	
mm64-3	199.6680	10.75771		0 IC	
mm64-3	200.4944	10.53037		- elect	
mm64-3	201.6062	10.28972		- elect	
mm64-3	202.7652	10.21073		- elect	
mm64-3	204.4805	9.273036		- elect	
mm64-3	207.6791	4.459406		- elect	
mm64-3	209.6333	2.316327		- elect	
mm64-3	213.6680	0.509513		- elect	
mm64-3	217.7652	0.221667		- elect	
mm64-3	221.625	0.157922		- elect	
mm64-3	225.7333	0		- elect	
mm64-3	231.4513	0		- elect	
mm64-4	188.5854	0.423865		0 IC	
mm64-4	188.7	0.604942		0 IC	
mm64-4	188.7736	0.659687		0 IC	
mm64-4	189.375	0.839940		- elect	
mm64-4	189.7520	0.857354		- elect	
mm64-4	190.5020	0.547751		- elect	
mm64-4	190.7104	0.681779		- elect	
mm64-4	190.9638	0.559107		- elect	
mm64-4	191.2937	0.688810		- elect	
mm64-4	191.4604	0.602798		- elect	
mm64-4	191.7868	0.745181		- elect	
mm64-4	191.9604	0.596645		- elect	
mm64-4	192.2937	0.705500		- elect	
mm64-4	192.5020	0.663378		- elect	
mm64-4	192.7104	0.854427		- elect	
mm64-4	192.9604	0.684115		- elect	
mm64-4	193.2937	0.578560		- elect	
mm64-4	193.5020	0.665651		- elect	
mm64-4	193.7104	0.927519		- elect	
mm64-4	193.9604	0.681779		- elect	
mm64-4	194.2937	0.715218		- elect	
mm64-4	194.8770	0.747734		- elect	
mm64-4	195.3215	1.158427		- elect	
mm64-4	195.7104	1.360438		- elect	
mm64-4	196.5854	2.009118		- elect	
mm64-4	196.8361	2.596598		- elect	
mm64-4	197.3	2.650431		- elect	
mm64-4	197.5541	3.460762		- elect	

Sample Point	Julian Day	Br ppm	NO3-N ppm	Method	Notes
mm64-4	197.8152	3.287698		- elect	
mm64-4	198.4638	2.605493		- elect	
mm64-4	198.7381	4.148525		- elect	
mm64-4	199.2937	5.007102		- elect	
mm64-4	199.6687	5.252680		- elect	
mm64-4	200.4604	5.981680		- elect	
mm64-4	201.6201	7.369326		- elect	
mm64-4	202.7736	8.713819		- elect	
mm64-4	204.4743	9.078883		- elect	
mm64-4	207.6895	7.945201		- elect	
mm64-4	209.6381	8.054640		- elect	
mm64-4	213.6756	5.663149		- elect	
mm64-4	217.7520	2.029838		- elect	
mm64-4	221.6409	0.511536		- elect	
mm64-4	225.7097	0.283084		- elect	
mm64-4	231.4423	0.257233		- elect	
mm64-5	188.5861	0.398598		0 IC	
mm64-5	188.7743	0.588098		0 IC	
mm64-5	189.3777	0.850472		0 IC	
mm64-5	189.7534	1.452384		0 IC	
mm64-5	190.5027	3.030827		0 IC	
mm64-5	190.7145	4.710290		0 IC	
mm64-5	190.9611	5.379549		0 IC	
mm64-5	191.2944	7.509394		0 IC	
mm64-5	191.4958	8.784776		0 IC	
mm64-5	191.7527	9.643449		0 IC	
mm64-5	191.9611	9.740260		0 IC	
mm64-5	192.2944	11.22610		0 IC	
mm64-5	192.5027	11.24714		0 IC	
mm64-5	192.7111	11.40288		0 IC	
mm64-5	192.9611	11.39446		0 IC	
mm64-5	193.2944	11.54178		0 IC	
mm64-5	193.5027	11.76066		0 IC	
mm64-5	193.7111	11.51232		0 IC	
mm64-5	193.9611	12.13107		0 IC	
mm64-5	194.2944	12.63196		0 IC	
mm64-5	194.9055	13.86104		0 IC	
mm64-5	195.2944	14.50926		0 IC	
mm64-5	195.7111	14.73655		0 IC	
mm64-5	196.5868	15.62469		0 IC	
mm64-5	196.8423	14.21040		0 IC	
mm64-5	197.3048	14.74497		0 IC	
mm64-5	197.5659	13.90313		0 IC	
mm64-5	197.7979	14.56818		0 IC	
mm64-5	198.4888	12.96028		0 IC	
mm64-5	198.7111	15.88145		0 IC	
mm64-5	199.2944	16.77800		0 IC	

Sample Point	Julian Day	Br ppm	NO3-N ppm	Method	Notes
mm64-5	199.6694	14.74918		0 IC	
mm64-5	200.4958	8.991554		- elect	
mm64-5	201.6076	4.374314		- elect	
mm64-5	202.7666	1.940098		- elect	
mm64-5	204.4819	0.947485		- elect	
mm64-5	207.6819	0.329657		- elect	
mm64-5	209.6347	0.202088		- elect	
mm64-5	213.6694	0		- elect	
mm64-5	217.7666	0		- elect	
mm64-5	221.6270	0		- elect	
mm64-5	231.4527	0		- elect	
mm64-6	188.5868	0		- elect	
mm64-6	188.775	0		- elect	
mm64-6	189.3784	0.285439		- elect	
mm64-6	190.5034	0		- elect	
mm64-6	190.7152	0		- elect	
mm64-6	190.9618	0		- elect	
mm64-6	191.2951	0		- elect	
mm64-6	191.4965	0		- elect	
mm64-6	191.7534	0		- elect	
mm64-6	191.9618	0		- elect	
mm64-6	192.2951	0		- elect	
mm64-6	192.5034	0		- elect	
mm64-6	192.7118	0		- elect	
mm64-6	192.9618	0		- elect	
mm64-6	193.2951	0		- elect	
mm64-6	193.5034	0		- elect	
mm64-6	193.7118	0		- elect	
mm64-6	193.9618	0		- elect	
mm64-6	194.2951	0		- elect	
mm64-6	194.9062	0		- elect	
mm64-6	195.2951	0		- elect	
mm64-6	195.7118	0		- elect	
mm64-6	196.5875	0		- elect	
mm64-6	197.3055	0		- elect	
mm64-6	197.5666	0		- elect	
mm64-6	197.7986	0		- elect	
mm64-6	198.4895	0		- elect	
mm64-6	198.7118	0		- elect	
mm64-6	199.2951	0		- elect	
mm64-6	199.6701	0		- elect	
mm64-6	200.4965	0		- elect	
mm64-6	201.6083	0		- elect	
mm64-6	202.7673	0		- elect	
mm64-6	204.4826	1.637956		- elect	
mm64-6	207.6833	7.548236		- elect	
mm64-6	209.6354	12.62468		- elect	

Sample Point	Julian Day	Br ppm	NO3-N ppm	Method	Notes
mm64-6	213.6701	14.41108		- elect	
mm64-6	217.7673	9.095029		- elect	
mm64-6	221.6277	3.082666		- elect	
mm64-6	225.7354	0.743735		- elect	
mm64-6	231.4541	0.278228		- elect	
mm64-7	188.5875	0		- elect	
mm64-7	188.7756	0		- elect	
mm64-7	189.3791	0		- elect	
mm64-7	190.5041	0		- elect	
mm64-7	190.7159	0		- elect	
mm64-7	190.9625	0		- elect	
mm64-7	191.2958	0		- elect	
mm64-7	191.4972	0		- elect	
mm64-7	191.7541	0		- elect	
mm64-7	191.9625	0		- elect	
mm64-7	192.2958	0		- elect	
mm64-7	192.5041	0		- elect	
mm64-7	192.7125	0		- elect	
mm64-7	192.9625	0		- elect	
mm64-7	193.2958	0		- elect	
mm64-7	193.5041	0		- elect	
mm64-7	193.7125	0		- elect	
mm64-7	193.9625	0		- elect	
mm64-7	194.2958	0		- elect	
mm64-7	194.9069	0		- elect	
mm64-7	195.2958	0		- elect	
mm64-7	195.7125	0		- elect	
mm64-7	196.5881	0		- elect	
mm64-7	197.3062	0		- elect	
mm64-7	197.5673	0		- elect	
mm64-7	197.7993	0		- elect	
mm64-7	198.4902	0.330976		- elect	
mm64-7	198.7125	0.646668		- elect	
mm64-7	199.2958	1.546388		- elect	
mm64-7	199.6708	2.125435		- elect	
mm64-7	200.4972	4.805175		- elect	
mm64-7	201.6090	10.82294		- elect	
mm64-7	202.7680	20.96874		- elect	
mm64-7	204.4833	32.34649		- elect	
mm64-7	207.6847	15.17991		- elect	
mm64-7	209.6361	6.856290		- elect	
mm64-7	213.6708	3.697903		- elect	
mm64-7	217.7680	1.142061		- elect	
mm64-7	221.6291	0		- elect	
mm64-7	225.7361	0		- elect	
mm64-7	231.4548	0		- elect	

Sample Point	Julian Day	Br ppm	NO3-N ppm	Method	Notes
mm66-3	200.8263	0	0	IC	
mm66-3	201.6006	0	0	IC	
mm66-3	202.7805	0	0	IC	
mm66-3	204.4652	0	0.110539	IC	Background nitrate
mm66-3	207.6354	0	0.045224	IC	
mm66-3	209.6431	0	0	IC	
mm66-3	213.684	0	0	IC	
mm66-3	217.8042	0	0	IC	
mm66-3	252.6097	0	0.015965	IC	
mm66-3	256.4541	0	0.088494	IC	
mm66-3	262.4388	0	0.093184	IC	
mm66-3	265.5625	0	0.025741	IC	
mm66-3	270.4583	0	0.068809	IC	
mm66-4	200.8270	0	0.294137	IC	Background nitrate
mm66-4	201.6013	0	0.575131	IC	
mm66-4	202.7812	0	0.556659	IC	
mm66-4	204.4659	0	0.846609	IC	
mm66-4	207.6389	0	0.700922	IC	
mm66-4	209.6438	0	0.344095	IC	
mm66-4	213.6847	0	0.060518	IC	
mm66-4	217.8049	0	0	IC	
mm66-4	252.6111	0	0.030894	IC	
mm66-4	256.4548	0	0.077727	IC	
mm66-4	262.4395	0	0.065506	IC	
mm66-4	265.5631	0	0.033932	IC	
mm66-4	270.4597	0	0.053881	IC	
mm66-5	200.8277	0	1.007257	IC	Background nitrate
mm66-5	201.6020	0	1.233956	IC	
mm66-5	202.7819	0	1.307843	IC	
mm66-5	204.4666	0	1.186937	IC	
mm66-5	207.6396	0	1.220253	IC	
mm66-5	209.6444	0	1.221958	IC	
mm66-5	213.6854	0	0.774978	IC	
mm66-5	217.8056	0	0.351498	IC	
mm66-5	262.4402	0	0.012002	IC	
mm66-5	265.5638	0	0.035187	IC	
mm66-5	270.4611	0	0.069470	IC	
mm66-6	200.8284	0	1.774114	IC	Background nitrate
mm66-6	201.6027	0	1.504314	IC	
mm66-6	202.7826	0	1.169585	IC	
mm66-6	204.4673	0	0.865081	IC	
mm66-6	207.6403	0	0.10318	IC	
mm66-6	209.6451	0	0	IC	
mm66-6	213.6861	0.258872	0	IC	Error in peak identification?
mm66-6	217.8063	0.35653	0	IC	Error in peak identification?

Sample Point	Julian Day	Br ppm	NO3-N ppm	Method	Notes
mm67-1	201.7083	0		0 IC	
mm67-1	202.7756	0		0 IC	
mm67-1	204.4680	0		0 IC	
mm67-1	207.6493	0		0 IC	
mm67-1	209.6389	0		0 IC	
mm67-1	213.691	0.310271		0 IC	Error in peak identification?
mm67-1	217.809	0		0 IC	
mm67-1	221.6166	0		0 IC	
mm67-1	225.4576	0	0.013448	IC	
mm67-1	231.4423	0	0.015057	IC	
mm67-1	234.5666	0	0.014999	IC	
mm67-1	239.4625	0	0.014137	IC	
mm67-2	201.7090	0		0 IC	
mm67-2	202.7763	0		0 IC	
mm67-2	204.4687	0		0 IC	
mm67-2	207.65	0		0 IC	
mm67-2	209.6396	0		0 IC	
mm67-2	213.6917	0		0 IC	
mm67-2	217.8097	0		0 IC	
mm67-2	221.6173	0	0.012701	IC	
mm67-2	225.4583	0	0.028672	IC	
mm67-2	231.4430	0	0.025168	IC	
mm67-2	234.5673	0		0 IC	
mm67-2	239.4631	0	0.020802	IC	
mm67-3	201.7097	0	0.101024	IC	Background nitrate
mm67-3	202.7770	0	0.107741	IC	
mm67-3	204.4694	0	0.099345	IC	
mm67-3	207.6521	0	0.04977	IC	
mm67-3	209.6403	0		0 IC	
mm67-3	213.6924	0.248592		0 IC	Error in peak identification?
mm67-3	217.8104	0		0 IC	
mm67-4	201.7104	0	0.179948	IC	Background nitrate
mm67-4	202.7777	0	0.122294	IC	
mm67-4	204.4701	0	0.186665	IC	
mm67-4	207.6528	0		0 IC	
mm67-4	209.641	0		0 IC	
mm67-4	213.6931	0.264012		0 IC	Error in peak identification?
mm67-4	217.8111	0.243452		0 IC	Error in peak identification?
mm67-5	201.7111	0	0.999421	IC	Background nitrate
mm67-5	202.7784	0	1.104654	IC	
mm67-5	204.4708	0	0.482773	IC	
mm67-5	207.6542	0	0.588988	IC	
mm67-5	209.6417	0	0.325913	IC	

Sample Point	Julian Day	Br ppm	NO3-N ppm	Method	Notes
mm67-5	213.6938	0		0 IC	
mm67-5	217.8118	0		0 IC	
mm67-5	221.6201	0		0 IC	
mm67-5	225.4604	0		0 IC	
mm67-5	231.4451	0	0.075259	IC	
mm67-5	234.5694	0		0 IC	
mm67-5	239.4652	0		0 IC	
mm67-6	201.7118	0		0 IC	
mm67-6	202.7791	0		0 IC	
mm67-6	204.4715	0		0 IC	
mm67-6	207.6556	0		0 IC	
mm67-6	209.6424	0		0 IC	
mm67-6	213.6944	0		0 IC	
mm67-6	217.8125	0		0 IC	
mm67-6	221.6208	0		0 IC	
mm67-6	225.4611	0		0 IC	
mm67-6	231.4458	0		0 IC	
mm67-6	234.5701	0		0 IC	
mm67-6	239.4659	0		0 IC	
mm68-1	207.6354	2.874940		- elect	
mm68-1	207.8021	3.254124		0 IC	
mm68-1	209.625	1.842014		0 IC	
mm68-1	209.7916	1.771976		- elect	
mm68-1	213.0277	1.164082		- elect	
mm68-1	213.4444	1.018556		0 IC	
mm68-1	217.4375	0.943510		- elect	
mm68-1	217.5069	0.908771		- elect	
mm68-1	217.5208	0.840890		0 IC	
mm68-1	217.7569	0.805357		0 IC	
mm68-1	221.7743	0.489363		- elect	
mm68-1	225.6638	0		- elect	
mm68-1	231.7166	0		- elect	
mm68-1	234.4708	0		- elect	
mm68-1	239.6402	0		- elect	
mm68-1	245.4666	0		- elect	
mm68-2	207.7583	0		- elect	
mm68-2	207.8	0.102594		0 IC	
mm68-2	209.6257	0.210139		0 IC	
mm68-2	209.7923	0.434006		- elect	
mm68-2	213.4451	1.263341		0 IC	
mm68-2	213.6534	1.273753		- elect	
mm68-2	217.4381	4.121309		- elect	
mm68-2	217.5076	4.681975		- elect	
mm68-2	217.5215	4.607416		0 IC	
mm68-2	217.7576	5.025918		0 IC	

Sample Point	Julian Day	Br ppm	NO3-N ppm	Method	Notes
mm68-2	221.775	7.165360		- elect	
mm68-2	225.6645	10.14324		- elect	
mm68-2	231.7173	6.627033		- elect	
mm68-2	234.4722	3.852201		- elect	
mm68-2	239.6416	1.726049		- elect	
mm68-2	240.4937	1.288170		- elect	
mm68-2	245.7597	0.416460		- elect	
mm68-3	207.7555	6.225641		- elect	
mm68-3	207.7972	6.690881		0 IC	
mm68-3	209.6264	5.942743		0 IC	
mm68-3	209.7930	5.584741		- elect	
mm68-3	213.4458	5.803702		0 IC	
mm68-3	213.6541	5.522240		- elect	
mm68-3	217.4388	4.824618		- elect	
mm68-3	217.5083	4.897561		- elect	
mm68-3	217.5222	5.025918		0 IC	
mm68-3	217.7583	5.085141		0 IC	
mm68-3	221.7763	3.809090		- elect	
mm68-3	225.6652	3.075778		- elect	
mm68-3	231.7180	0.925978		- elect	
mm68-3	234.4736	0.372132		- elect	
mm68-3	239.6430	0		- elect	
mm68-3	245.4687	0		- elect	
mm68-3	251.7520	0		- elect	
mm68-3	259.5972	0		- elect	
mm68-3	263.6986	0		- elect	
mm68-3	272.6006	0		- elect	
mm68-4	207.5444	0		- elect	
mm68-4	207.7944	0		0 IC	
mm68-4	209.6271	0		0 IC	
mm68-4	209.7937	0		- elect	
mm68-4	213.4465	0.572417		0 IC	
mm68-4	213.6548	0.645943		- elect	
mm68-4	217.4395	1.726049		- elect	
mm68-4	217.5090	1.798766		- elect	
mm68-4	217.5229	1.693688		0 IC	
mm68-4	217.7590	1.780547		0 IC	
mm68-4	221.7770	1.975630		- elect	
mm68-4	225.6659	1.812313		- elect	
mm68-4	231.7187	1.208582		- elect	
mm68-4	234.4743	1.168458		- elect	
mm68-4	239.6444	1.414829		- elect	
mm68-4	240.4951	1.668745		- elect	
mm68-4	245.7618	2.578583		- elect	
mm68-4	251.7548	3.378204		- elect	
mm68-4	259.5986	3.266049		- elect	

Sample Point	Julian Day	Br ppm	NO3-N ppm	Method	Notes
mm68-4	263.7006	2.962530		- elect	
mm68-4	272.6013	2.697316		- elect	
mm68-4	280.5659	1.931658		- elect	
mm68-5	207.7125	0		- elect	
mm68-5	207.7958	0		0 IC	
mm68-5	209.6278	0		0 IC	
mm68-5	209.7944	0		- elect	
mm68-5	213.4472	0		0 IC	
mm68-5	213.6555	0		- elect	
mm68-5	217.4402	1.425484		- elect	
mm68-5	217.5097	1.571529		- elect	
mm68-5	217.5236	1.318615		0 IC	
mm68-5	217.7597	1.437059		0 IC	
mm68-5	221.7784	3.655104		- elect	
mm68-5	225.625	3.738308		- elect	
mm68-5	231.7611	4.560626		- elect	
mm68-5	234.4756	4.915969		- elect	
mm68-5	239.6458	5.200530		- elect	
mm68-5	240.4965	5.027875		- elect	
mm68-5	245.7625	4.752761		- elect	
mm68-5	251.7562	3.766462		- elect	
mm68-5	259.6	1.758731		- elect	
mm68-5	263.7020	1.063854		- elect	
mm68-5	272.6020	0.407191		- elect	
mm68-5	280.5659	0		- elect	
mm68-6	207.809	0		0 IC	
mm68-6	209.6285	0		0 IC	
mm68-6	213.4479	0		0 IC	
mm68-6	217.5243	0		0 IC	
mm68-6	217.7604	0		0 IC	
mm68-6	221.7375	0		- elect	
mm68-6	225.4590	0		- elect	
mm68-6	231.6368	1.100386		- elect	
mm68-6	234.7687	1.496726		- elect	
mm68-6	239.6472	1.589315		- elect	
mm68-6	240.7895	4.934445		- elect	
mm68-6	245.4722	3.217406		- elect	
mm68-6	251.7576	1.051948		- elect	
mm68-6	272.6027	0		- elect	
mm68-6	280.5694	0		- elect	
mm68-7	207.8153	0		0 IC	
mm68-7	209.6292	0		0 IC	
mm68-7	213.4486	0		0 IC	
mm68-7	217.525	0		0 IC	
mm68-7	217.7611	0		0 IC	

Sample Point	Julian Day	Br ppm	NO3-N ppm	Method	Notes
mm68-7	221.7388	0		- elect	
mm68-7	225.6263	0		- elect	
mm68-7	231.7625	0		- elect	
mm68-7	234.4784	0		- elect	
mm68-7	239.6486	0		- elect	
mm68-7	245.4729	0		- elect	
mm68-7	251.7590	0		- elect	
mm68-7	272.6034	0		- elect	
mm69-1	213.7048	0		0 IC	
mm69-1	217.5263	0		0 IC	
mm69-1	217.75	0		0 IC	
mm69-2	213.7055	0		0 IC	
mm69-2	213.7881	0.524128		- elect	
mm69-2	217.4743	0.266388		- elect	
mm69-2	217.5270	0		0 IC	
mm69-2	217.7506	0		0 IC	
mm69-2	217.7666	0		- elect	
mm69-3	213.4958	1.958905		- elect	
mm69-3	217.5027	4.240239		0 IC	
mm69-3	217.7513	5.025918		0 IC	
mm69-3	217.7680	0.600625		- elect	
mm69-3	217.7937	1.273421		- elect	
mm69-3	221.7062	5.649142		- elect	
mm69-3	225.5277	4.655912		- elect	
mm69-3	231.7513	4.843753		- elect	
mm69-3	234.6722	4.951365		- elect	
mm69-3	239.7902	7.372139		- elect	
mm69-3	240.475	7.428977		- elect	
mm69-3	245.6506	4.822513		- elect	
mm69-4	213.4972	0.526437		- elect	
mm69-4	213.7069	8.734534		0 IC	
mm69-4	217.5285	7.506103		0 IC	
mm69-4	217.6013	0.208274		- elect	
mm69-4	217.7521	7.506103		0 IC	
mm69-4	217.7694	0.323216		- elect	
mm69-4	221.7069	7.428977		- elect	
mm69-4	225.5284	7.040126		- elect	
mm69-4	231.7520	6.932812		- elect	
mm69-4	234.6736	4.995076		- elect	
mm69-4	239.7916	4.320747		- elect	
mm69-4	245.4756	2.858589		- elect	
mm69-4	251.6520	1.694455		- elect	
mm69-5	213.625	0.524128		- elect	

Sample Point	Julian Day	Br ppm	NO3-N ppm	Method	Notes
mm69-5	213.7076	0.222893		0 IC	
mm69-5	217.5292	0.485027		0 IC	
mm69-5	217.5361	1.635918		- elect	
mm69-5	217.7222	1.301712		- elect	
mm69-5	217.7528	0.510726		0 IC	
mm69-5	221.7076	0.348288		- elect	
mm69-5	225.5291	0.390447		- elect	
mm69-5	231.7527	0.231441		- elect	
mm69-5	234.675	0.409786		- elect	
mm69-5	239.7930	0.417053		- elect	
mm69-5	245.4763	0.542883		- elect	
mm69-5	251.6534	0.584995		- elect	
mm69-5	263.4986	0.582430		- elect	
mm69-5	272.7708	0.831456		- elect	
mm69-5	280.6020	0.633150		- elect	
mm69-6	213.6263	1.628744		- elect	
mm69-6	213.7083	0		0 IC	
mm69-6	217.5299	0		0 IC	
mm69-6	217.5368	0.277136		- elect	
mm69-6	217.7222	0		- elect	
mm69-6	217.7535	0		0 IC	
mm69-6	221.7083	0		- elect	
mm69-6	225.5298	0		- elect	
mm69-6	231.7534	0		- elect	
mm69-6	234.6763	0.362340		- elect	
mm69-6	239.7944	3.721062		- elect	
mm69-6	240.4770	7.428977		- elect	
mm69-6	245.6548	7.013143		- elect	
mm69-6	251.5	6.620584		- elect	
mm69-6	259.7951	6.697298		- elect	
mm69-6	263.7715	4.843753		- elect	
mm69-6	272.6034	4.475355		- elect	
mm69-6	280.6902	2.784199		- elect	
mm69-7	0.5375	0		- elect	
mm69-7	0.627777	1.874682		- elect	
mm69-7	0.71875	0		- elect	
mm69-7	213.709	0		0 IC	
mm69-7	217.5306	0		0 IC	
mm69-7	221.7090	0		- elect	
mm69-7	225.5305	0		- elect	
mm69-7	231.7541	0		- elect	
mm69-7	234.6770	0		- elect	
mm69-7	239.7979	0		- elect	
mm69-7	240.4777	0		- elect	
mm69-7	245.6562	0.399122		- elect	
mm69-7	251.5013	1.786212		- elect	

Sample Point	Julian Day	Br ppm	NO3-N ppm	Method	Notes
mm69-7	263.7965	1.993645		- elect	
mm69-7	272.7722	1.716943		- elect	
mm69-7	280.6048	2.527618		- elect	
mm70-1	225.7687	1.583801		- elect	
mm70-1	231.5173	0.587660		- elect	
mm70-1	234.6618	0.353971		- elect	
mm70-1	251.6194	0		- elect	
mm70-1	272.5486	0		- elect	
mm70-2	225.7708	1.946804		- elect	
mm70-2	231.5180	1.576711		- elect	
mm70-2	234.6652	1.903622		- elect	
mm70-2	239.5062	2.148745		- elect	
mm70-2	251.6180	2.120020		- elect	
mm70-2	263.6284	1.288483		- elect	
mm70-2	272.5493	1.199239		- elect	
mm70-3	225.7743	0.277818		- elect	
mm70-3	251.6194	1.878174		- elect	
mm70-3	263.6291	1.243061		- elect	
mm70-3	272.55	0.556861		- elect	
mm70-4	251.6069	0.232182		- elect	
mm70-4	263.6298	0		- elect	
mm70-4	272.5506	0		- elect	
mm70-5	251.6083	0		- elect	
mm70-5	263.6312	0		- elect	
mm70-5	272.5513	0		- elect	
mm70-6	251.6097	0		- elect	
mm70-6	263.6326	0		- elect	
mm70-6	272.5520	0		- elect	
mm71-1	231.5583	0.326512		- elect	
mm71-1	239.4833	0		- elect	
mm71-5	231.5555	0.953987		- elect	
mm71-6	231.5569	0.572053		- elect	
mm72-5	239.4763	0		- elect	
mm73-1	239.4631	0		- elect	
mm73-2	239.4638	0		- elect	
mm73-3	239.4645	0		- elect	
mm73-4	239.4652	0		- elect	
mm73-5	239.4659	0		- elect	
mm73-6	239.4666	0		- elect	

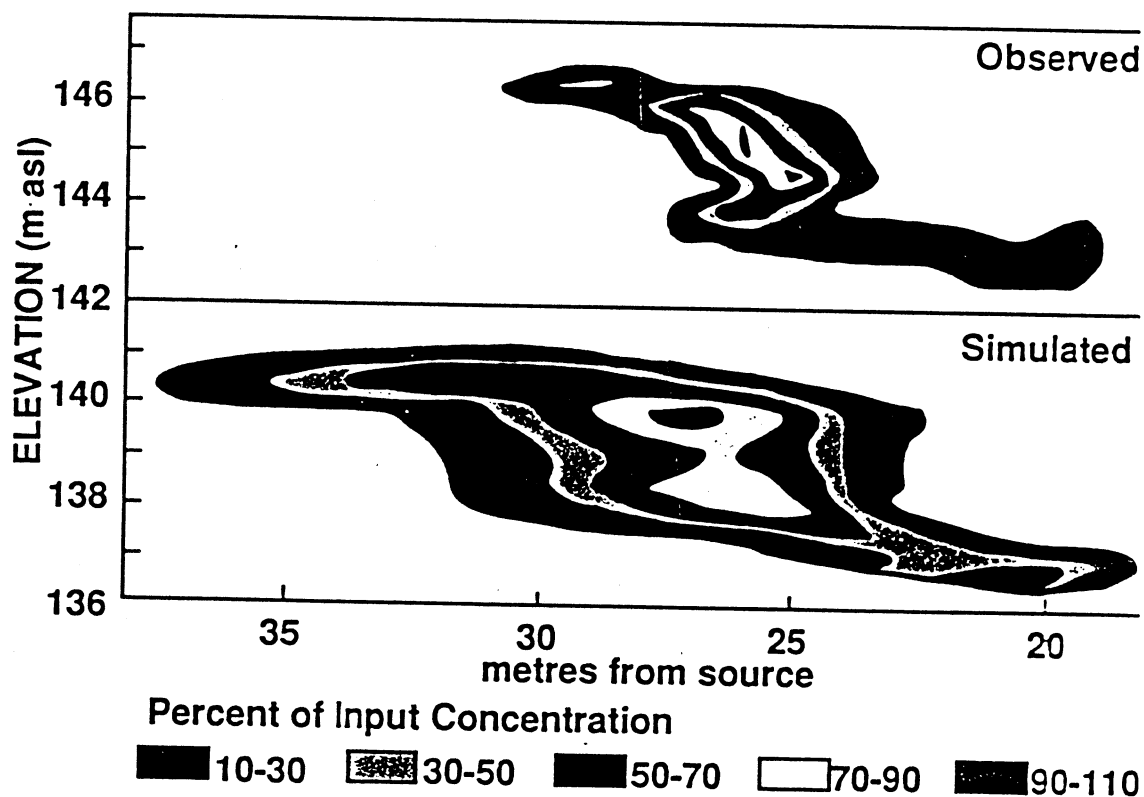
Sample Point	Julian Day	Br ppm	NO3-N ppm	Method	Notes
mm74-1	234.6701	0.344749		- elect	
mm74-1	239.4513	0		- elect	
mm74-1	245.7819	0		- elect	
mm74-2	234.7541	0.826296		- elect	
mm74-2	239.4520	0.402671		- elect	
mm74-2	240.8020	0.358795		- elect	
mm74-2	245.7833	0.212545		- elect	
mm74-2	251.6284	0		- elect	
mm74-3	234.6715	3.086567		- elect	
mm74-3	239.4527	1.438864		- elect	
mm74-3	240.8034	1.097661		- elect	
mm74-3	245.7847	0.436151		- elect	
mm74-3	251.6298	0		- elect	
mm74-4	234.6722	9.883439		- elect	
mm74-4	239.4534	8.483311		- elect	
mm74-4	240.8048	7.889557		- elect	
mm74-4	245.7861	2.145142		- elect	
mm74-4	251.6312	0.390356		- elect	
mm74-4	272.5722	0		- elect	
mm74-4	280.7305	0		- elect	
mm74-5	234.6729	4.789120		- elect	
mm74-5	239.4541	3.653461		- elect	
mm74-5	240.8062	3.183943		- elect	
mm74-5	245.7875	2.887817		- elect	
mm74-5	251.6326	0.422813		- elect	
mm74-5	280.7277	0.120980		- elect	
mm74-6	234.6736	0.746128		- elect	
mm74-6	239.4548	1.276406		- elect	
mm74-6	240.8076	0.883165		- elect	
mm74-6	245.7888	0.426581		- elect	
mm74-6	251.6340	0.969416		- elect	
mm74-6	280.7291	0.129881		- elect	
mm74-7	234.6743	3.343205		- elect	
mm74-7	239.4555	6.277794		- elect	
mm74-7	240.8090	6.418631		- elect	
mm74-7	245.7902	3.702420		- elect	
mm74-7	251.6354	0.480876		- elect	
mm74-7	272.5763	0.766259		- elect	
mm74-7	280.7256	0.390356		- elect	
mp 8	217.5208	0.742435		- elect	

Sample Point	Julian Day	Br ppm	NO3-N ppm	Method	Notes
mp 8	217.6458	0.813253		0 IC	
mp 8	221.6625	1.835930		- elect	
mp 8	225.7076	3.163148		- elect	
mp 8	231.7902	1.806999		- elect	
mp 8	234.6368	1.219628		- elect	
mp 8	239.5006	1.082657		- elect	
mp 8	240.5180	0.945924		- elect	
mp 8	245.8180	0.350524		- elect	
mp 9	225.7590	0.393306		- elect	
mp 9	231.7916	1.011984		- elect	
mp 9	239.5430	0		- elect	
mp 9	240.5194	0		- elect	
mp 9	245.8194	0		- elect	
ditch	225.4270	0.367631		- elect	
ditch	234.7979	0.334213		- elect	
ditch	239.6319	0		- elect	

APPENDIX D - Paper published in Ottawa Conference Proceedings

Transport and Mass Exchange Processes in Sand and Gravel Aquifers: Field and Modelling Studies

G. Moltyaner, Editor



Twin Lake Tracer Test

Proceedings of the International Conference and Workshop held in Ottawa, Canada
October 1 - 4, 1990

AECL-10308

Volume 1 pp 355-372

TRACER STUDY IN A COMPLEX THREE-DIMENSIONAL FLOW SYSTEM

Lucy W. Chambers and Jean M. Bahr, Department of
Geology and Geophysics, University of Wisconsin - Madison

ABSTRACT

An ongoing series of natural gradient tracer tests are being conducted in Wisconsin's central sand plain, a region of thick sandy glacial outwash. The initial motivation for the tracer tests was to determine the flow path around a drainage ditch in order to evaluate the role of ditches in limiting the spread of agricultural contamination. The tests were also designed to permit a detailed evaluation of the tracer movement within the aquifer. These tracer tests involve the simultaneous introduction of bromide and iodide tracers, each at a different depth, up-gradient of the ditch. The path of the tracer is monitored by frequent synoptic sampling from a dense three-dimensional array of multilevel sampling wells.

The overall movement of the tracer plume suggests that the drainage ditch acts as a barrier to the shallow flow within the aquifer. A more detailed examination of the groundwater flow pattern reveals that it is quite complex. The direction and velocity of the flow varies spatially and includes a significant component of vertical flow across aquifer stratification. A variation in groundwater velocity, from an average rate of 0.4 ft/day at a depth of 20 ft to more than 1 ft/day near the water table, clearly affected the movement of the tracer plume. The transient nature of the flow system and small scale aquifer heterogeneities also appear to have affected the shape and path of the tracer plume. A detailed examination of breakthrough curves along with plume and water table maps calculated for over 40 different days during the test, were used to assess the combined effects of aquifer heterogeneity, flow across stratification, and fluctuating gradients on macroscale dispersion. Additional tracer tests are being conducted in order to refine our interpretations.

INTRODUCTION

The central sand plains of Wisconsin is a region of thick sandy sediment of glaciofluvial and glaciolacustrine origin. The glacial sands form the principal aquifer for both municipal use and for irrigation in this important agricultural region. High nitrate concentrations and pesticide contamination have resulted in the closing of a municipal well (Borne et al., 1988) and a number of domestic wells (Lulloff, 1987). A number of recent research and monitoring efforts have been designed to determine the extent of contamination and to characterize the processes that control contaminant migration in the unsaturated zone and groundwater of the central sand plain (Brasino, 1986; Chesters et al., 1982; Harkin et al. 1986; Jones, 1987; Manser, 1983; Kung, 1990a,b; Rothschild et al., 1982; Stoertz, 1983).

The results of these studies have highlighted the need for effective measures to control shallow contaminant migration. Interceptor ditches have been used with success to remove shallow contamination at waste management sites (Cantor and Knox, 1986; Gilbert and Gress, 1987). In the sand plain an existing network of drainage ditches serves to lower the water table and may act as passive controls on contamination. Zheng et al. (1988a, 1988b) developed an analytical and a numerical model to evaluate the effectiveness of existing ditches by identifying the "capture zone" of a ditch (Figure 1). The capture zone is the region above the dividing streamline from which all water flows into the ditch.

The objectives of the field experiment described in this paper were to verify the existence of a capture zone in the vicinity of a drainage ditch in central sand plain and to generate a data set that could be used to conduct a detailed evaluation tracer movement in a complex flow system. An ongoing series of natural gradient tracer tests are being used to evaluate the flow system and to assess the combined effects of aquifer heterogeneity, flow across aquifer stratification, and fluctuating gradients on macroscale dispersion.

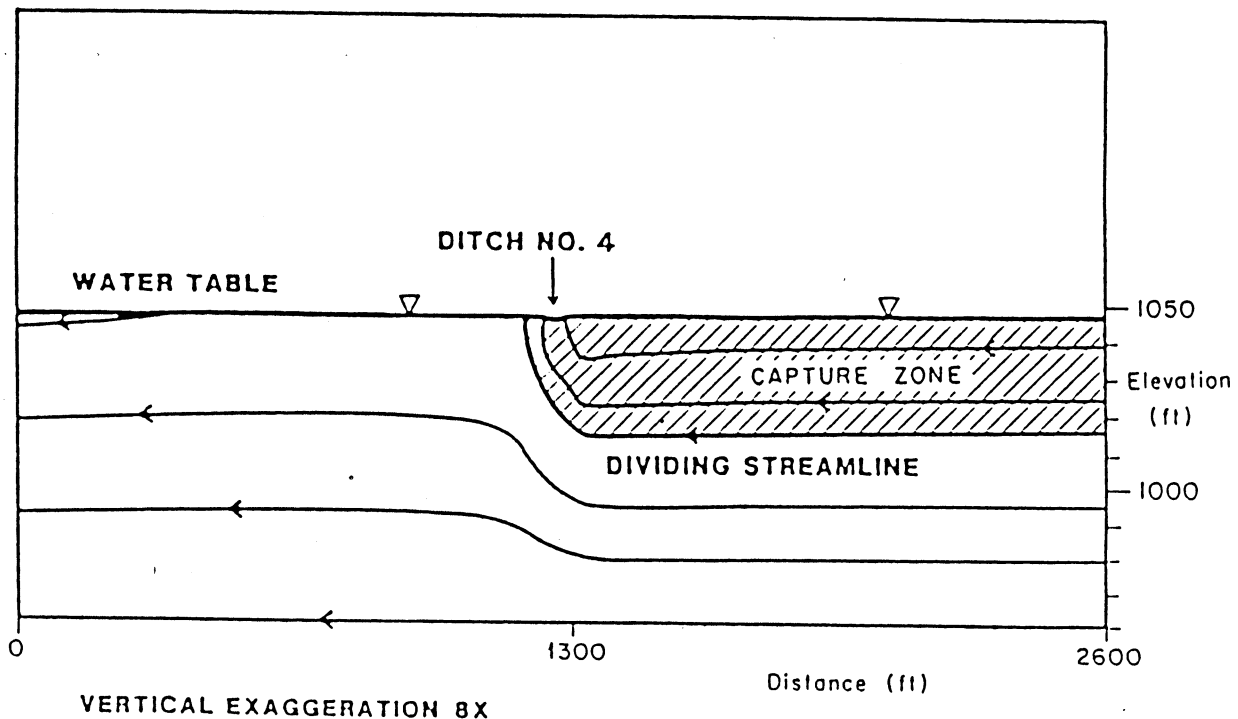


Figure 1. The capture zone of ditch no. 4 in the central sand plain on August 22, 1984 (modified from Zheng et al., 1988a)

FIELD SITE DESCRIPTION

Geology and Hydrology of the Central Sand Plain

The field site for this study is located about 100 miles north of Madison, Wisconsin within the region known as the central sand plain (Figure 2). The sand plain is a region of sandy glacial outwash just west of the maximum extent of Pleistocene glaciation delimited by a terminal moraine. The sandy glaciolacustrine and glaciofluvial sediments, primarily derived from the poorly-lithified Cambrian sandstone bedrock, were deposited in this area during several episodes of filling and draining of Glacial Lake Wisconsin. A relatively extensive silt and clay bed, known as the New Rome Member, was probably deposited during the last filling of Glacial Lake Wisconsin (Clayton and Attig, 1989). A meter or more of windblown sediment covers the outwash in some portions of the sand plain (Clayton, 1986; 1987). The total thickness of sediments above the bedrock ranges from 0 to over 150 feet (Faustini, 1985; Weeks and Stangland, 1971).



Figure 2. The location of the field site within the central sand plain of Wisconsin (modified from Anderson, 1986)

The regional groundwater flow within the eastern portion of the central sand plain is towards the Wisconsin River. The mean hydraulic conductivity in this region as computed by Stoertz (1989) from results of eleven pumping tests is 250 ft/day. The vertical hydraulic conductivity appears to be somewhat lower due to horizontal layering within the aquifer. Weeks and Stangland (1971) evaluated 5 pumping tests and concluded that the probable anisotropy ratio for the central sand plain is between 1 to 7.

Site Characteristics

According to the maps of Clayton and Attig (1989), the field site for this study is located near the edge of the maximum extent of Glacial Lake Wisconsin. Drilling at the site revealed the presence of a silt and clay layer, presumably the New Rome Member, at a depth of approximately 30 ft. The sediment above the silt and clay layer is predominantly well sorted fine sand, based on the Folk (1980) classification. A vibracore of the relatively shallow sediment at the site revealed distinct narrow zones of coarser and finer sediment. A number of slug tests and grain size analyses are currently being conducted in order to evaluate variations in hydraulic conductivity at the site.

A ditch approximately 9 feet wide runs north-south across the field site. Mini-piezometers installed in the ditch indicate that head in the aquifer exceeds ditch stage by 0.1 to 0.2 feet. Based on a water table map of Adams County, regional flow is to the west-southwest, roughly perpendicular to the ditch, and the gradient is about 0.0015. Water table measurements at the site indicate that the local water table gradient near the east side of the ditch ranges from greater than 0.007 to around 0.003. The local groundwater gradient on the west side of the ditch varies from about 0.004 to being undetectable. Figure 3 shows the water table configuration in the vicinity of the ditch as water levels dropped from mid-July (when the tracer test was begun) until late September when the fall recharge caused water levels to rise.

TRACER TEST METHODOLOGY

Conceptual Design

Figure 4 is a schematic of a tracer test designed to identify the capture zone of a ditch. Distinct tracers are introduced and different depths and tracer paths are monitored by sampling from multilevel sampling wells located on both sides of the ditch. Based on preliminary estimates using the analytic solution by Zheng et al. (1988a), the capture depth at the field site was predicted to be above the silt and clay layer. Bromide and iodide were selected as tracers because they were expected to behave conservatively in the sandy sediments at the site. Background concentrations of these anions were below the limit of detection for specific ion electrodes, permitting introduction of tracers at relatively low concentrations.

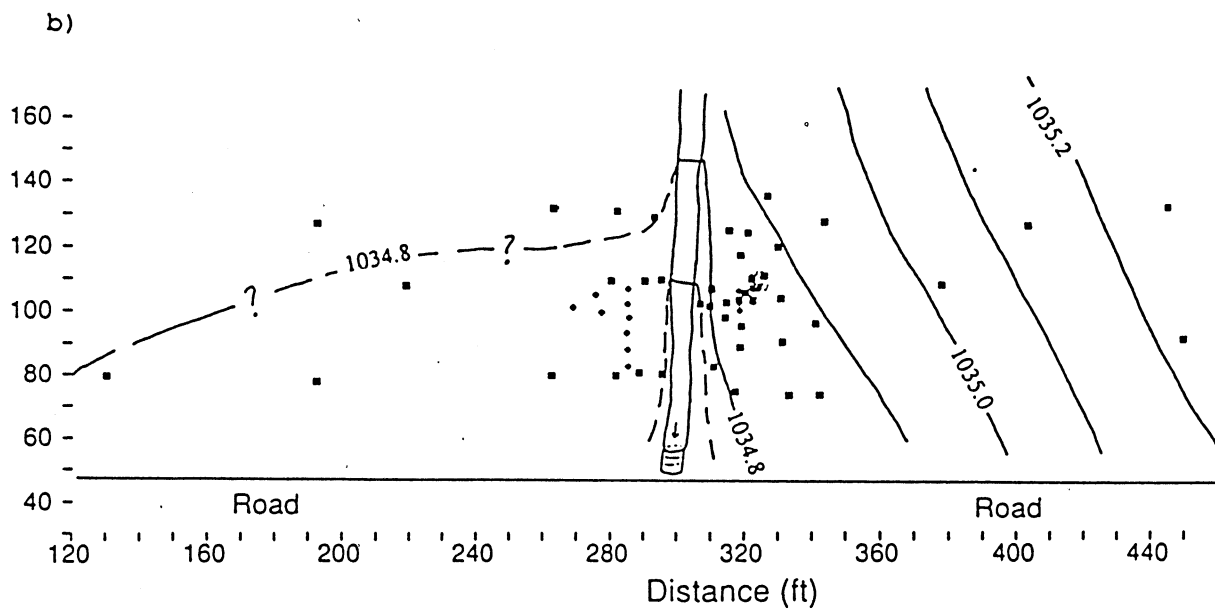
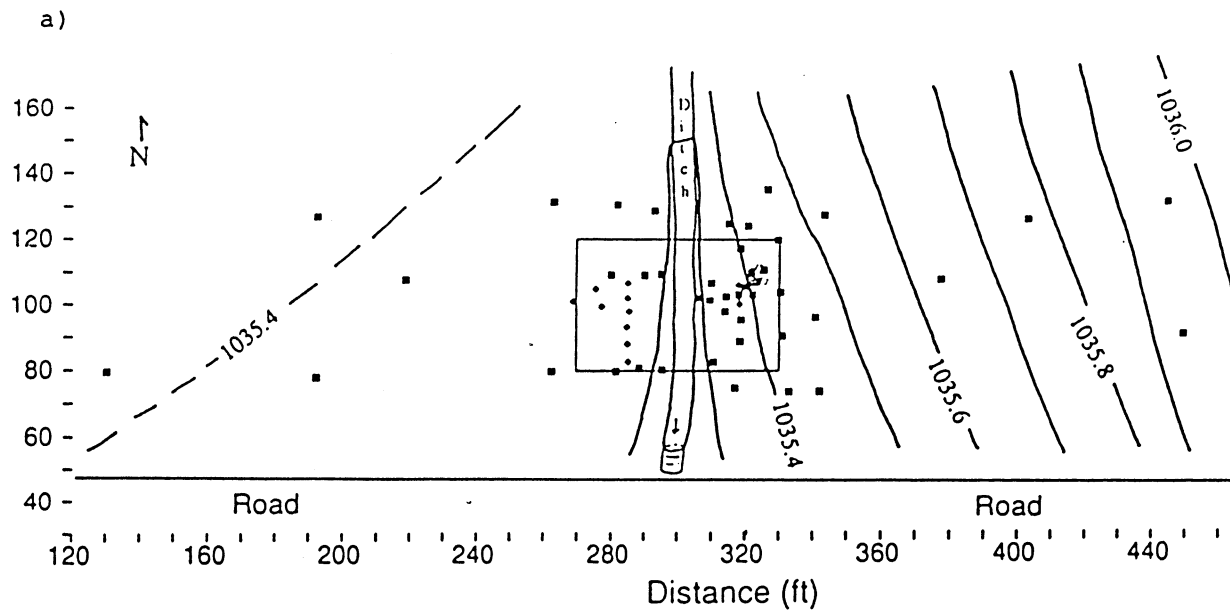


Figure 3. Water table maps for the field site on a) July 16, 1989 and b) September 23, 1989. Squares represent water table wells, diamonds, represent multilevel wells and upside down triangles represent injection wells. The rectangle on Figure 3a delineates the area instrumented for the tracer test as shown in Figure 5a.

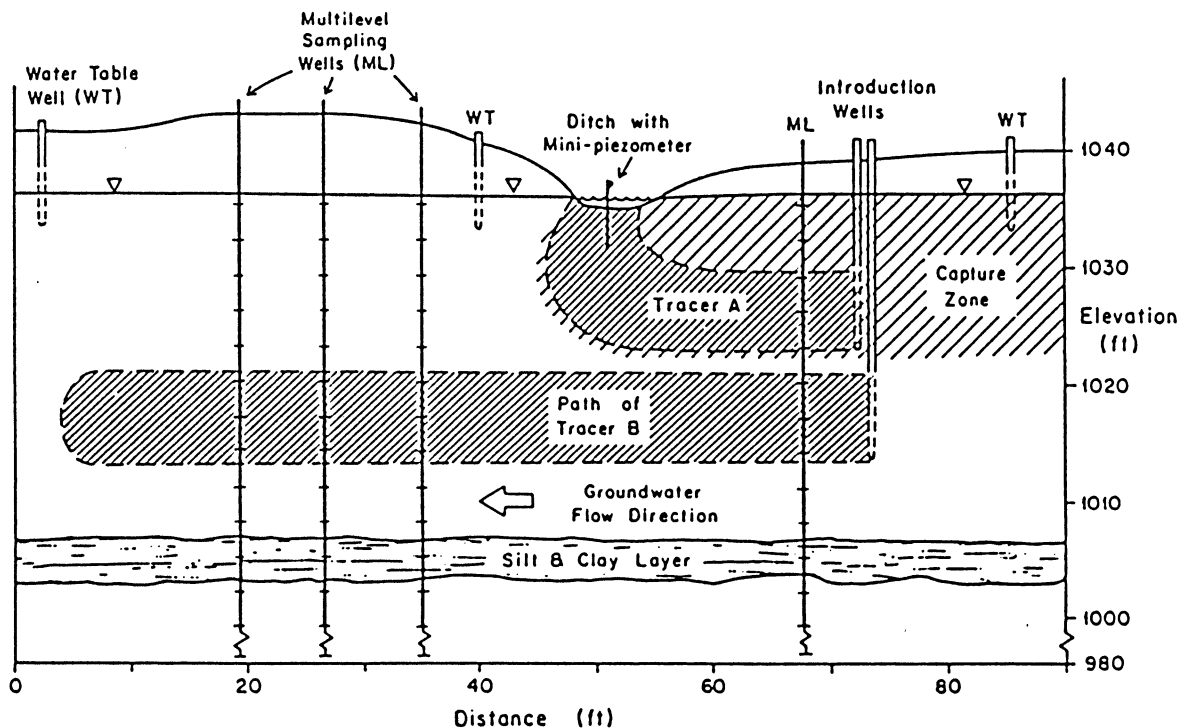


Figure 4. A schematic of a tracer test designed to identify the capture zone.

Monitoring Network

A dense array of monitoring points has been installed at the field site. Over 50 water table wells have been installed either by hand auguring or using a trailer mounted auger. Mini-piezometers of the type described by Lee and Cherry (1978) were installed in the ditch to depths of 2 to 7 feet below the sediment surface. Seven 2-inch diameter injection wells, installed using a truck mounted auger, were used for the test described in this paper: one well screened 0.6 to 2.0 feet below the water table, a set of three wells screened from 6.4 to 11.1 feet below the water table, and another set of three wells screened from 16.4 to 21.1 feet below the water table. Twelve bundle-type multilevel sampling wells of the type described by Jackson et al. (1985) were installed in borings completed using hollow stem auger. Each multilevel consists of approximately twenty 0.25-inch polyethylene tubes attached to a PVC backbone. Nylon mesh at the end of each tube forms the sampling point. Sampling points were spaced at intervals of either 1.5 or 3 feet. Miniature multilevels, consisting of three 0.25-inch tubes with nylon mesh points, were installed using the method described by Stites and Chambers (in press). Most of these were added during the tracer test in order to obtain improved definition of tracer paths. A number of these were installed through the base of the ditch, permitting monitoring of the tracer within the capture zone prior to

discharge into the ditch. Figure 5 shows the location of multilevels, miniature multilevels and injection wells employed during the tracer test.

Tracer Injection

A number of preliminary tests were conducted at the site between August of 1988 and June of 1989 (Chambers, 1990). Only the results of the multiple tracer test initiated in July of 1989 will be described in this paper. Another multiple tracer test begun in the summer of 1990 is currently still in progress. For the test begun in mid-July of 1989, two different tracer solutions were injected into three different levels within the aquifer: iodide solution at a concentration of 0.5 g/l in the shallowest injection well, bromide solution at a concentration of 1 g/l in the three intermediate injection wells, and iodide at a concentration of 1 g/L in the three deep injection wells. Each tracer solution was mixed in carboys by combining a measured amount of crystalline potassium bromide or potassium iodide with approximately 20 liters of water from the aquifer. Injection was accomplished by draining solution through the carboy spigot into the well while carefully monitoring the flow rate. At the intermediate and deep levels, three injection wells were used to ensure that the resulting tracer plume would be sufficiently wide to be detected should the tracer travel beyond the ditch. Because the shallow iodide plume was expected to have a much shorter flow path, a single injection well was judged to be sufficient to generate a plume that could be traced to the ditch. Additional injection characteristics are summarized in Table 1.

Sampling and Analysis

Samples were collected from multilevel and miniature multilevel points using a peristaltic pump. A volume of 150 to 500 mL, corresponding to two or three tube volumes, was removed from each multilevel point prior to sampling. Field measurements of electrical conductance provided a preliminary estimate of tracer concentration. Samples for laboratory analysis were stored in 120 mL polypropylene cups. Sampling frequency for points at which tracer arrival was expected ranged from at least once a day during the first eleven days of the test, to at least once a week after the first two months of monitoring. Over 2500 samples were analyzed during the course of the test.

Laboratory analyses were performed using Orion specific ion electrodes and a Chemcadet electrode meter. Ionic strength adjuster (ISA, 5 M sodium nitrate) was added to samples prior to analysis, using 2 mL of ISA per 100 mL of sample. Electrodes were standardized before and after each set of analyses, using solutions with concentrations in the range anticipated for the samples. When periods of analysis extended over several hours, electrodes were restandardized to check for drift at least every two hours.

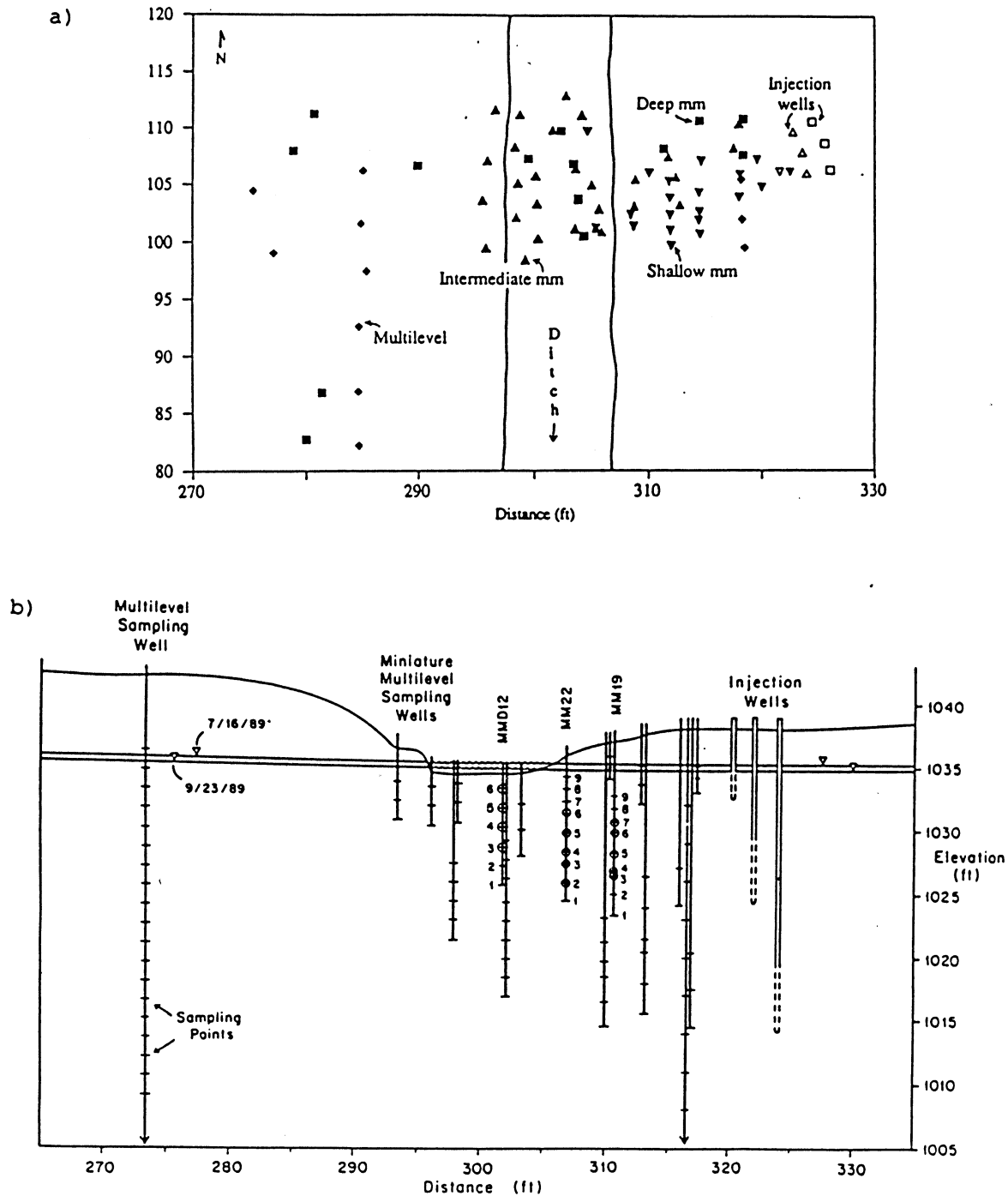


Figure 5. a) This diagram shows the location of all multilevels and miniature multilevels wells at the field site. The open triangles and squares represent miniature multilevel wells (mm). The squares represent the deeper miniature multilevels of the depth for monitoring the tracer injected into the deeper injection wells (squares). The triangles are for monitoring at an intermediate depth and the upside down triangles are very shallow miniature multilevels. The diamonds represent the multilevel wells. b) A cross-section of the wells along the axis of the plumes. Breakthrough curves for some of the circled points are shown in Figure 8.

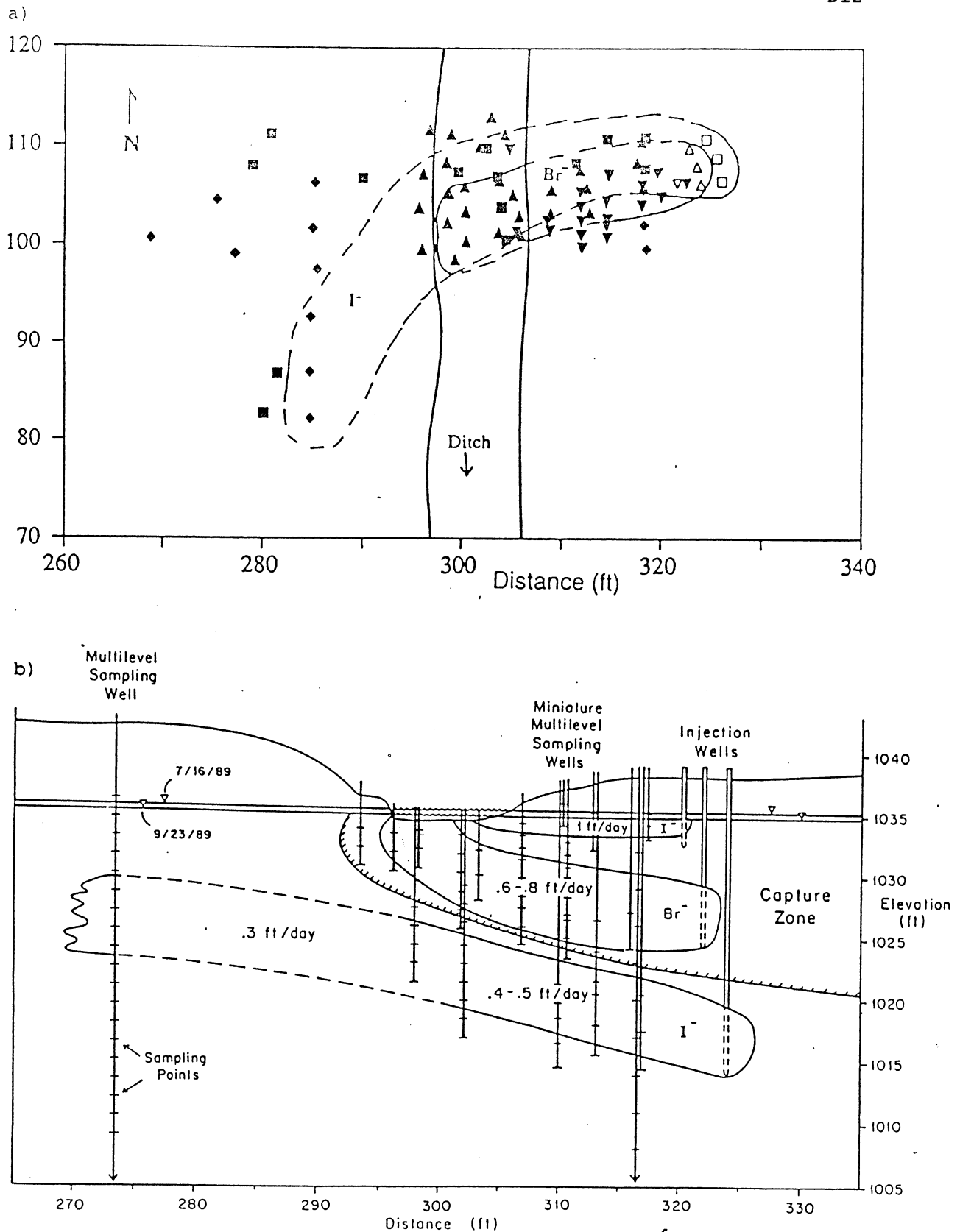
Table 1 - Injection Information

	Shallow	Inter- mediate	Deep
Elevation of Screen (ft)	1033.5- 1034.9	1024.4- 1029.1	1014.4- 1019.1
Tracer	Iodide	Bromide	Iodide
Concentration (g/l)	0.5	1.0	1.0
Injection Rate (l/hr)	45	235	235
Duration of Injection (hr)	2.3	3.0	3.0
Volume (l)	102	705	800

RESULTS

Tracer Paths

Figure 6a illustrates the total horizontal movement of the deep iodide and intermediate bromide plumes between the time of injection on July 17, 1989 and the last sampling round on December 5, 1989. The shallow iodide plume followed a horizontal path similar to that of the bromide and is not shown on this figure. The total movement of the tracer plumes and the range of average velocities for each plume are shown in cross section on Figure 6b. The flow paths of the bromide and deep iodide plumes appear to bracket the dividing streamline of the capture zone for the summer and fall of 1989. At a lateral distance of 25 feet from the ditch, the dividing streamline lies between 11.3 and 15.7 feet below the average water table position for the test. Given that the deep iodide plume showed an upward component of flow even at this distance, it is likely that the depth to the dividing streamline is even greater at larger distances from the ditch. The capture depth falls within the range predicted using the analytic model by Zheng et al. Preliminary evaluations of the tracer test begun in the summer of 1990 indicate that there may be significant transient variations in the depth of the capture zone.



Plume Dispersion

The areal distributions of the deep and intermediate tracer plumes are illustrated by a series of plan views (Figure 7a) for days 15, 45 and 131 following injection. Maximum concentrations measured within each multi-level were used to contour the plumes in order to define the edges of the plumes. Evaluation of frequent synoptic sampling suggests that there was very little horizontal transverse dispersion in the intermediate bromide plume; the plume width appeared relatively constant until the plume began discharging to the ditch. The width of the deep iodide plume appears to increase once the plume is beneath the ditch. This increase in plume width is probably due to the change in flow path of the plume as it curved off toward the south-west.

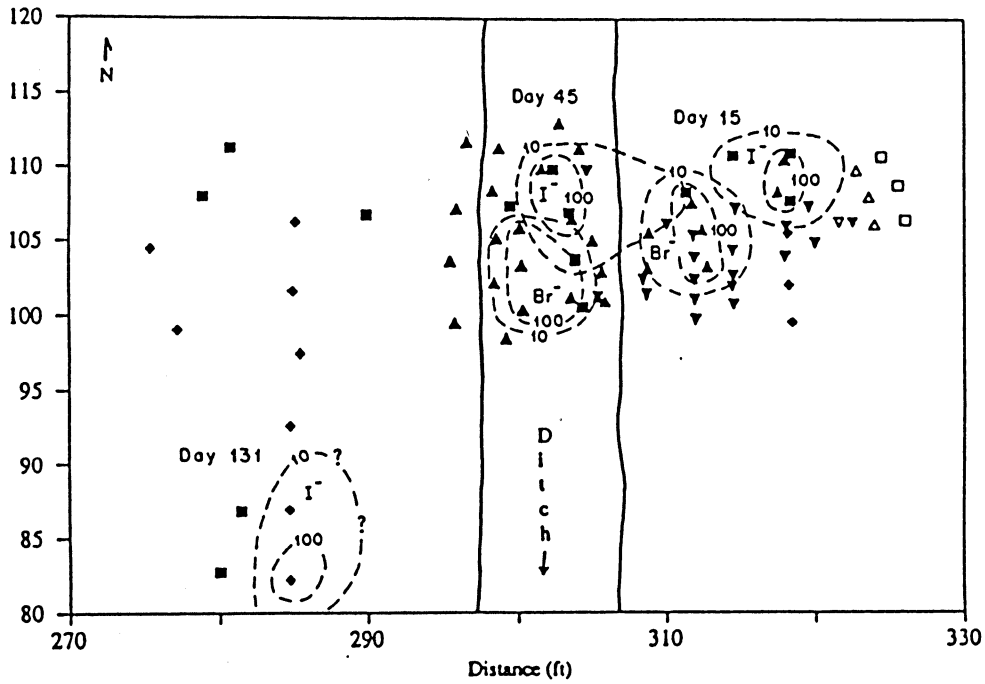
The cross sections in Figure 7b show the vertical distributions of the three plumes on days 15, 45, and 131, projected from the approximate longitudinal axis of each plume. There appears to be very little vertical transverse dispersion based on the examination of numerous synoptic sampling rounds. Examination of the plumes, for example the bromide plume on day 15, shows that there are clearly zones of higher and lower velocity within the aquifer, presumably due to variations in the hydraulic conductivity of the sediment. On day 15, bromide was found at points 2 and 5 in miniature multilevel (mm) 22 (location on Figure 5) and not at the points in between. Near the center of the plume, concentrations of over 300 mg/l were found in points 3,4 and 7 in mm19, and concentrations of less than 100 mg/l were found at points 5 and 6 in between. A peak concentration of 700mg/l was measured on day 11 in point 6 in mm19; point 5 reached its peak of a bit over 200 mg/l on about day 20 of the test. The dramatic variations in velocity seen in mm19 appeared to have decreased by the time the center of mass of the plume reached mm22. It appears that as the plume moved upward toward the ditch, the portion of the plume that had been flowing in a higher hydraulic conductivity zone reached a zone of slightly lower conductivity.

All 3 plumes clearly lengthened along the axis of flow as they migrated through the aquifer. The longitudinal dispersion of the plumes appears to be predominantly due to velocity variations caused by aquifer heterogeneity and intensified by flow across aquifer stratification. Fluctuating gradients within this shallow flow system also appear to have contributed to plume dispersion.

Apparent Dispersivities

In order to evaluate the apparent dispersivity, breakthrough curves from the bromide plume were modeled. The one-dimensional analytic solution used by Moltyaner and Killey (1988) to model two tracer tests at the Twin Lake site was used to evaluate a series of breakthrough curves. The

a)



b)

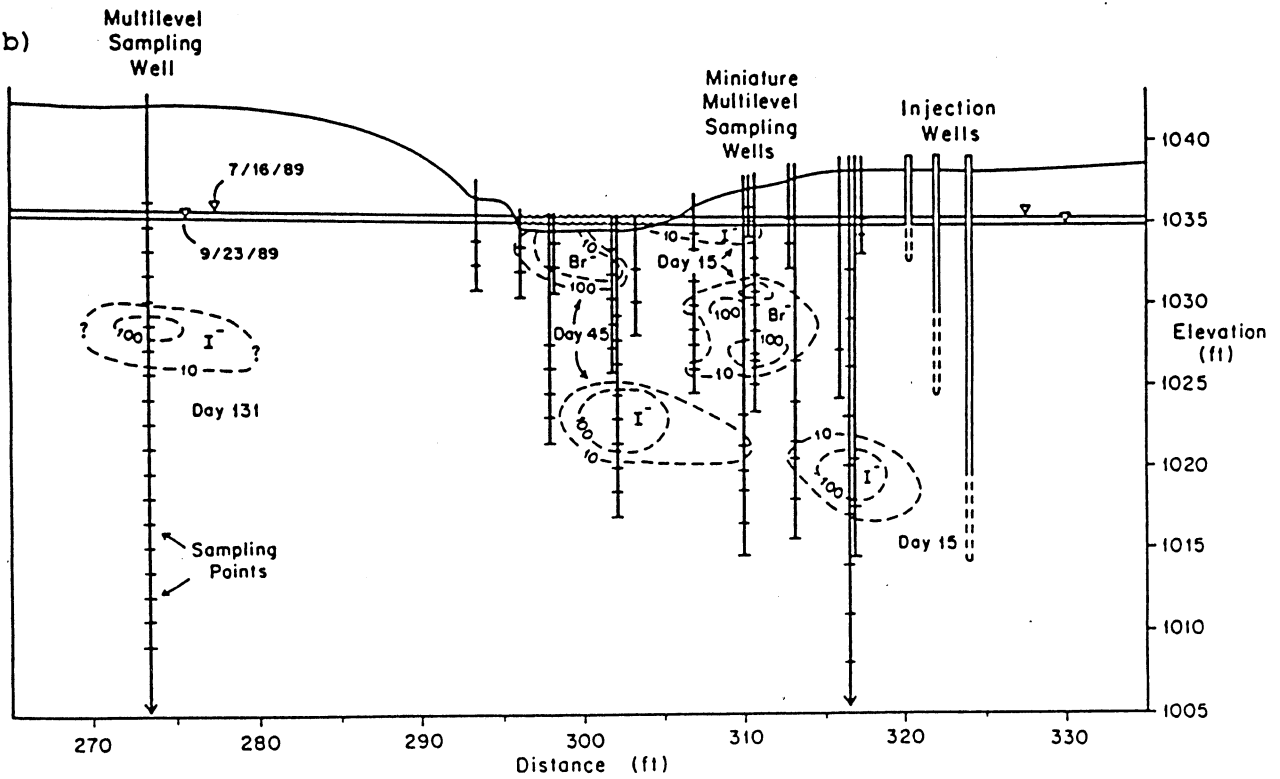


Figure 7. a) A plan view of tracer plumes on day 15, 45, and 131 of the test. b) A cross-sectional view of plume movement. Contours represent concentrations of 10 and 100 mg/l.

model, Moltaner and Killey's equation 6,

$$c(x,t) = 0.5c_0 \left[\operatorname{erf} \left(\frac{x + x_0/2 - vt}{2 DL t} \right) - \operatorname{erf} \left(\frac{x - x_0/2 - vt}{2 DL t} \right) \right]$$

assumes that the tracer is instantaneously added to the aquifer at time $t = 0$. At the moment the tracer is added to the system the plume has a width of x_0 and a concentration of c_0 . DL is the coefficient of longitudinal dispersion, v is the plume velocity and x is the distance from the source. An one-dimensional model should be a good initial approximation with which to evaluate the longitudinal dispersion of the bromide plume because there appears to be little transverse dispersion.

Figure 8 shows the observed and calculated breakthrough curves for 3 miniature multilevels along the apparent axis of the plume. See Figure 5b for the location of each sampling point. The breakthrough curves for points 5 and 6 in mm19 show the extremes in velocity variation which were discussed earlier. Between the injection of the plume and breakthrough at mm19 the flow of the tracer had been predominantly horizontal, so extremes of velocity variations due to layers of higher and lower hydraulic conductivity may have developed. During transport between mm19 and mmd12 the vertical component of flow becomes more important. Flow across aquifer stratification is likely to cause a dampening in the extremes of flow rates, as a portion of the tracer flowing in a low hydraulic conductivity zone reaches a higher hydraulic conductivity zone. A lessening of velocity variations in is visible in the breakthrough curves for mm22 and mmd12.

It is not possible to match the model to point 5 in mmd12 because the dispersion is very large given the peak concentration. The large apparent dispersivity observed at point 5 was probably due to the fact that the point is only 1.5 feet below the base of the ditch. The long period of tracer breakthrough may reflect a combination of different portions of the bromide plume as the plume rose up into the ditch. The large apparent dispersivity is also likely to have been partially caused by transient variations in gradients directly beneath the ditch.

Table 2 shows the parameter values which were used in the model in order to match the model to the actual breakthrough curve data. At times it was necessary to adjust the value of the initial plume width or initial concentration value in order to obtain a good fit. The need to adjust the parameters may be partially due to the fact that the initial plume was not perfectly homogeneous. With the exception of the slow moving region of tracer at point 5 in mm19, the apparent dispersivity values show a general trend of increasing as the upward component of flow increases. The increase in apparent dispersivity probably reflects the plume flowing across rather than parallel to aquifer stratification.

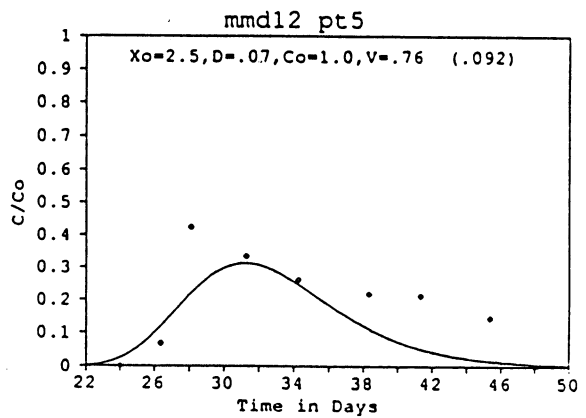
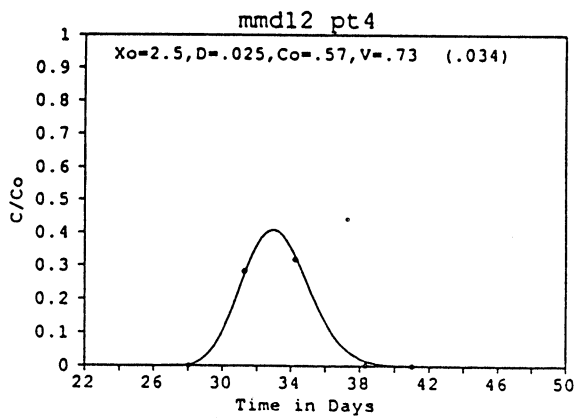
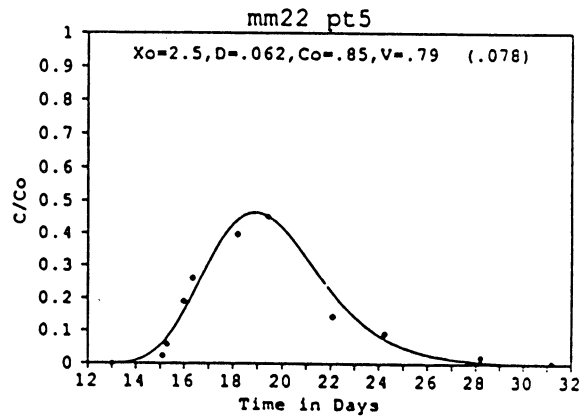
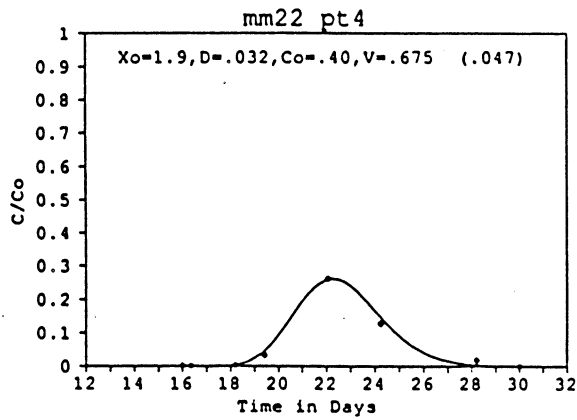
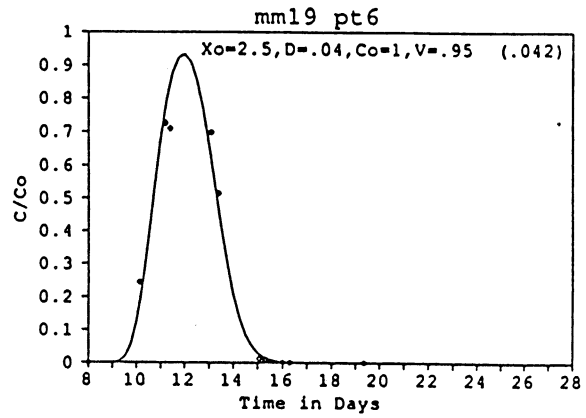
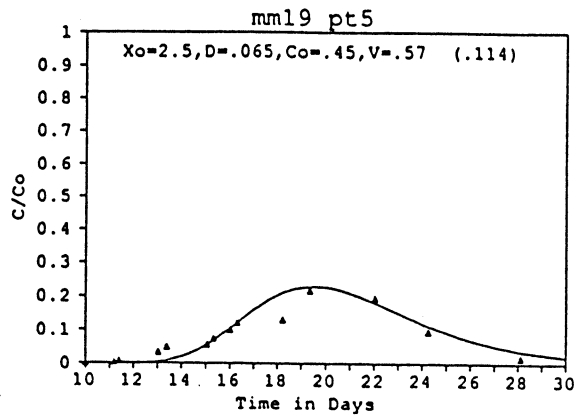


Figure 8. Observed (diamonds) and calculated (solid curves) breakthrough curves. The location of the points can be found in Figure 5b.

Table 2 - Breakthrough Curve Information

Sampling point	Elevation (ft)	v (ft/day)	x ₀ (ft)	C ₀ (%)	α _L (ft)
mm19 pt7	1030.65	0.73	1.6	0.7	0.027
mm19 pt6	1029.89	0.95	2.5	1.0	0.042
mm19 pt5	1028.14	0.57	2.5	0.45	0.11
mm19 pt4	1026.39	0.72	1.6	0.63	0.027
mm22 pt6	1031.50	0.76	1.8	0.38	0.039
mm22 pt5	1030.00	0.79	2.5	0.85	0.078
mm22 pt4	1028.50	0.675	1.9	0.40	0.047
mm22 pt3	1027.73	0.71	2.5	0.80	0.066
mm22 pt2	1026.23	0.805	2.5	0.36	0.037
mm12 pt6	1032.97	0.77	2.5	0.40	0.042
mm12 pt5	1031.47	0.76	2.5	1.0	0.092*
mm12 pt4	1029.97	0.73	2.5	0.57	0.034
mm12 pt3	1028.54	0.82	2.5	1.0	0.046

* Questionable value. A good match was not achieved.

SUMMARY AND CONCLUSIONS

The tracer test described in this paper verified the existence of a capture zone in the vicinity of a drainage ditch in the central sand plain of Wisconsin. For conditions during the summer and fall of 1989, the capture depth of the ditch was at least 12 below the water table. At distances greater than 25 feet from the ditch, the dividing streamline was probably deeper than that inferred from the tracer test. These results are encouraging because they confirm the hypothesis that drainage ditches in the sand plain can provide an effective means to control shallow groundwater contamination.

Heterogeneities within the aquifer are reflected in the breakthrough curves and plume diagrams. There appear to be distinct zones of higher and lower hydraulic conductivity within the aquifer. This conclusion is supported by the bands of coarser and finer sediment which were visible in a vibracore from the site. Flow across aquifer stratification appears to cause an increase in the apparent dispersivity. The macroscale dispersion of the plume seems to be a result of velocity variations due to aquifer heterogeneity, flow across stratification and fluctuating gradients.

REFERENCES

- Anderson, M. P., 1986, Field validation of ground water models, pp. 396-412 in Garner, W. Y., R. C. Honeycutt, and H. N. Nigg (editors), Evaluation of Pesticides in Ground Water, A C S symposium series 315, American Chemical Society, Washington, D.C.
- Born, S. M., D. A. Yanggen, A. R. Czecholinski, R. J. Tierney, and R. G. Hennings, 1988, Well head protection districts in Wisconsin: an analysis and test application, Wisconsin Geological and Natural History Survey Special Report, no 10., 75 p.
- Brasino, J. S., 1986, A simple stochastic model predicting conservative mass transport through the unsaturated zone into groundwater, Ph.D. thesis in Civil and Environmental Engineering, University of Wisconsin, Madison, Wisc., 255pp.
- Canter, L. W. and R. C. Knox, 1986, Ground water pollution control, Lewis Publishers., Michigan, 526 pp.
- Chambers, L.W., 1990, A field evaluation of drainage ditches as barriers to contaminant migration, M.S. Thesis in Geology, University of Wisconsin, Madison, Wisc., 130p.
- Chesters, G., M. P. Anderson, B.H. Shaw, J. M. Harkin, M. Meyer, E. Rothschild, and R. Manser, 1982, Aldicarb in groundwater, Water Resources Center Report, Madison, Wisc. 38 p.
- Clayton, L., 1986, Pleistocene geology of Portage County, Wisconsin: Wisconsin Geological and Natural History Survey Information Circular, 19 p.
- Clayton, L., 1987, Pleistocene geology of Adams County, Wisconsin: Wisconsin Geological and Natural History Survey Information Circular, no. 59, 14 p.
- Clayton, L., and J. W. Attig, 1989, Glacial Lake Wisconsin, Geological Society of America Memoir 173, Boulder, Co., 80 p.
- Faustini, J. M., 1985, Delineation of groundwater flow patterns in a portion of the central sand plains of Wisconsin, M. S. thesis in Geology, University of Wisconsin, Madison, Wisc., 117 p.
- Folk, R. L., 1980, Petrology of Sedimentary Rocks, Hemphill publishing Co., Austin, Texas.
- Gilbert, S. G. and J. J. Gress, 1987, Interceptor trenches for positive groundwater control, Ground Water Monitoring Review, vol 7 n.2, pp. 55-59.

- Harkin, J. M., G. Chesters, F. A. Jones, R. N. Fathulla, E. K. Dzantor, and D. G. Kroll, 1986. Fate of Aldicarb in Wisconsin groundwater, Water Resources Center Tech., Rept., WIS-WRC, 86-01.
- Jackson, R. E., R. J. Patterson, B. W. Graham, J. Bahr, D. Belanger, J. Lockwood and M. Priddle, 1985, Contaminant hydrogeology of toxic organic chemicals at a disposal site, Gloucester, Ontario. 1. Chemical concepts and site assessment. Inland Water Directorate Scientific Series, no. 141, Environment Canada, Ottawa, Ontario, 114 p.
- Jones, F. A., 1987, Computer simulation of aldicarb migration and degradation in the sand plain of central Wisconsin, Ph.D. thesis in Soil Science, University of Wisconsin, Madison, Wisc.
- Kung, K. J. S., 1990, Preferential flow in a sandy vadose zone: 1. Field observations, Geoderma, vol 46, pp. 51-58.
- Kung, K. J. S., 1990, Preferential flow in a sandy vadose zone: 2. Mechanisms and Implications, vol 46, pp.59-71.
- Lee, D. R. and J. A. Cherry, 1978, Flow using seepage meters and mini-piezometers: Journal of Geological Education, 27, pp. 6-10.
- Lulloff, A. R., 1987, Groundwater quality in Wisconsin, Wisconsin DNR, PUBL WR-156-87.
- Manser, R. J., 1983, An investigation into the movement of aldicarb residue in groundwater in the central sand plains of Wisconsin, M.S. Thesis in Geology, University of Wisconsin, Madison, Wisc., 193 p.
- Moltzaner, G. L. and R. W. D. Killey, 1988, Twin Lake Tracer Test: Longitudinal Dispersion, Water Resources Research, vol. 24, n. 10, pp. 1613-1627.
- Rothschild, E. R., R. J. Manser, and M. P. Anderson, 1982, Investigation of aldicarb in ground water in selected areas of the central sand plain of Wisconsin: Ground Water, vol. 20, n. 4, pp. 437-445.
- Stites, W. and L. W. Chambers, in press, A method for installing miniature multilevel sampling wells, Ground Water, in press
- Stoertz, M. W., 1985, Groundwater recharge processes in the central sand plain of Wisconsin: M. S. thesis in Geology, University of Wisconsin, Madison, Wisc.
- Stoertz, M. W. and K. R. Bradbury, 1989a, Mapping recharge areas using a groundwater flow model--a case study, Ground Water, vol. 27, n. 2, pp. 220-228.